276

ORNL-3415
Special

THE JOINT NATIONAL INSTITUTES OF HEALTH–ATOMIC ENERGY COMMISSION ZONAL CENTRIFUGE DEVELOPMENT PROGRAM SEMIANNUAL REPORT

FOR PERIOD JULY 1–DECEMBER 31, 1962

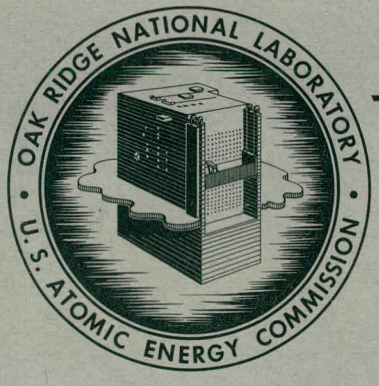

OAK RIDGE NATIONAL LABORATORY
operated by
UNION CARBIDE CORPORATION
for the
U.S. ATOMIC ENERGY COMMISSION

DISCLAIMER

ORNL-3415

Contract No. W-7405-eng-26

BIOLOGY DIVISION

THE JOINT NATIONAL INSTITUTES OF HEALTH–ATOMIC ENERGY COMMISSION ZONAL CENTRIFUGE DEVELOPMENT PROGRAM

SEMIANNUAL REPORT

For Period July 1–December 31, 1962

Prepared by
N. G. Anderson

DATE ISSUED

MAR 4 1963

OAK RIDGE NATIONAL LABORATORY
Oak Ridge, Tennessee
operated by
UNION CARBIDE CORPORATION
for the
U. S. ATOMIC ENERGY COMMISSION

THIS PAGE

WAS INTENTIONALLY

LEFT BLANK

Summary

This report describes development work done on zonal centrifuge systems at the Oak Ridge National Laboratory and the Oak Ridge Gaseous Diffusion Plant during the period July 1 to December 31, 1962 under the joint National Institutes of Health–Atomic Energy Commission Zonal Centrifuge Program. A basic purpose of this project is to develop new methods for isolating virus particles associated with cancerous cells and tissues. Three classes of rotor systems capable of separating particles ranging in size from whole animal or plant cells to protein or nucleic acid molecules on the basis of either sedimentation rate or density alone have been developed. Experiments with phage particles indicate the feasibility of large-scale virus isolation by continuous-flow centrifugation, followed by isopycnic banding in cesium chloride and velocity sedimentation in sucrose—all steps being carried out sequentially in the same rotor. Zonal rotors using the reorienting gradient principle for molecular separations have been tested to 141,000 rpm (310,000 $\times g$ at R_{max}). Previous work on zonal centrifugation and future plans for this program are discussed.

THIS PAGE

WAS INTENTIONALLY

LEFT BLANK

Contents

1 c

I. Introduction

N. G. Anderson C. L. Burger

This is the first semiannual report on work done at Oak Ridge under the joint National Institutes of Health–Atomic Energy Commission Zonal Centrifuge Development Program.

The purpose of the program is to explore the theory and techniques of particle separation by zonal centrifugation and their application to biological materials. The range of particle sizes of interest is that resolved by the electron microscope – roughly from whole cells to protein and nucleic acid molecules. While excellent analytical centrifuge methods for particles up to the size of viruses were perfected by Svedberg and Pedersen,[1] both true preparative counterparts of the present analytical ultracentrifuge and an analytical centrifuge for larger particles have been lacking. As is illustrated in subsequent sections of this report, zonal centrifuges may be employed as both preparative and analytical instruments.

The work has been divided into three concurrently pursued phases (1) development of basic theory and methods, (2) perfection of suitable instruments, and (3) application of the developed centrifuges to specific biological problems.

The basic methodological problems have been to overcome the capacity and speed limitations inherent in swinging-bucket rotors, to accelerate large-volume gradients to the desired rotational speed without mixing, and to recover the gradient undisturbed at the end of centrifugation. Two general types of zonal centrifuge rotors have been developed to solve these problems. These, in turn, require the solution of numerous problems concerned with the development of leakproof fluid-line seals and stable large-capacity rotors operating over a wide range of speeds, as well as the perfection of suitable drive systems.

The central biological problem is the quantitative mass separation of subcellular organelles and particles on the basis of either density or sedimentation rate to generate a profile, or spectrum, of separated fractions. Because relatively few particles having the physical properties of most viruses are found in normal tissues, the zonal centrifuge is expected to be of considerable assistance in detecting and isolating viruses found in tissues. Since the subcellular particulates are physically separated in reasonable quantity, the localization of drugs, carcinogens, or enzymic activities in the profile may be determined. Further, changes in the amount or centrifugal behavior of cell components in response to drugs or experimental treatment may be observed.

[1] The Svedberg and Kai O. Pedersen, *The Ultracentrifuge*, Oxford at Clarendon Press (Oxford Univ. Press), 1940.

1 F

For a variety of reasons, it is desirable to concentrate and to purify extensively virus materials used for the preparation of vaccines. To this end, an integrated system for concentrating virus particles from large volumes of fluid, for isolating from the concentrate (by isopycnic banding) only particles having the density of the desired virus, and for the further purification of the virus by rate-zonal centrifugation through a sucrose density gradient is being perfected. With the development of these methods, the potential hazards involved in handling large quantities of purified virus must be considered and minimized.

Since the fractions separated in zonal centrifuges are recovered as a stream, so-called "on stream" analytical methods are being explored for enzymes, protein, and other cell constituents.

A method for the ultra-fast freezing of cells by centrifugation through liquid nitrogen is also being perfected.

This program is in its very early stages, so that attention must be directed chiefly to the physical problems involved. As rotor systems are perfected, more experimental studies with biological materials will be included in these reports.

II. Background

N. G. Anderson C. L. Burger

A. DENSITY GRADIENT CENTRIFUGATION

Centrifugation ordinarily performed using tubes results in the simultaneous sedimentation, though at differing rates, of all species of particles present. For a multicomponent system, good separations can be made from only a part of the most slowly sedimenting component. When a complex mixture is to be fractionated, repeated centrifugations are often required to obtain acceptable (though generally not quantitative) results. The Svedberg analytical ultracentrifuge, the exact analytical counterpart of the ordinary centrifuge, measures the rate of movements of boundaries without physically separating each of the components observed (except part of the most slowly sedimenting component).

The resolution obtained in a centrifuge could be vastly improved by restricting at the outset all the particles to one level near the top of the tube and allowing each species of particle to move a distance from the starting level, or zone, proportional to its sedimentation rate. Since particles sediment only when they are denser than the suspending liquid, a zone of particles will also be denser than the underlying fluid, resulting in gravitational instability and rapid streaming of the particle zone to the bottom of the tube. It appears, then, that only by positioning the sample zone in a liquid density gradient can stable sedimenting particle zones be obtained. Attempts to use supporting media, such as is done in zonal electrophoresis, have led to the discovery of a new sedimentation anomaly,[1] but have not provided a substitute for a density gradient.

Separations based on rate of sedimentation have been termed "rate zonal centrifugation,"[2] while those based on density alone are termed either "isopycnic gradient centrifugation"[3] or "isopycnic zonal centrifugation." These terms are used in this report.

Previous work on centrifugation through gradients using swinging-bucket centrifuge rotors has been extensively reviewed.[4-6] While excellent separations have been made in density gradients set up in

[1]N. G. Anderson, *Nature* 181, 45–46 (1958).

[2]M. K. Brakke, *Virology* 2, 463–76 (1956).

[3]N. G. Anderson, *Exptl. Cell Research* 9, 446–59 (1955).

[4]N. G. Anderson, pp 299–352 in *Physical Techniques in Biological Research, Vol. III. Cells and Tissues* (eds. Gerald Oster and Arthur W. Pollister), Academic Press, New York, 1956.

[5]Ch. de Duve, J. Berthet, and H. Beaufay, *Prog. Biophys. Biophys. Chem.* 9, 325 (1959).

[6]M. K. Brakke, *Advan. Virus Res.* 7, 193–224 (1960).

tubes, the method has had certain disadvantages. Considerable time is required to set up the gradients, wall anomalies occur, only small amounts of sample material can be handled in each centrifuge tube, care must be taken to avoid disturbances during acceleration and deceleration, and the gradient must be recovered with the tubes at rest. In high-speed rotors, the capacity of the centrifuge tube is severely limited, and the lack of a sector shape gives rise to wall effects, which include clumping and premature sedimentation of particles, and convection currents. In the ensuing chapters of this report, methods and systems for overcoming these difficulties are presented.

B. THE ZONAL CENTRIFUGE

We wished to achieve simultaneously in one rotor system the following: (1) ideal sedimentation in sector-shaped compartments, (2) rapid gradient formation in the rotor with minimal stirring or convection, (3) sharp starting or sample zones, (4) high rotational speed, (5) large capacity, and (6) rapid recovery of the gradient after centrifugation without loss of resolution. Initially a swinging-bucket system was used to demonstrate that high resolution could be obtained (Fig. II-B-1) using glass tubes of modified sector shape.[7,8] Because density gradients are greatly stabilized in a centrifugal field, a second rotor system was developed in which the density gradient was introduced into the centrifuge tubes through a central distributor cup (Fig. II-B-2) while the centrifuge was running.[9] The gradients were recovered from the tubes at rest, however.

It appeared that the centrifuge tubes could be eliminated entirely by using a hollow centrifuge head filled and emptied *during rotation*. The first rotor of this type[10] is shown in Figs. II-B-3 and II-B-4. The gradient was introduced to the edge of the rotor, light end of the gradient first, through radially oriented tubes attached to an annular groove near the rotor center. After the gradient was in position, the sample was introduced manually to its inner surface. When a sufficient particle separation had occurred (Fig. II-B-3) the gradient was displaced toward the center by allowing a very dense fluid to flow to the rotor edge. The gradient was collected as a stream flowing out the exit tubes in the bottom of the rotor near the axis of rotation. This relatively crude rotor (A-III) demonstrated the feasibility of the zonal centrifuge. A more refined design (rotor A-IV), shown in Fig. II-B-5, demonstrated that gradients could be introduced into and recovered from rotors operating at speeds up to 18,000 rpm. Based on this work, construction of an intermediate-speed zonal rotor was proposed, and was built on subcontract by the Spinco Division of Beckman Instruments, Inc. Rotor B-I, constructed under this contract, was unstable for reasons not fully understood. Rotor B-II, tested extensively under the present joint NIH–AEC program, has produced excellent separations but has never reached the maximum design speed for reasons which are discussed in chapters IV-A and B, and VI-B-3.

---

[7] N. G. Anderson, *Exptl. Cell Research* 9, 446–59 (1955).

[8] N. G. Anderson, *Science* 121, 775 (1955).

[9] J. F. Albright and N. G. Anderson, *Exptl. Cell Research* 15, 271–81 (1958).

[10] N. G. Anderson, *Bull. Am. Phys. Soc. I, Series II*, 267 (1956).

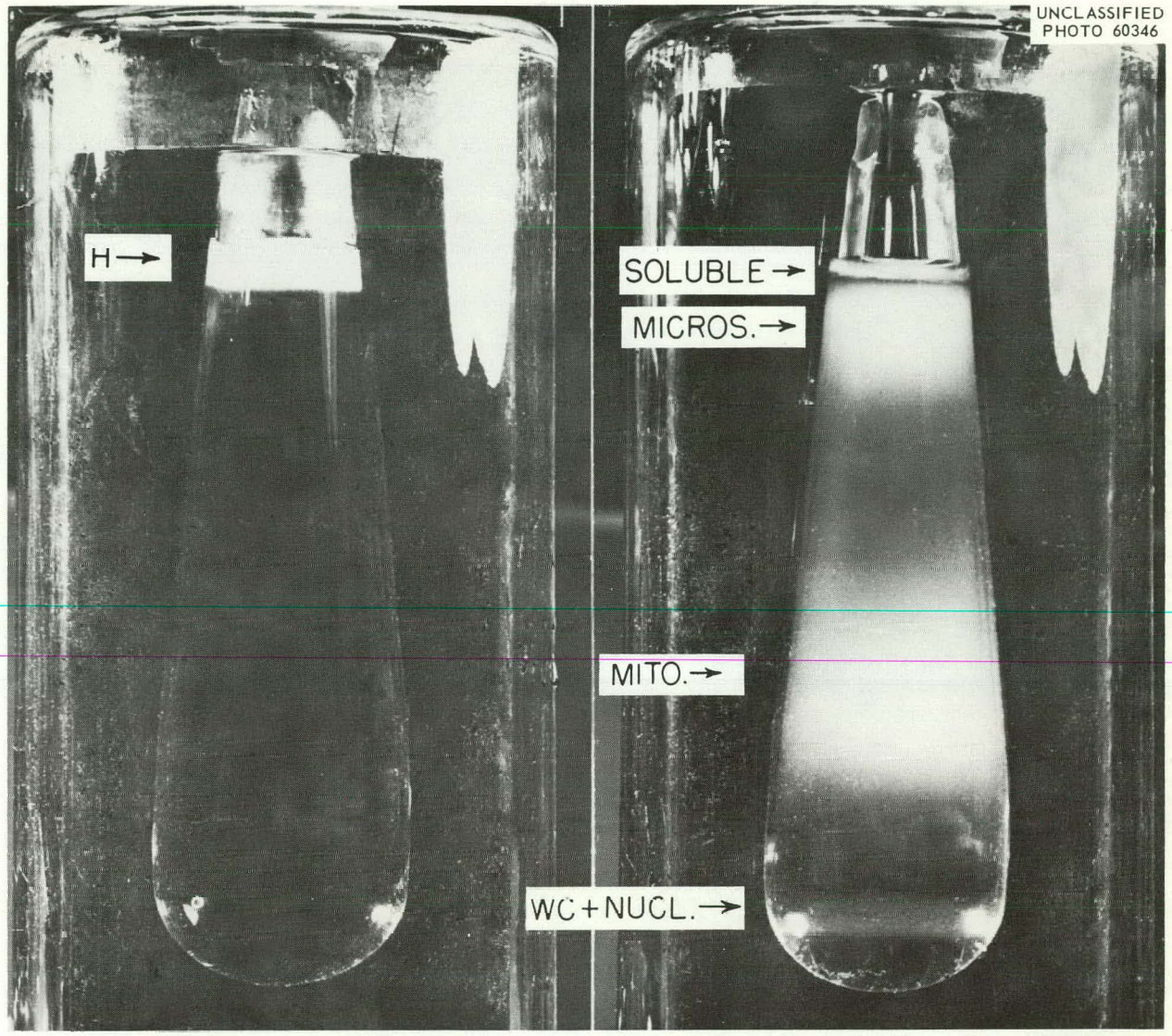

Fig. II-B-1. Fractionation of Rat Liver Subcellular Particulates in a Sucrose Density Gradient Using Pyrex Tubes of Modified Sector Shape. In tube on left, homogenate or brei has been layered over gradient at rest. On right, tube is shown after prolonged centrifugation. Whole cells and nuclei are banded near the bottom of the gradient, mitochondria in the middle, and microsomes near the top. A small zone of cleared soluble material is visible at the very top. The gradient volume was 65 ml; the sample volume, 2 ml; and the centrifugation time, 18 hours at 3000 rpm.[8] Reprinted from *Science* by permission.

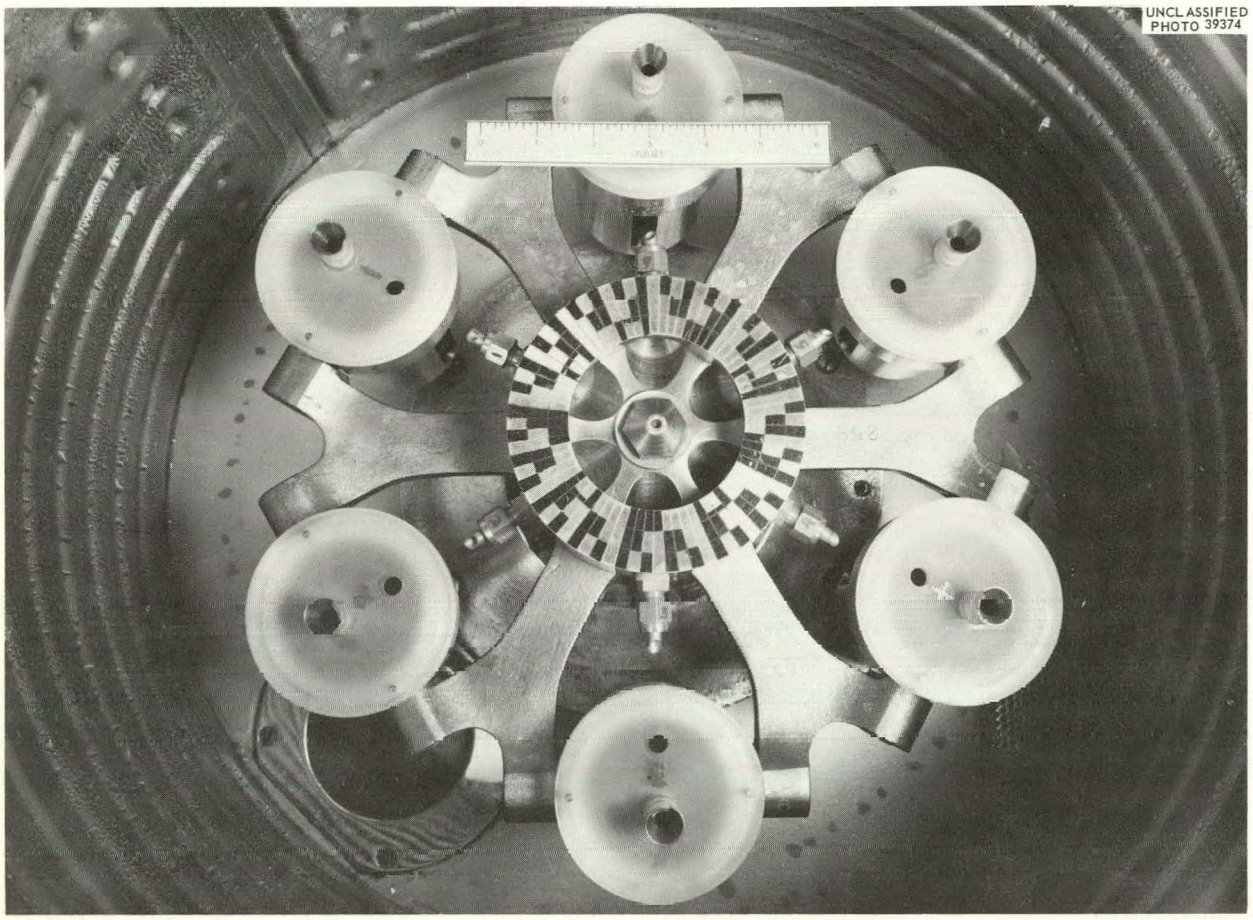

Fig. II-B-2. Zonal Centrifuge System A-II. During rotation the flared tubes on the top of each centrifuge cup make contact with the center distributing vessel. As fluid is introduced into the distributing vessel during rotation, it is proportioned evenly to the bottom of each centrifuge cup. In this manner, identical density gradients are set up in all tubes at one time. Modified from Albright and Anderson.[9]

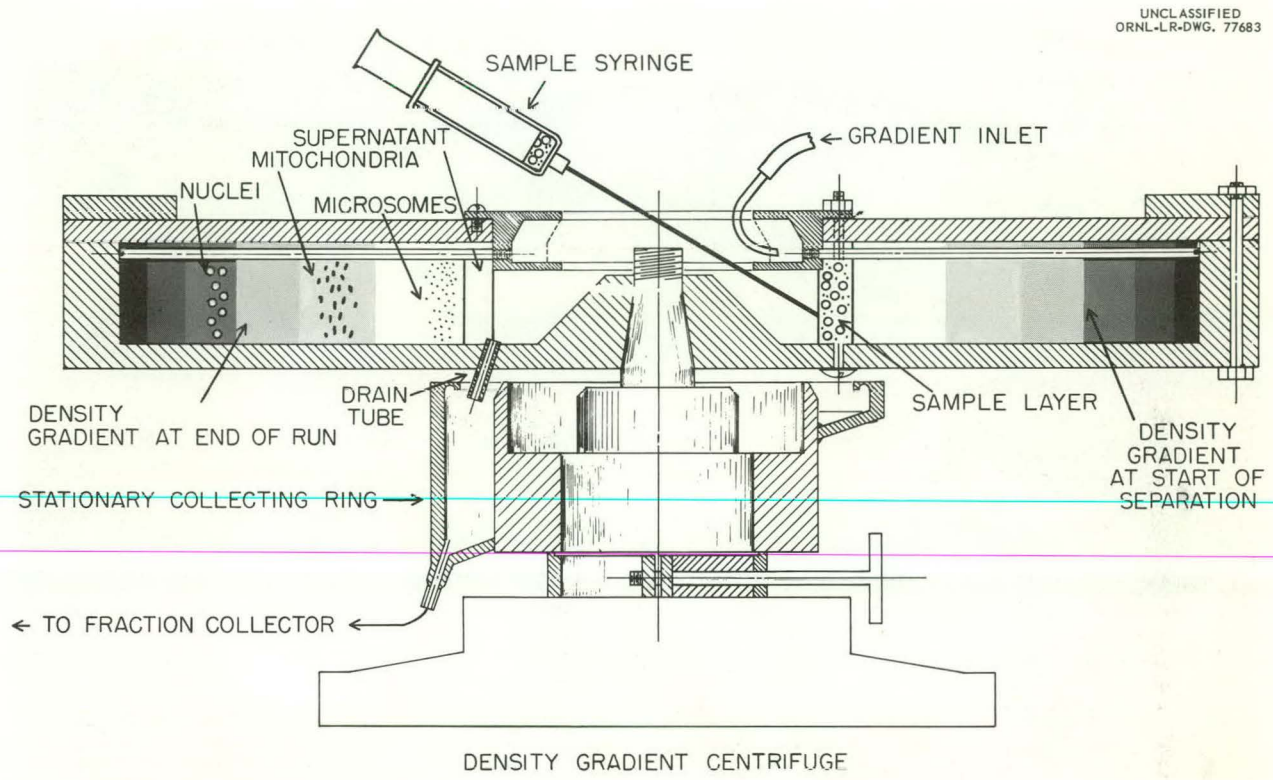

Fig. II-B-3. Schematic Drawing of Operation of Zonal Rotor A-III. The density gradient flows into the spinning rotor through the center annular ring, and thence through small tubes to the rotor edge. The sample layer is then manually layered on the central (light) edge of the gradient. After separation of the particles, the gradient is recovered by displacement toward the center drain tube using a dense sucrose solution introduced to the rotor edge.

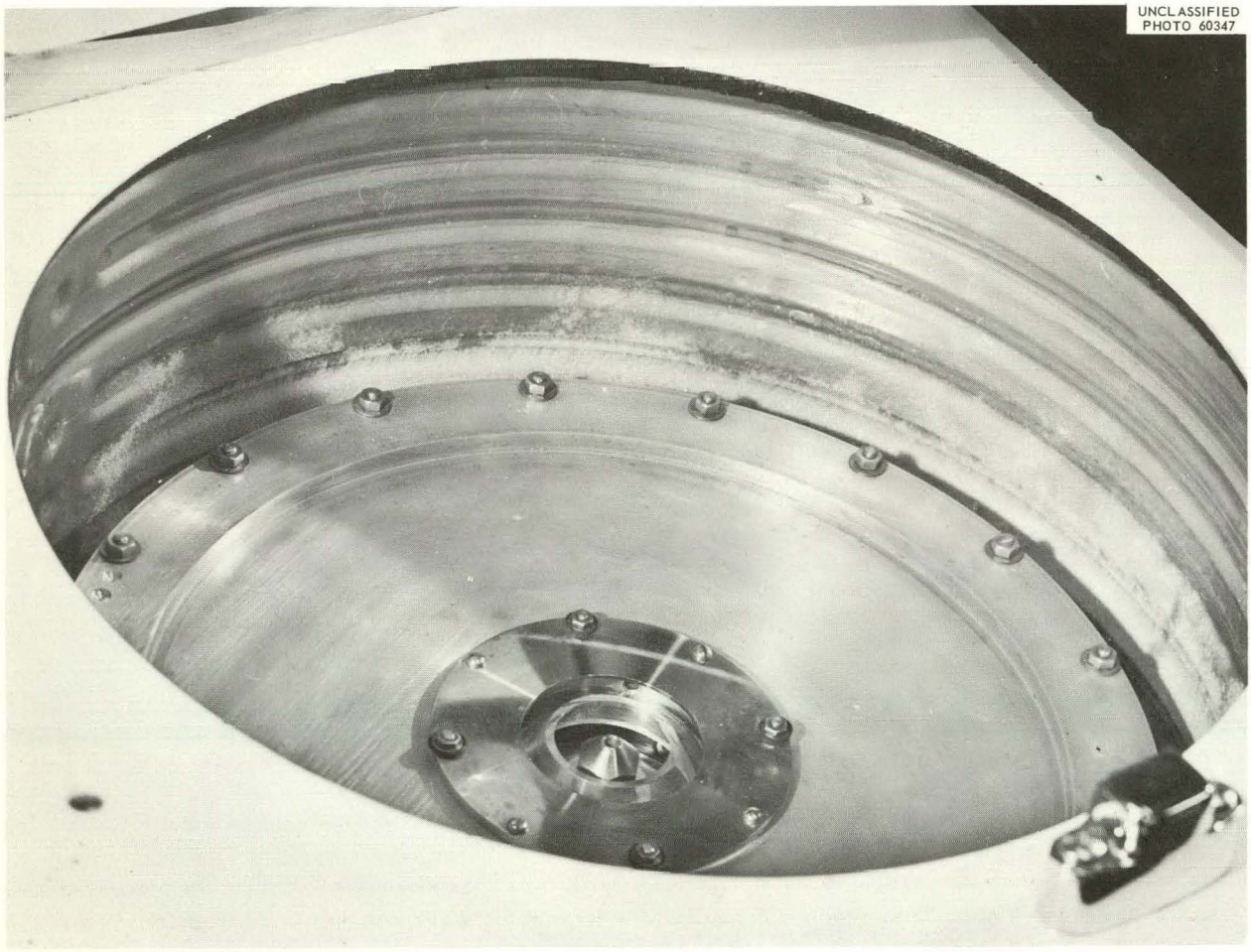

Fig. II-B-4. Zonal Rotor A-III Mounted in International PR-2 Refrigerated Centrifuge.

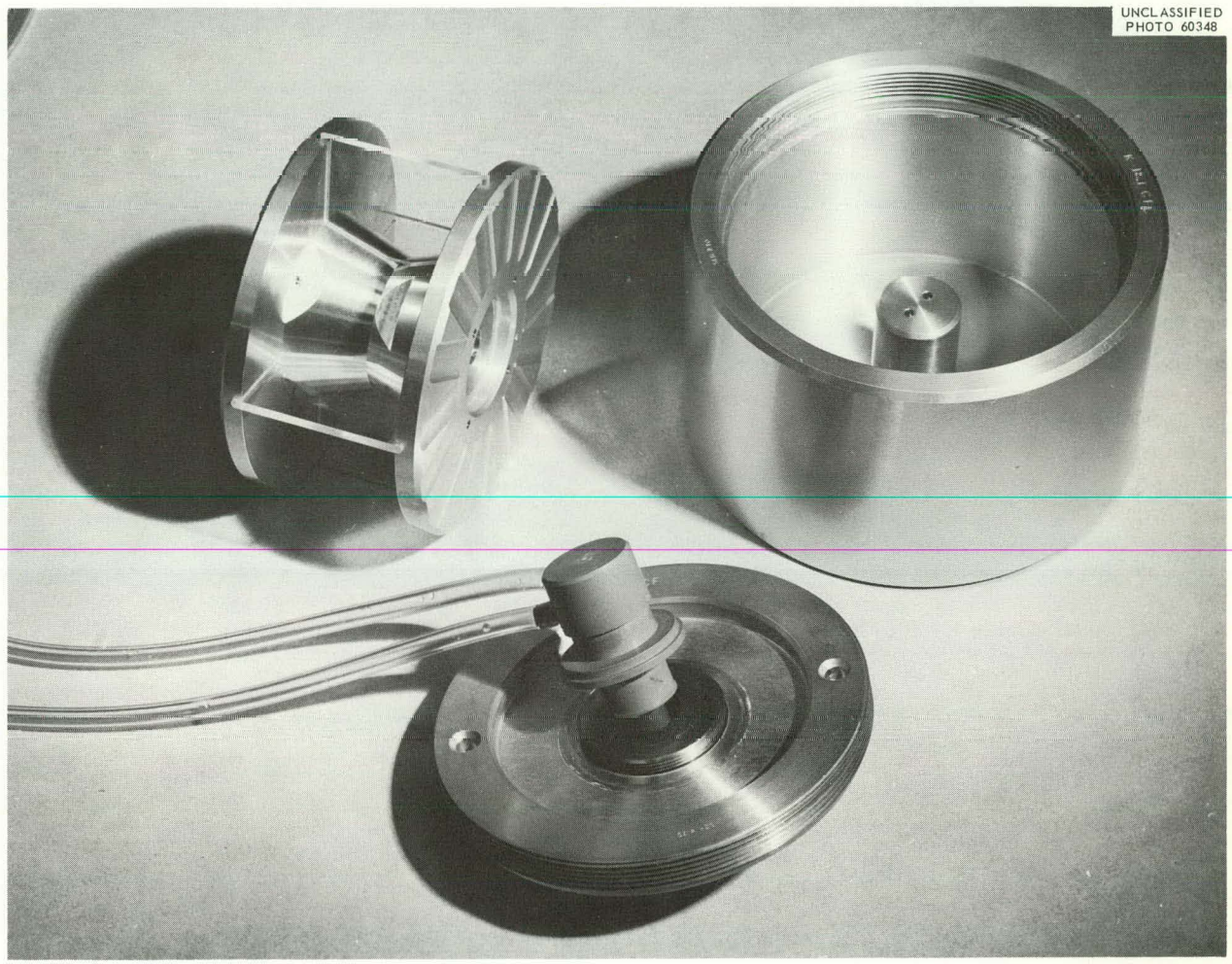

Fig. II-B-5. Zonal Rotor A-IV. Rotor used to demonstrate gradient introduction and recovery from rotor at speeds up to 18,000 rpm. Used in Spinco Model K centrifuge.

III. Theory of Zonal Centrifuges

A. CONTINUOUSLY ROTATING ZONAL ROTORS

N. G. Anderson C. L. Burger

1. General Principles

Consider a sector-shaped compartment, similar to the cell of an analytical ultracentrifuge, continuously rotating about a vertical axis. If fluid line connections are made to the inner and outer edges of the compartment, fluid may be pumped through it in either direction. If the fluid lines are brought back to the center of rotation, the pressure produced by the centrifugal field will be equal along both lines and will cancel. As long as the fluid in both lines has the same density, negligible resistance to flow owing to centrifugal force will be observed.

When a density gradient is caused to flow into the compartment through the connection to the outer edge, it will be stabilized with the gradient extending horizontally while the meniscus and all equidensity surfaces are oriented vertically (chapter II-B). When the compartment is completely filled and the light end of the gradient begins to flow out the connection to the inner edge of the compartment, the direction of fluid flow is reversed, and the sample layer backed in. In order to form the sample layer into a thin zone, an overlay of fluid lighter than the sample layer is introduced after it. This forces the sample layer out into the rotor chamber clear of the center core.

The rotational speed is first increased to effect the desired separation of particles, then decreased to the speed used for loading when recovery of the gradient is desired. This is done by pumping a dense fluid to the rotor edge, thereby displacing the gradient to the center and out the line leading to the inner edge of the compartment.

It is evident that the sample layer may also be introduced first to the rotor edge and then be picked off the rotor wall by the in-flowing gradient. This method has two disadvantages: it allows some particles to sediment to the rotor wall at once, and it increases mixing by both diffusion and laminar flow as the gradient streams in under the sample layer, which is initially spread over the entire inner wall of the rotor.

It is also evident that the gradient may be backed into a compartment containing a dense fluid which is withdrawn through the outer edge line. The gradient may also be recovered in the reverse direction, that is, through the connection to the outer edge. The method used in the continuously rotating zonal rotors described in the present report is believed to give higher resolution than any other method.

In practice, there is no reason why many sector-shaped compartments cannot be used in the same rotor. The rotor may be simply a hollow tube divided by thin, vertically arranged septa into sector-shaped compartments so that nearly the entire internal volume of the rotor can be used. This is the configuration used in the zonal rotor shown in Fig. III-A-1.

2. Operating Sequence

The rotor system, shown diagrammatically in Fig. III-A-1*a* is a hollow cylinder divided into a number of sectors by septa that intersect the core. The core has one or more (in Fig. III-A-1, two) constrictions where the center fluid line opens to the rotor chamber.

The rotor is filled during rotation at a low speed, as shown in Fig. III-A-1*b*. The light end of the gradient is pumped to the rotor wall first, followed by denser fluid, which displaces the lighter fluid end of the gradient toward the rotor core. When the gradient is in the rotor, additional dense fluid, termed the "cushion," is pumped in until the light end of the gradient begins to flow out the center line. At this point the sample layer is introduced through the center line (Fig. III-A-1*c*), reversing the direction of fluid flow through the rotor and causing part of the cushion to flow back out through the edge line. To push the sample layer further into the rotor chamber clear of the core, additional light fluid (the overlay) is pumped in as is shown in Fig. III-A-1*d*. The connection to the rotor edge is then closed, and the center line attached to a reservoir of water to allow a small volume of fluid to flow into the rotor during acceleration to compensate for rotor expansion. The rotor is then accelerated to a speed sufficient to effect the desired particle separation (Fig. III-A-1*e*).

After deceleration to low speed, the gradient is displaced by a dense solution toward the core and out through the center line (Fig. III-A-1*f*). The gradient flows through an ultraviolet absorbance monitor and into a fraction collector. Part of the gradient may be pumped through automated systems to assay for enzyme or total protein activity (Fig. III-A-1*g*). A radioactivity analyzer can also be used in this system.

3. Rotor Length

The length of a zonal rotor is limited by rotor stability considerations and by the fact that two forces act on particle or density zones during rotation. These are centrifugal and gravitational forces. The net result is that all zones of equal density form paraboloids of revolution about the axis of rotation. The equation for the intersection of an axial plane with the paraboloid of revolution is given by

$$L = \frac{r^2\omega^2}{2 \times 980} \qquad (1)$$

where L (cm) is the height from the apex of the paraboloid of a given point on the isodensity surface, and r (cm) is the radius at that point.

It is evident that at various heights, L, isodense zones in a long rotor will be subjected to different centrifugal forces. Indeed, if the rotor is long enough to allow the apex of a zone to be in the rotor, the centrifugal field in a given zone will vary down to zero. For this reason, low-speed rotors generally have a very short height and are of large diameter, while high-speed rotors may be long and narrow. Fortunately considerations of rotational stability and strength of materials generally favor the same configurations.

Fig. III-A-1. Diagrammatic Representation of Zonal Centrifuge Operation.

(*a*) Schematic diagram of zonal centrifuge rotor. Rotation is about the core axis.

(*b*) During low-speed rotation, the liquid density gradient is introduced to the rotor edge, light end of the gradient first. After the gradient is in, additional dense fluid, termed the "cushion," is pumped in to fill the rotor completely and to cause the light end of the gradient to begin to flow out the center line.

(*c*) The sample layer is introduced through the core, displacing back out part of the cushion.

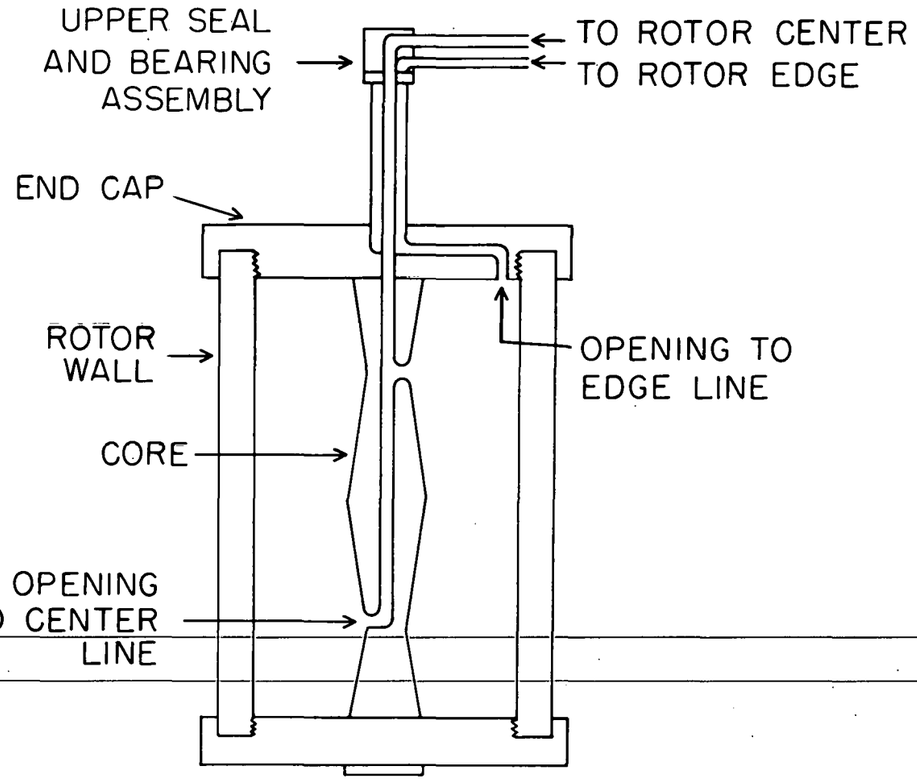

VERTICAL SECTION

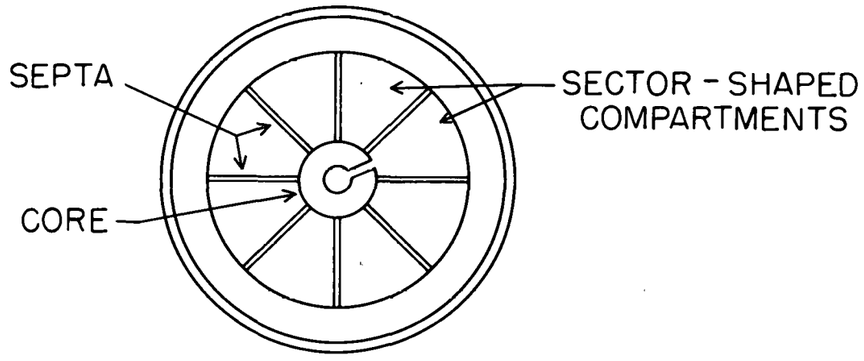

HORIZONTAL SECTION

a

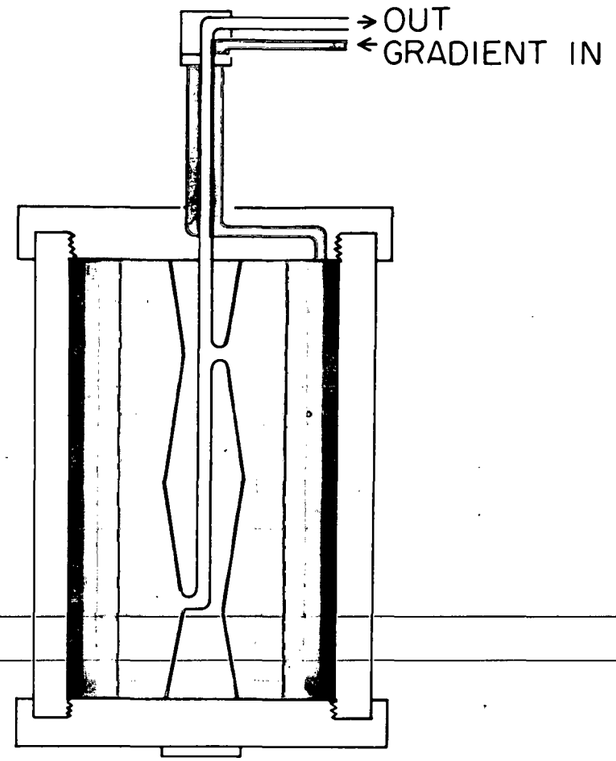

LOW SPEED

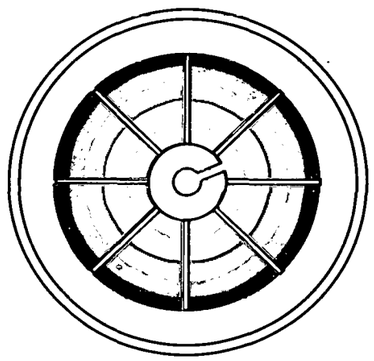

GRADIENT LOADED DURING ROTATION

b

UNCLASSIFIED
ORNL-LR-DWG. 77837

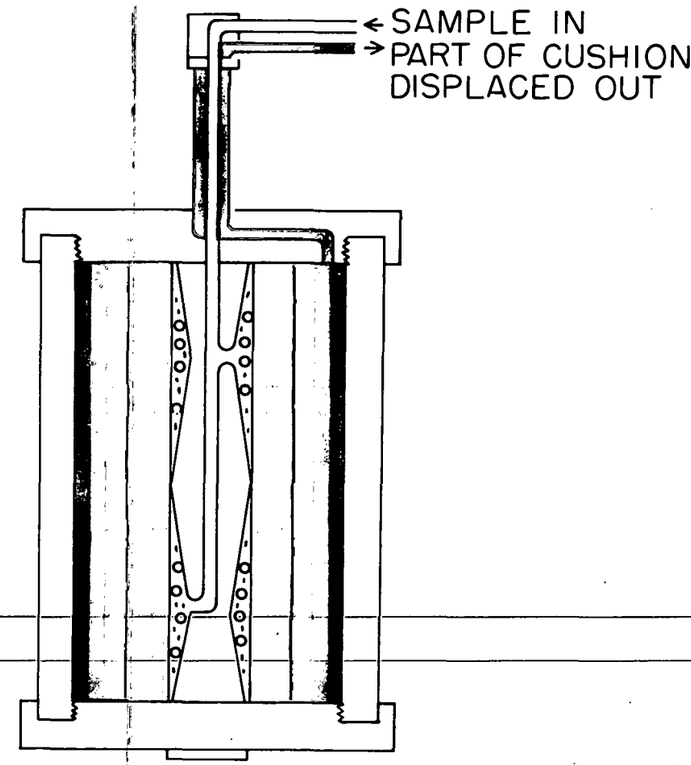

LOW SPEED

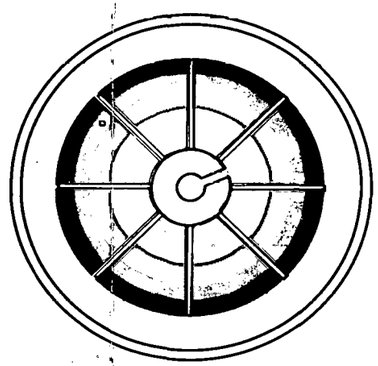

INTRODUCTION OF SAMPLE

c

Fig. III-A-1

UNCLASSIFIED
ORNL-LR-DWG. 77708

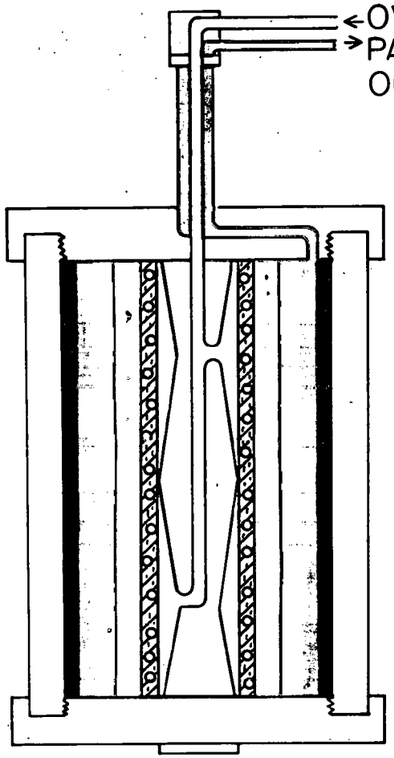

LOW SPEED

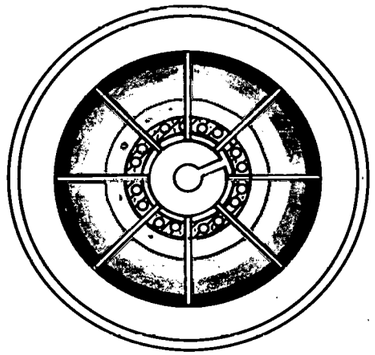

SAMPLE MOVED CLEAR OF CORE BY INTRODUCTION OF OVERLAY

d

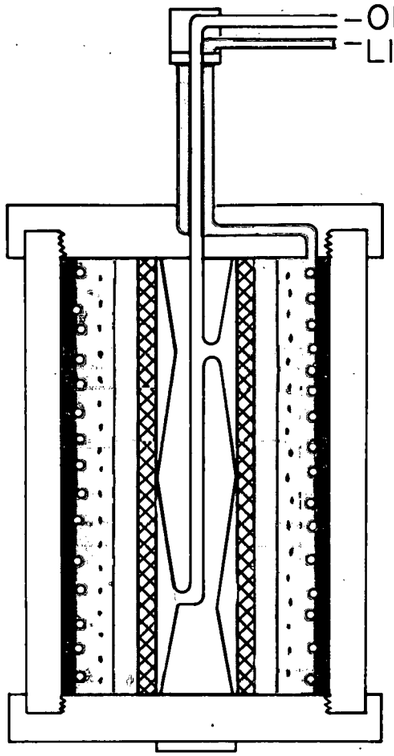

OPERATING SPEED

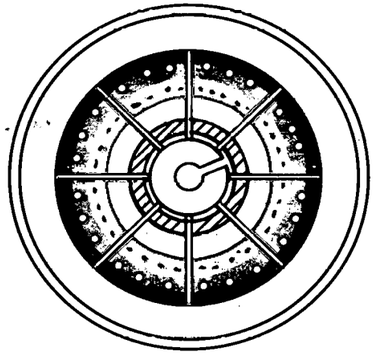

PARTICLES SEPARATED AT OPERATING SPEED

e

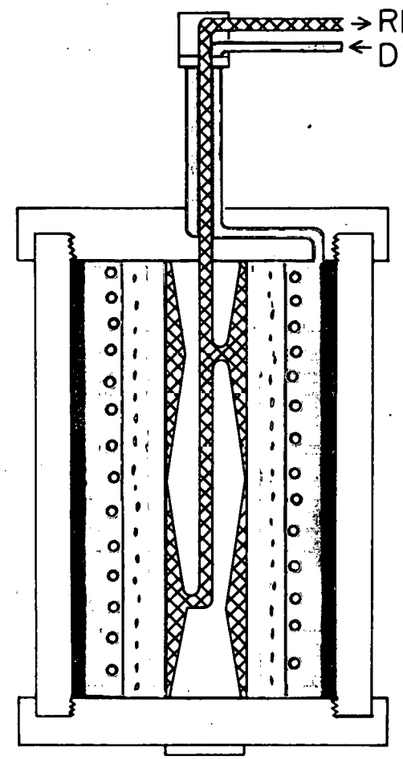

LOW SPEED

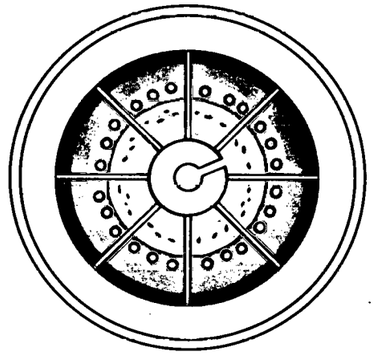

RECOVERY OF GRADIENT

f

Fig. III-A-1 (continued)

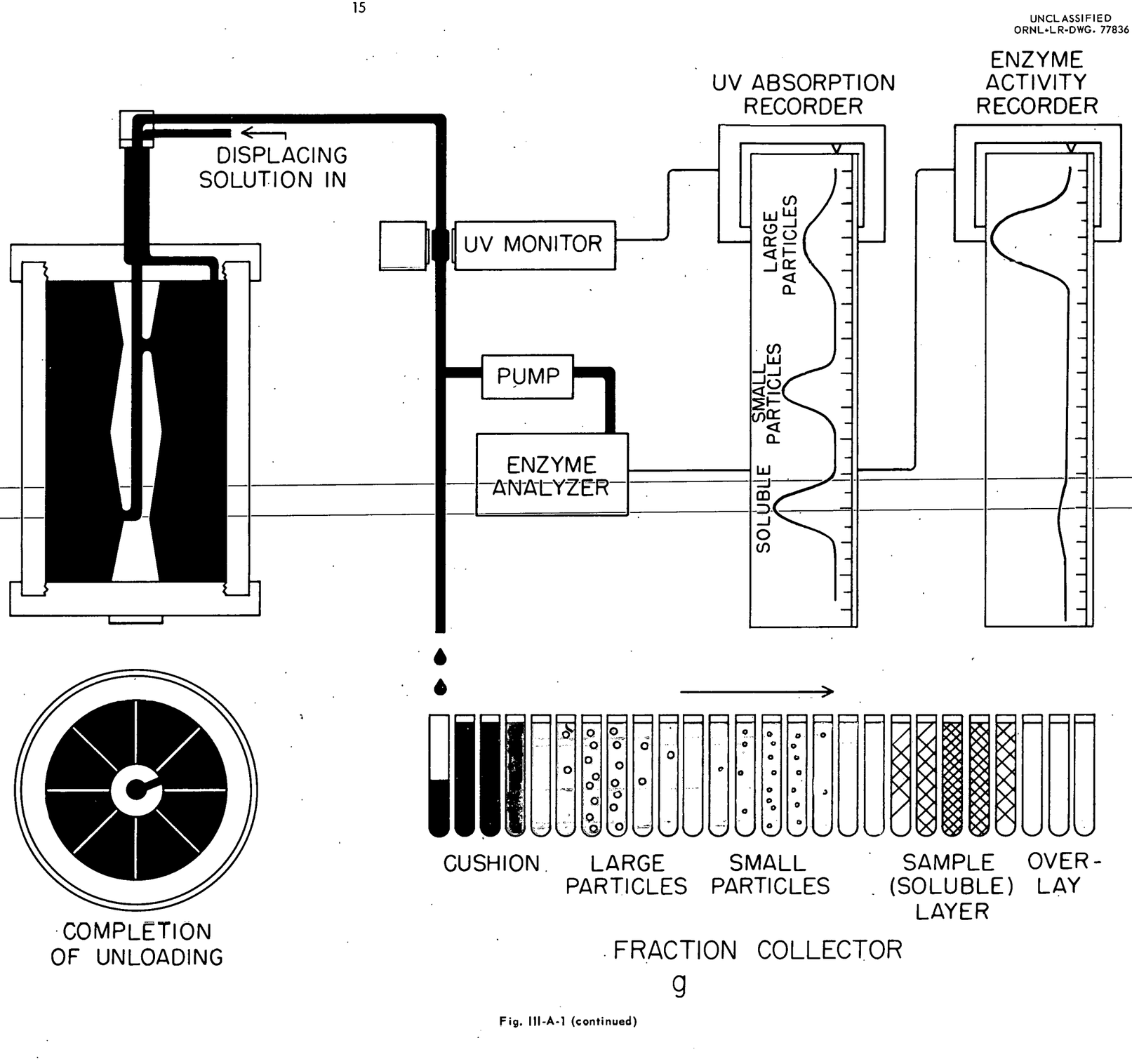

Fig. III-A-1 (continued)

Fig. III-A-1 (continued)

(*d*) A light overlay solution is used to displace the sample layer out clear of the rotor core.

(*e*) The rotor is accelerated to operating speed long enough to effect the desired separations.

(*f*) The gradient is recovered after deceleration to a relatively low speed by pumping a dense fluid to the rotor edge. The overlay, followed by the sample layer, begins to flow out through the center line.

(*g*) The entire gradient, as it is recovered, flows through an ultraviolet absorption monitoring system, and into fraction collector tubes. Part of the gradient may also be pumped through automated analyzers for determining enzymatic activity or total protein. As each fraction is collected, a mark is automatically made on a recorder chart.

B. REORIENTING GRADIENT (REOGRAD) SYSTEMS

N. G. Anderson C. A. Price W. D. Fisher C. L. Burger

The shearing forces occurring in a liquid confined in a closed cylinder during the transition from rest to a stable orientation in a high centrifugal force field may be considered qualitatively by examining Fig. III-B-1. The horizontal lines indicate levels, or surfaces, of equal density in a continuous density gradient.

During acceleration, each isodense surface becomes part of a paraboloid of revolution, as described in chapter III-A. At a given rotational speed, all isodensity curves are identical, being merely transposed vertically. Acceleration results in a series of configurations shown diagrammatically in Fig. III-B-1*b* and *c*. At high speed, where the ratio between the centrifugal force and the acceleration due to gravity is very high, the isodensity surfaces will approach verticality (Fig. III-B-1*d*).

Deformations occurring at the various levels may be best understood by describing the changes occurring in layers originally at the top, middle, and bottom of the rotor. The fluid originally against the upper rotor cap becomes squeezed into a small paraboloid of revolution during acceleration (Fig. III-B-1*b*) and then occupies the center of the rotor at high speed (Fig. III-B-1*d*). A zone in the middle of the rotor (III-B-1*a*) at rest increases in area during acceleration, and then decreases in area slightly as an approximately vertical position is approached. The zone at the very bottom of the rotor at rest (Fig. III-B-1*a*) decreases markedly in surface area during acceleration (Fig. III-B-1*b*) but covers the entire surface of the rotor wall at high speed (Fig. III-B-1*d*). The greatest area changes, therefore, occur in those zones near the top and bottom when at rest but near the center and the edge at high speed.

The reoriented gradient, before the particles have sedimented appreciably, is shown at the left (Fig. III-B-1*d*), and after sedimentation at the right. The distribution during deceleration is shown in Fig. III-B-1*e*, with the distribution at rest shown in Fig. III-B-1*f*. The separated zones are recovered by draining the gradient out of the bottom of the rotor, or displacing it out the top.

A mathematical analysis of the areas of isodensity surfaces (W. D. Fisher, C. A. Price, and N. G. Anderson, in preparation) shows that very little shearing occurs in the center of the gradient in a sector-compartmented rotor. While increases and decreases in area occur, the difference in rate of increase or decrease in the areas of adjacent zones is rather small. By placing a dense "cushion" in the bottom, and an overlay of light fluid above the sample layer at the top, the sample layer and density gradient may be restricted to that part of the rotor where least shearing occurs. As the fluid layers change position during acceleration and deceleration, their tangential velocity will change, since the velocity at any point in the rotor is a function of both the rotational speed and the radius of the point. Fluid in the upper layer, originally near the edge of the rotor, decreases in tangential velocity relative to previously underlying fluid during acceleration, for example. Vertical septa, therefore, are considered necessary to prevent swirling during reorientation of the gradient.

UNCLASSIFIED
ORNL-LR-DWG. 77684

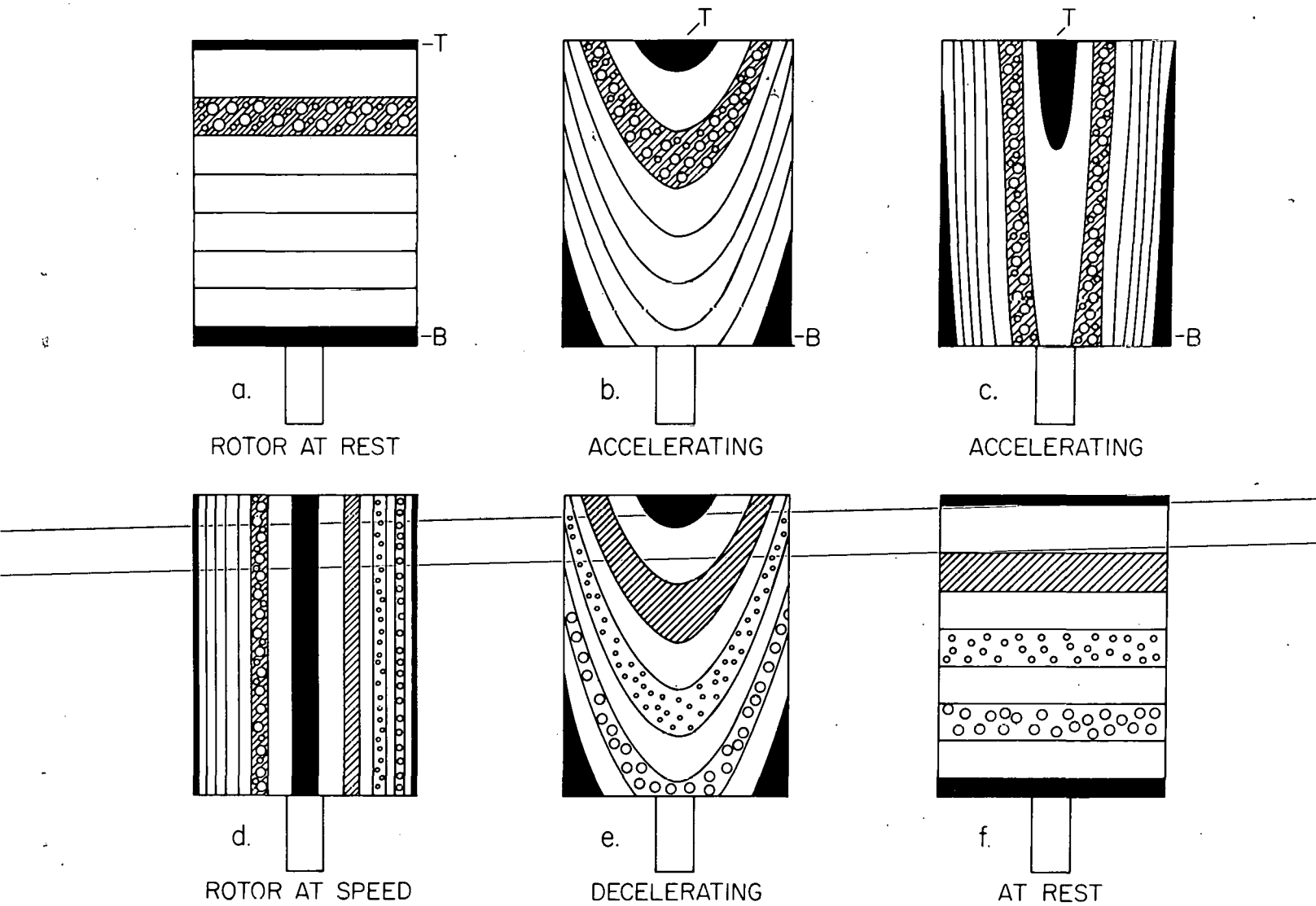

Fig. III-B-1. Schematic Diagram of Reograd Rotor System. (*a*) Rotor is filled at rest with density gradient and sample layer. To indicate extremes of zone deformation, a thin upper layer, *T*, and bottom layer, *B*, are also indicated. (*b*) During acceleration, each zone forms a paraboloid of revolution about the axis. Note *T* and *B*. (*c*) Near operating speed, the zones approach a vertical orientation. (*d*) At a sufficiently high speed, the zones become nearly vertical. Separation of particle zones is shown at right. (*e*) During deceleration, zones again form paraboloids of revolution. (*f*) At rest, various zones may be recovered by draining rotor contents out the bottom, or displacing the gradient out through the top.

C. THEORY OF ZONE CAPACITY

N. G. Anderson

1. Graphical Presentation

A density gradient stabilizes a particle zone by preventing convective disturbances. As was first explicitly shown by Svensson *et al.*,[1] a stable sample zone can exist only so long as all portions of the gradient remain positive (i.e., increase in density in a centrifugal direction). At a level in the gradient where the particles have the same density as the solvent (the isopycnic level) the gradient capacity is equal to the volume, that is, a sheet of packed particles may be supported. At other levels, the capacity is a function of the steepness of the gradient, and the difference between the density of the particles and solvent. Assuming that the particles are impermeable and non-osmotic, the theoretical capacity of a gradient may be approximated graphically as shown in Fig. III-C-1. If rotor radius is plotted along the ordinate, and density along the abscissa, a linear gradient may be indicated as shown. A sample zone may be represented by a triangle whose horizontal length L equals the maximum volume fraction of particles times C, which is the distance along the density abscissa from zero to the isopycnic level. The density (from 0 to the value at the isopycnic level) is plotted along L, and L is shifted horizontally until the intersection of L and the gradient curve is at a point on the scale of L equal to the density at the point of intersection. Since no zone having a density which exceeds that of any point on the gradient underneath it is allowed, it is evident that a thin, dense particle zone must be supported by a decreasing or negative gradient of particles underneath. As shown in Fig. III-C-1 the maximum capacity indicated in the upper zone occurs when the density does not change through a zone. By dropping a perpendicular line from L as shown, a triangle is formed which indicates graphically the distribution of particles as a function of rotor radius. The area to the right of the density curve is proportional to the excess density, while the dark area to the left is proportional to the buoyancy. As the zone sediments, the intersection of L and the gradient density curve shifts until at the isopycnic point no excess density exists. When a zone is placed below the isopycnic level a reverse situation, with an excess buoyancy, occurs.

2. Shape of the Gradient

The following factors favor the use of convex gradients:

1. The capacity of a gradient increases as the difference between the particle and solvent density decreases. If the capacity of a gradient is to be the same along its length, a desirable situation when a single virus species is being purified, then dc/dx should decrease as $\rho_p - \rho_s$ decreases.

2. In a multicomponent system a series of zones will leave the starting zone with little separation between them, but these will become widely distributed throughout the gradient during centrifugation. It is evident that the greatest gradient capacity is required through and just below the sample zone, that is, the gradient should be convex.

---

[1] H. Svensson, L. Hagdahl, and K-D. Lerner, *Sci. Tools* 4, 1–10 (1957).

Concave gradients may be employed when it is desirable to band a rapidly sedimenting or dense particle at its isopycnic point while allowing a slowly sedimenting component to sediment through a shallow gradient. Complex gradients have been employed for cell component isolation in the present work when a linear gradient ends in a second, small steep gradient.

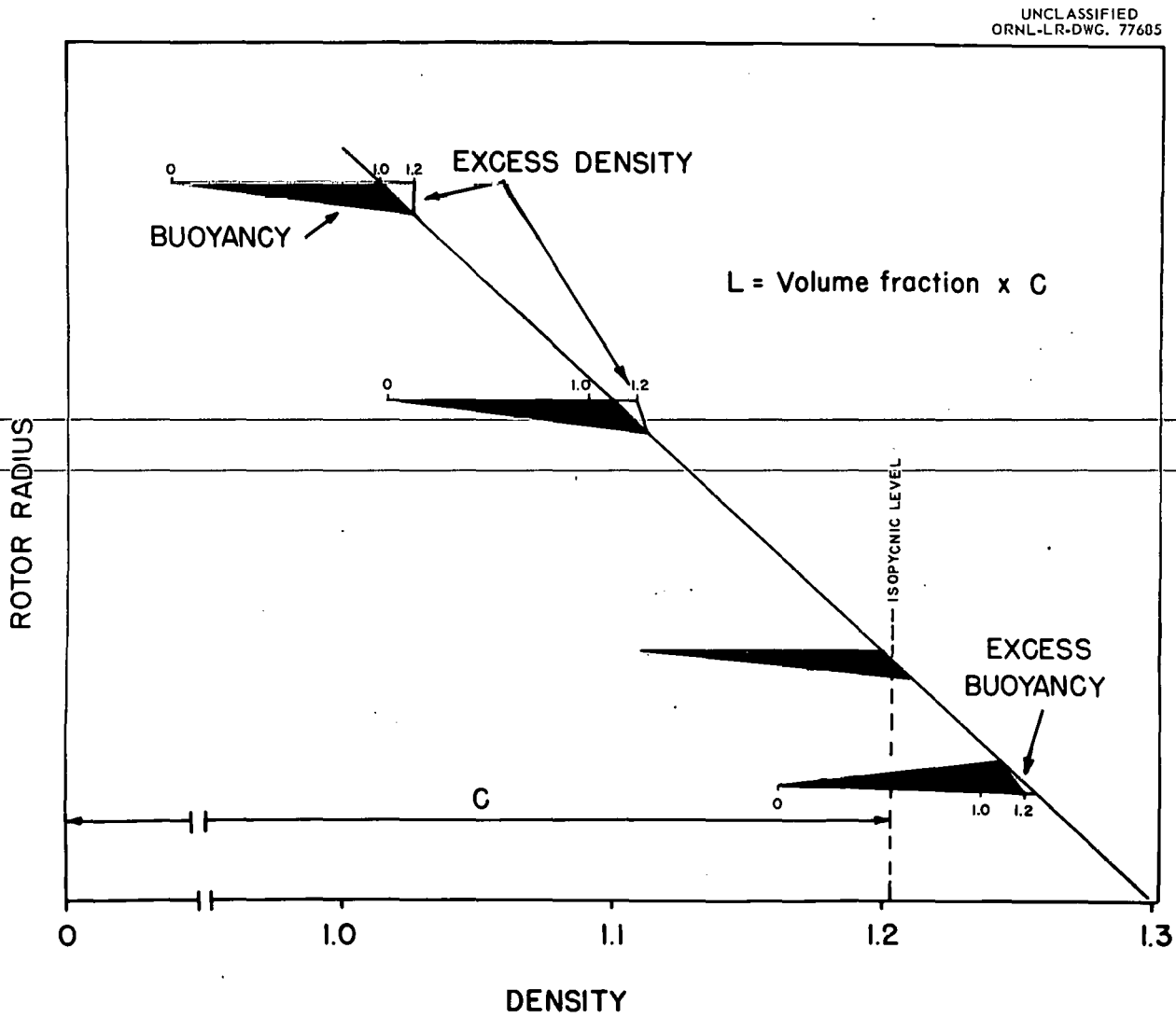

Fig. III-C-1. Graphic Representation of Gradient Capacity. Particle zones are represented as triangles whose length, L, is equal to the particle volume fraction multiplied by C, the distance along the abscissa from zero density to the particle isopycnic point. Along L is plotted a scale from zero to the isopycnic density number. L is shifted horizontally until the intersection between L and the gradient curve is at the gradient density (as read on scale L) existing at the level of intersection. Displacement buoyancy is indicated in black, excess density or buoyancy in white.

3. Equation for Zone Capacity

The capacity of a zone in terms of the amount of particulate material supported in a thin, stable zone in a zonal centrifuge may be calculated approximately by using equation 2 (derived from an equation of Svensson *et al.*[1] and Brakke[2] for gradients in tubes of circular cross section). It is based on the assumption that the negative concentration gradient of a particle zone may increase until the sum of the solvent and particle gradient approaches zero.

$$A_i' = \frac{Lb^2[2\pi(x_0 + 0.29b) - cn][d\rho_1'/dx - (d\rho/dx)_e]}{2(1 - \rho_{1x}'/\phi_i')} \tag{2}$$

where symbols with prime marks indicate values in sucrose solutions, symbols without prime marks refer to values under standard conditions, that is, water at 20°, ρ_1' the density of the sucrose solution, ρ_{1x}' the density of the bottom (outer edge) of a zone, ϕ_i the effective density for sedimentation in solution of component i, letter b the thickness of the zone, c the thickness of one septum, n the number of septa, L the height of the internal rotor chamber, and x_0 the distance from the axis of rotation to the top (inner edge) of the particle zone. The term $(d\rho/dx)_e$ is a correction factor for the minimum overall density gradient necessary for gravitational stability. Theoretically it should approach zero for centrifugation, but have a small positive value for electrophoresis.

Half the particles in a wedge distribution of particles lie above a point $0.29b$ down the zone. The area of the zone perpendicular to the direction of sedimentation is taken to be $L[2\pi(x_0 + 0.29b) - cn]$.

In practice, the amount of material which may be supported in a zone of given thickness is much smaller than predicted by equation (2). The reasons are not understood and series E rotor systems are proposed for the specific purpose of studying this and several other problems in connection with gradient theory.

In subsequent reports theoretical studies on particle-particle interactions in density gradients will be presented.

---

[2] M. K. Brakke, *Advan. Virus Res.* 7, 193–224 (1960).

IV. Rotor Design

A. ROTOR STABILITY STUDIES

D. A. Waters A. A. Brooks

1. Introduction

The purpose of this section is to define *stability*, as used in this report, and to describe generally the types of instability that can affect the operation of a liquid centrifuge. The stability problem will be considered in more detail in section B. The centrifuge test stand and the methods used to investigate rotor motion will also be described.

2. The General Problem

To operate a liquid centrifuge at high rotational speeds without imposing any adverse acceleration upon the material being processed, the rotor must remain stable at all times. The word *stability* is not used here in the usual mathematical context, but refers to any type of motion of the rotor that would disturb the orientation of its contents. Using this definition, there are five basic sources of excitation in a centrifuge rotor which could lead to an unstable condition. These are: (1) external vibration, (2) shaft whirl, (3) the rigid body modes of vibration of the rotor in its suspension system, (4) precession, and (5) liquid instabilities.

The vacuum and refrigeration equipment associated with the liquid centrifuge is the usual source of external vibration. The effect of such vibration upon a rotor can be minimized by using proper isolation techniques.

Shaft whirl in this instance is essentially independent of the rotor and suspension system design. There are two types: (1) half-speed whirl of the supporting shafts in their journal bearings, and (2) shaft whirl at the critical speeds of the shafts. Half-speed whirl, caused by improper journal bearing design, can transmit large amplitude motion to the rotor with a frequency of one-half the operating speed. Shaft whirl at the critical speed of the shaft is a phenomenon that is associated with high-speed rotors supported by flexible shafting. At high speeds the rotor effectively behaves as a rigid, immovable mass and the shaft can whirl between the rotor and the shaft bearings. As shown in Fig. IV-A-1, the shaft behaves as though it is nearly clamped at the rotor, and, depending upon the type of bearing used, either clamped or pinned at the bearing. A typical model that will illustrate the rigid body modes of vibration is shown and

discussed by Den Hartog.[1] If the damping and stiffness properties of the suspension systems are symmetric about the axis of rotation, then there are but four basic modes of vibration. The first can be described as a whirling of the rotor symmetry axis about the vertical axis of the total assembly. The second, which occurs at a slightly higher speed, is a whirl of the rotor symmetry axis about the vertical axis with a node near the rotor's center of gravity. The third and fourth types of motion are suspension system vibrations.

Precession usually describes the behavior of celestial bodies, tops, or gyroscopes. It can be demonstrated quite easily that, under certain conditions, a high-speed centrifuge rotor will precess like a top or gyroscope. In most cases, the top or gyroscope precesses due to the moment exerted by the earth's gravitational field. If a flexibly suspended centrifuge rotor is deflected from the vertical, it experiences not

[1] J. P. Den Hartog, *Mechanical Vibrations*, McGraw-Hill, New York, 1947.

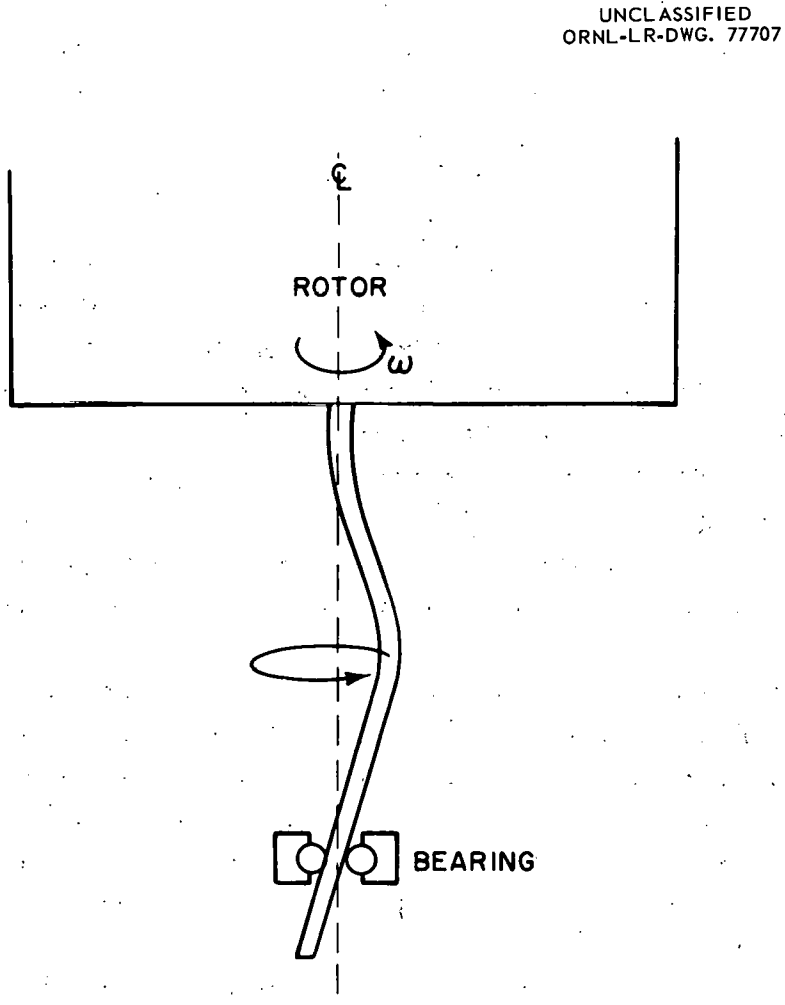

Fig. IV-A-1. Shaft Whirl at Shaft Critical Speed.

only gravitational torque but a much stronger torque due to the deflection of the shafts and the suspension systems. There are two basic forms of rotor precession. The first is a slow backward (opposite to the spin of the rotor) whirl of the rotor symmetry axis about the vertical axis. This form of motion is similar to the first type of rigid body motion, and at high rotational speeds its frequency is approximately inversely proportional to the operating speed. The second type of precession is a fast forward whirl of the rotor symmetry axis about the vertical axis, with a node near the rotor center of gravity. This form of motion is similar to the second type of rigid body motion, and at high rotational speeds its frequency is nearly directly proportional to the operating speed of the rotor. Typical curves for slow and fast precession are shown in Fig. IV-A-2.

All of these types of instability must be considered in evaluating a particular centrifuge design.

In addition to the mechanical stability of the centrifuge rotor, the stability of the liquid in the rotor must be considered. The effects of accelerations throughout the entire operation of the centrifuge must be evaluated.

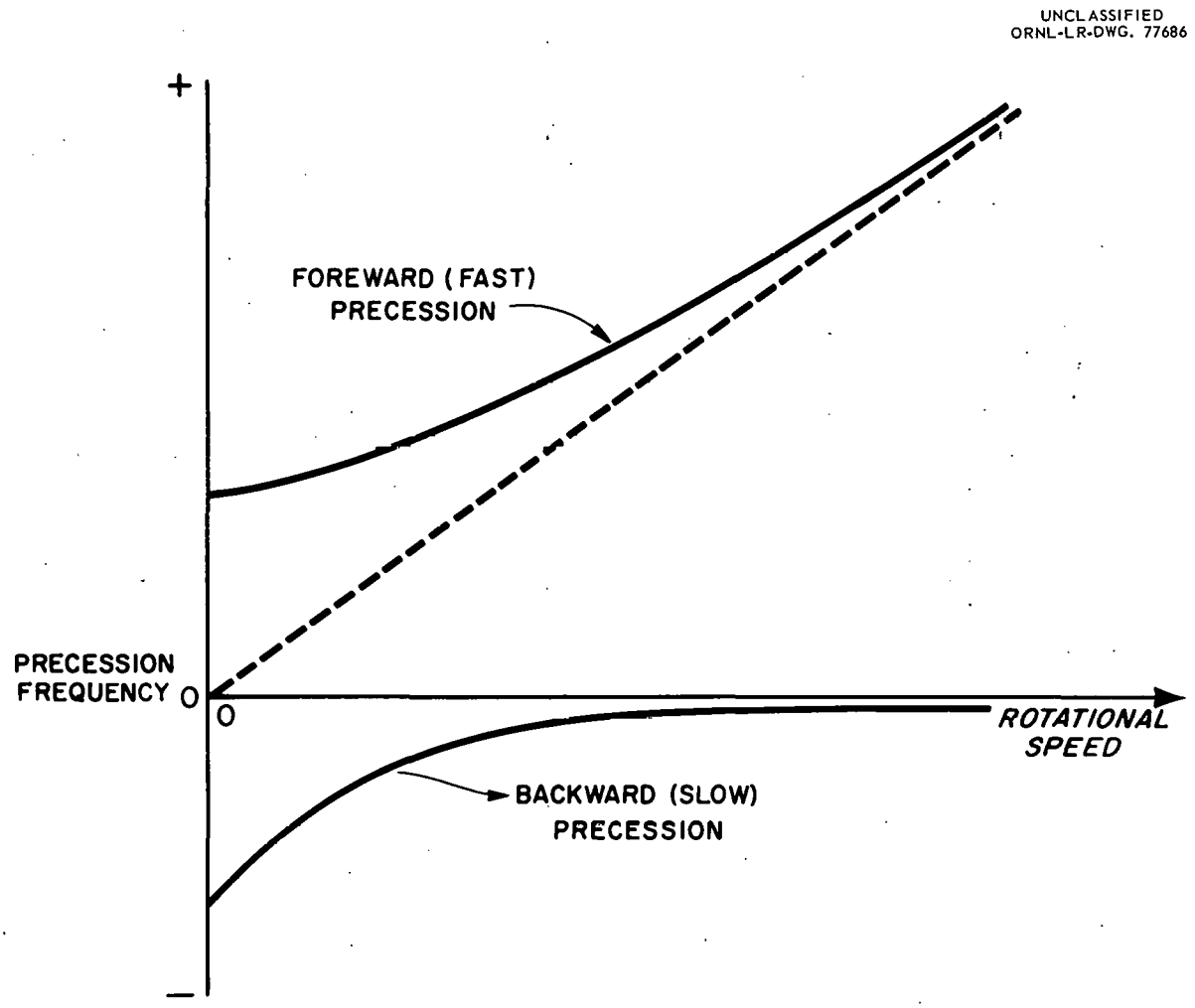

Fig. IV-A-2. Precession Curves for a Flexibly Supported Centrifuge Rotor.

3. Test Facilities

To evaluate and understand the mechanical behavior of liquid centrifuges, a mechanical test stand has been built. The stand is a vacuum jacket 50 inches high and 10 inches in diameter.

Any high-speed rotor presently under consideration can be operated within this chamber. The nature of most instabilities can be determined quite accurately with relative ease using extremely sensitive proximity probes. Rotor movements with amplitudes of 1/10,000 inch can be measured accurately up to frequencies of 10 kilocycles. Four-channel oscilloscopes are used so that rotor and suspension system movements at four positions can be displayed simultaneously. Phase relations between the various components of the system can be determined as well as runout amplitudes and vibration or whirl frequencies and amplitudes.

B. BASIC DESIGN CONCEPTS

D. A. Waters

1. General Considerations

The primary consideration in the design of a liquid centrifuge is the application, which dictates the overall capacity, the loading and unloading procedure, and the rotational speed and *g* force. However, once this has been decided, there are four critical areas that must be investigated before the centrifuge can be designed. These are (1) the ratio of the polar and transverse moments of inertia and the effect of this ratio upon shaft stiffness and damping required to operate the machine, (2) the critical speed of the rotor, (3) the stress in the rotor, and (4) the stability of the liquid throughout the operating cycle of the rotor.

2. Essential Areas of Investigation

Could a rotor be balanced and aligned perfectly and connected rigidly to its damping and suspension systems, it would be theoretically possible to operate any rotor configuration to its ultimate speed without concern for mechanical stability. However, a rotor cannot be so balanced and aligned. In addition, no matter how close the tolerances are between the shafting and bearings, some movement is possible. In reality then, some means must be found to support the rotor to minimize the effect of the inherent unbalance and misalignment on the operating characteristics of the machine. This problem may be solved by using flexible shafting to couple the rotor with its suspension systems. A shaft can be designed which is capable of bending to compensate for both the rotor unbalance and its misalignment without imposing any undue force on the rotor or its suspension systems. A second criteria is that the stiffness of the supporting shafts must be such that the rotor movements are transmitted to the suspension system at the highest expected precession frequency and the suspension system must contain adequate damping to remove the energy of precession. This problem also has been solved.

The second area, critical speed of the rotor itself must be determined when the required length-to-diameter ratio of the rotor is large. If flexible shafting is used to support the rotor, the shafting itself exerts a negligible influence, and the rotor can be treated as a free beam.

The third area of investigation becomes extremely important in the design of a high-speed centrifuge. It can be shown that there is an optimum wall thickness for minimum stress in the rotor that depends upon density of the rotor material, the density of the liquid, and the peripheral speed of the rotor. An analysis of the rotor wall stress for a rotor full of liquid has been made, and the optimum wall thickness is given by

$$b - a = a \left\{ \left[1 + \left(\frac{4\rho}{(3+\mu)\delta} \right)^{1/2} \right]^{1/2} - 1 \right\} \tag{1}$$

and the maximum shear stress in an optimized rotor is

$$\tau_{opt} = V_p^2 \left\{ \frac{\delta + \rho}{2} + \frac{1}{2} [(3+\mu)\rho\delta]^{1/2} \right\} \tag{2}$$

where

τ_{opt} = maximum allowable shear stress at optimum conditions,
$V_p = \omega a$ = peripheral speed,
δ = density of metal,
μ = Poisson's ratio,
ρ = density of fluid,
a = inside rotor radius,
b = outside rotor radius.

The maximum allowable shear stress determines the inside radius, which, in turn, determines the optimum wall thickness. The details of this analysis will be published in a subsequent report. In addition to the stress analysis in which equations (1) and (2) were derived, an IBM 7090 computer program that solves for the hoop stress in the rotor as a function of speed, liquid, film thickness, and rotor wall thickness is used in the design of liquid centrifuges. Some areas of a liquid rotor, such as the junction of the end cap to the rotor, defy stress analysis. Stress-coat techniques are often used to investigate the stress in these areas of the centrifuge.

At this writing, little work has been done in the final area of investigation. However, the dynamics of loading and unloading the centrifuge must be well understood as must the effects of heat and vibration upon the liquid being processed. A thorough hydrodynamic study of the liquid centrifuge is therefore being undertaken and will be described in subsequent reports.

C. MATERIALS STUDIES

H. P. Barringer

It now appears that the limits in the development of each of the several classes of rotors are set by the strengths of available materials. A comprehensive review has been undertaken of the strengths, fabrication costs, and corrosion resistance of metallic, ceramic, and plastic materials which might be used. Of special interest are high-strength rocket motor and solid fuel casing materials.

In most of the rotors described here, 7075 aluminum alloy with a T-6 heat treatment has been employed.

V. Low-Speed Zonal Rotors

A. ROTOR A-V

N. G. Anderson R. E. Canning C. T. Rankin

1. Design

Rotor A-V was designed to examine the possibility of separations at relatively low speeds (500–1000 rpm). Loading and unloading Type B rotors at very much higher speeds is feasible.[1,2] At very low speeds, however, the stabilizing effects of centrifugal force are much less and the possibility of mixing during introduction of the sample layer correspondingly increased. Since the pressures and stresses are relatively small, large-diameter rotors of transparent materials may be considered. Rotor A-V has therefore been constructed of methacrylate resin. The rotor is shown diagrammatically in Fig. V-A-1.

The interior is divided into eight sector-shaped compartments, each 2.72 cm deep, with maximum and minimum radii of 13.60 and 3.49 cm. The upper and lower end plates are of 3.26-cm-thick clear plastic. The internal volume is 1300 ml.

All parts of a zone of one density in a zonal centrifuge constitute a paraboloid of revolution about the axis of rotation. A single conical-section core, therefore, has been used which allows the sample layer to slope 45° or more as it approaches the rotor center. The rotating seal was constructed of filled Teflon while the static fluid-line seal was made of stainless steel and was flexibly mounted to allow alignment with the rotating seal during operation. Chilled water was circulated through the upper seal to remove frictional heat.

Water was added to the rotor in 100-ml increments and the position of the meniscus carefully determined at 1000 rpm. From this data, a chart of volume as a function of radius was drawn. The position of any portion of the gradient recovered during unloading could then be related to its original position in the rotor. All work was performed in an International Equipment Co. Model PR-2 Refrigerated Centrifuge with a transparent plastic lid.

---

[1] N. G. Anderson and C. L. Burger, *Science* 136, 646–48 (1962).

[2] N. G. Anderson, *J. Phys. Chem.* 66, 1984–89 (1962).

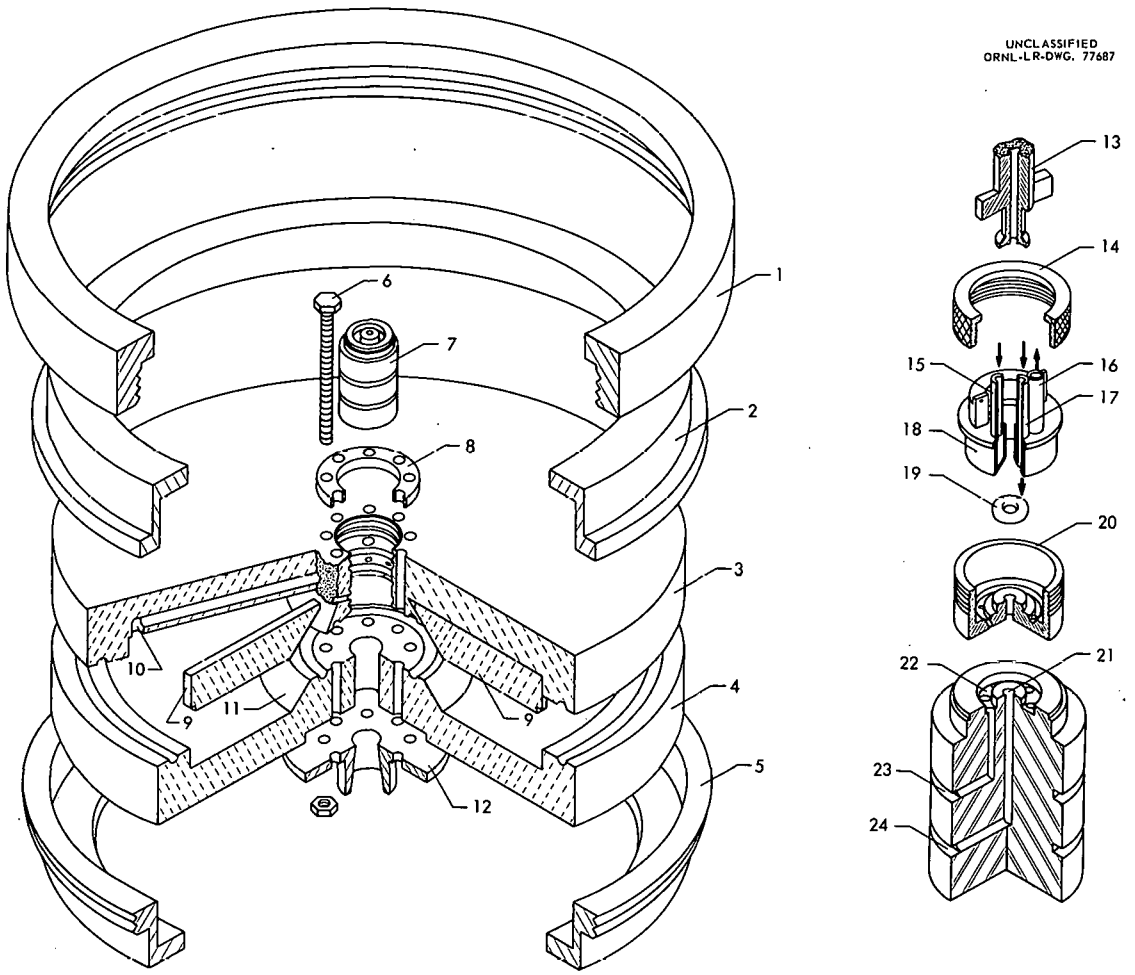

Fig. V-A-1. Schematic Drawing of Rotor A-V. (1) Coupling ring; (2) upper retaining ring; (3) upper end plate; (4) lower end plate; (5) lower retaining ring; (6) retaining bolts; (7) filled Teflon rotating seal; (8) bolt locating ring; (9) septa; (10) fluid line to edge of rotor; (11) conical-section core; (12) drive shaft adapter; (13) stationary seal flexible mount and fluid line to center of rotor; (14) stationary seal coupling ring; (15) coolant inlet; (16) coolant outlet; (17) fluid line to edge of rotor; (18) cooling jacket; (19) "O" ring; (20) stationary seal; (21 & 24) flow passage through rotating seal to center of rotor; (22 & 23) flow passage through rotating seal to edge of rotor.

2. Performance

To determine whether density gradients could be introduced into the rotor and recovered without extensive mixing, a density gradient was analyzed refractometrically both before introduction and after spinning in the rotor for 15 min at 1000 rpm. Negligible differences between the two gradients were seen.

A sample zone introduced into the rotor is widened by laminar flow through the tubing and rotor core, by any turbulence or convection in the rotor, and by diffusion. To determine how much widening would occur in practice, a sample zone containing 4% bovine serum albumin (BSA) having a total volume of 20 ml was introduced over a sucrose gradient. When moved to a position just external to the core, the sample zone should have a calculated width of 0.1 cm. The rotor was spun 20 min at 1000 rpm at 5°C ($152 \times g$ at

R_{max}, 39 × g at R_{min}). When the gradient was recovered, the absorbance recording of the sample zone showed a peak whose width at half-height was equivalent to a zone width of 0.3 cm in the centrifuge. This amount of broadening is not considered excessive.

Three types of experiments were performed to determine the resolution obtainable with the rotor. In the first, ragweed pollen grains were used to form a sharp band at their isopycnic point; in the second, the sedimentation of rat red blood cells was followed. In the third series of experiments (Section XI, A), a method for isolating calf thymus nuclei that retained their ability to incorporate amino acids was developed.

Preliminary experiments with ragweed pollen suggested that more uniform behavior could be obtained if the grains were first fixed in alcohol. Two hundred mg of pollen, therefore, was suspended in 10 ml of 95% ethanol, centrifuged briefly, and the pollen resuspended in 10 ml of 8.5% sucrose. This volume of material was used as the sample layer and was introduced centripetally to a 1200-ml gradient extending from 17% to 55% (w/w) sucrose. Fifty-five percent sucrose was also used as the "cushion" outboard of the gradient. After 10 min at 1000 rpm the gradient was displaced with 55% sucrose through the core and the monitoring system, and into 40-ml collecting tubes. Photographs of the rotor during the run are shown in Fig. V-A-2. The fractions were examined by dark field phase-contrast microscopy. No particles were observed through the gradient except at the level of the zone, shown in Fig. V-A-2.

Additional experiments with rat red cells are shown in Fig. V-A-3. When the cells reached their isopycnic position, two bands have been obtained repeatedly. The basis of this fractionation is now under investigation.

Separations of mitochondria from rat liver have also been made in rotor A-V. However, because of its very low operating speed, 8- to 10-hr runs are required.

The results reported here indicate that the principles previously employed in the zonal ultracentrifuge[1,2] can be applied to large particles in a low-speed rotor.

B. ROTOR A-VI

H. P. Barringer C. E. Nunley

Rotor A-VI is the largest zonal centrifuge rotor presently contemplated. It is designed to explore large-scale nuclear isolation and the separation of different cell types in a mixture as occurs, for example, in bone marrow cell suspensions.

1. Design and Performance

Rotor A-VI has a 3-liter capacity, is designed for operation at 6000 rpm and a maximal centrifugal force of 7100 × g. The design specifications were fixed by the speed, permissible diameter, and thrust bearing capacity of the International Model PR-2, which was used to drive the rotor. The design is not an optimum one from the point of view of the strength of the rotor material (7075-T6 aluminum). The partially disassembled rotor is shown in Fig. V-B-1, while the rotor and seal system assembled for use are shown in Fig. V-B-2.

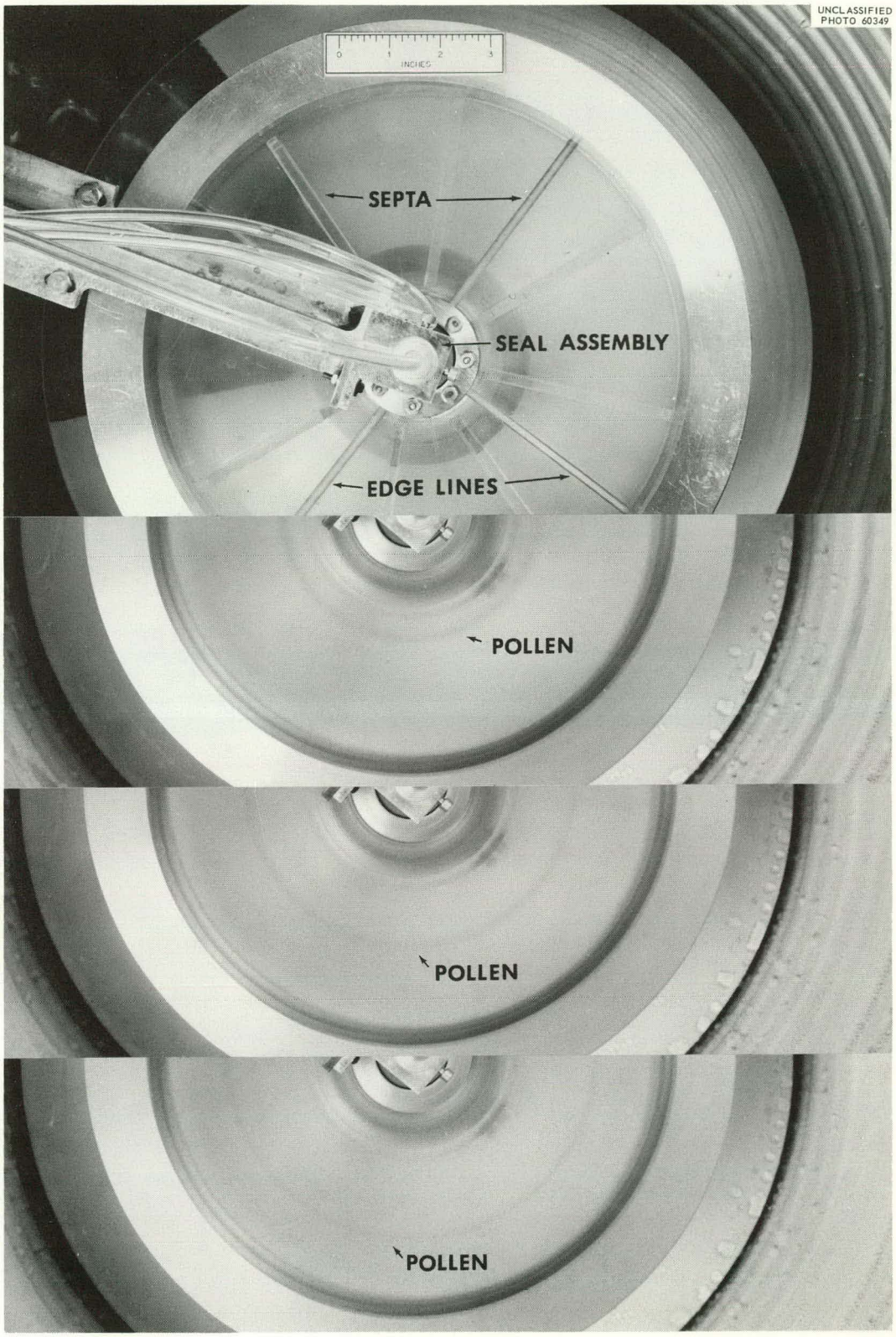

Fig. V-A-2. Sedimentation of Ragweed Pollen in Rotor A-V.

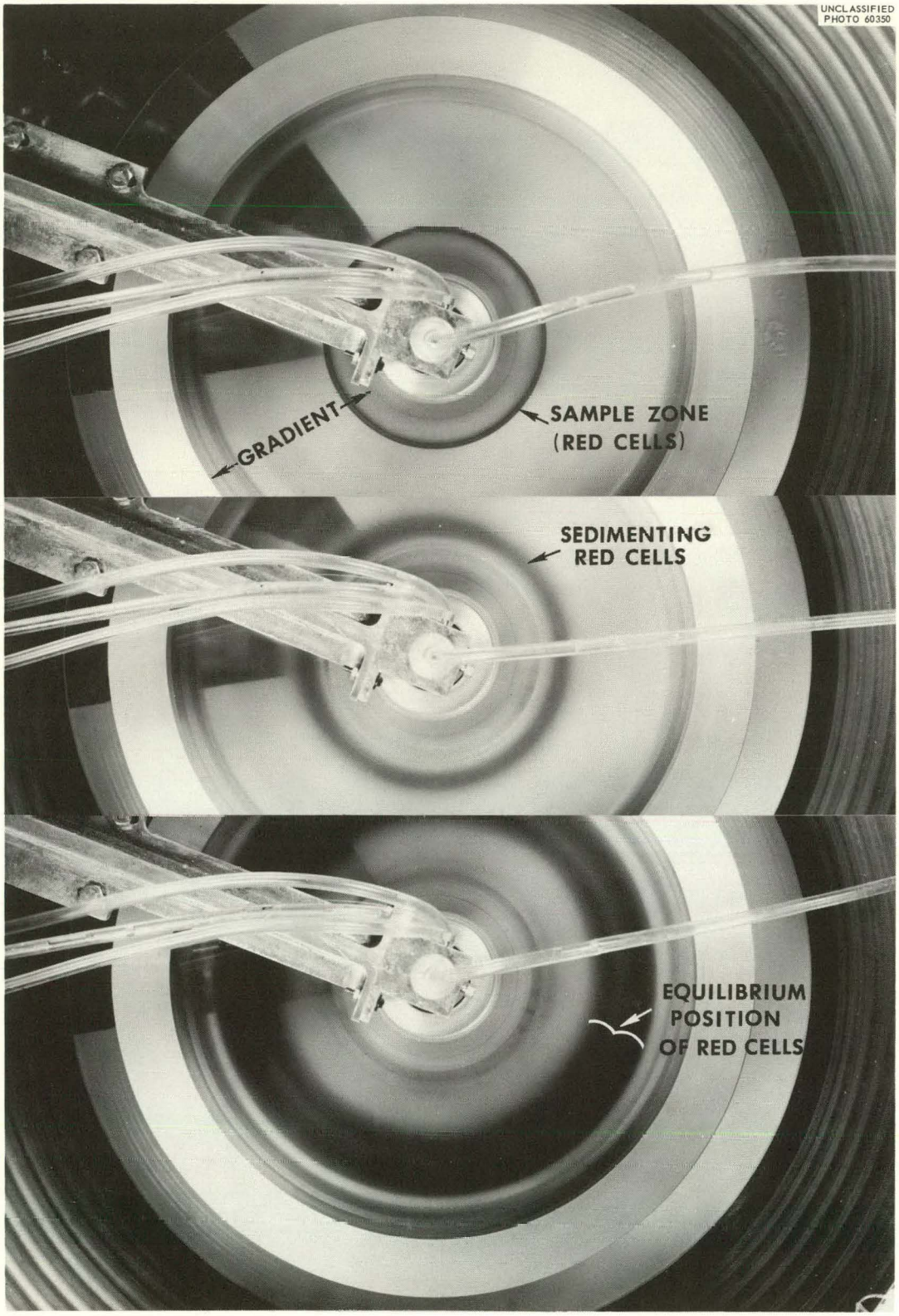

Fig. V-A-3. Separation of Rat Red Blood Cells in Rotor A-V.

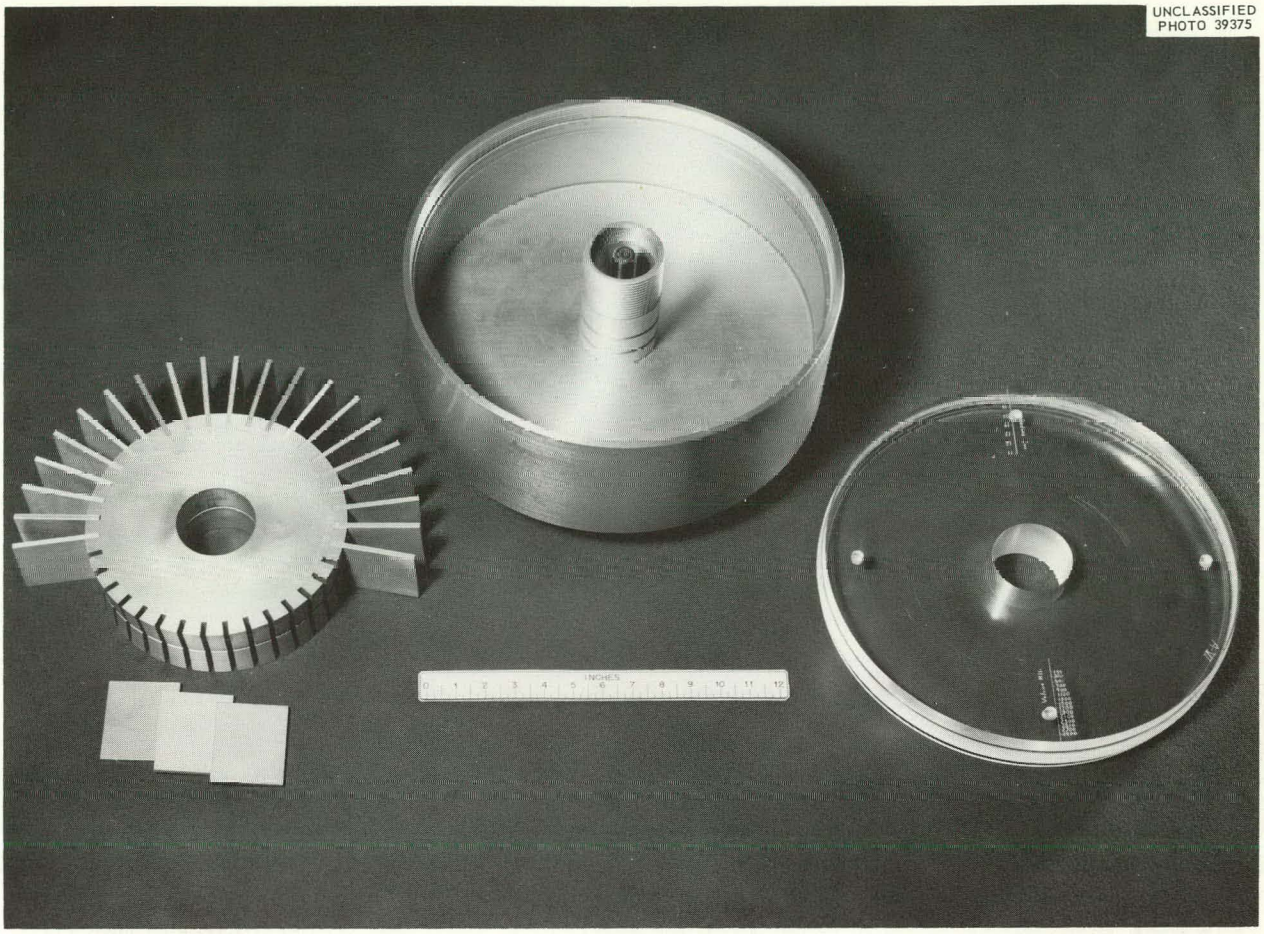

Fig. V-B-1. Rotor A-VI Partially Disassembled. Core with septa shown at left, main body of rotor in center, with transparent upper end plate at right.

The initial intent was to provide a fairly uniform centrifugal field by using a large-diameter central core to keep the entire gradient close to the rotor edge. The length was held to a minimum to give a ratio of $I_{spin}/I_{transverse} > 1$ for the moments of inertia, thus providing a configuration which spins about its most stable axis. The central core diameter is 9 inches and the inside diameter is 14 inches, giving a gradient chamber length of $2\frac{1}{2}$ inches. At the design speed of 6000 rpm with a sucrose density gradient in position, a rather large radial growth (approximately $\frac{1}{64}$ inch) occurs. Since the end caps increase in diameter by only a few thousandths of an inch, a mechanism was needed to center the rotor chamber wall with the end caps, and maintain concentricity to the drive spindle. Plated brass plates (one in each end cap), which expanded during centrifugation at a rate intermediate between that of the rotor wall and the end plates, were employed. Without the brass plates the run-out (departure from circularity) increased from the normal 0.004 in. total indicator reading (TIR) to 0.010 in. TIR, demonstrating the effectiveness of the brass plates.

By very accurate machining, the necessity of balancing the rotor has been obviated. The only metals in contact with fluid are anodized aluminum, nickel, monel or stainless steel. "O" rings are used to seal the rotor chamber and all components in the liquid lines.

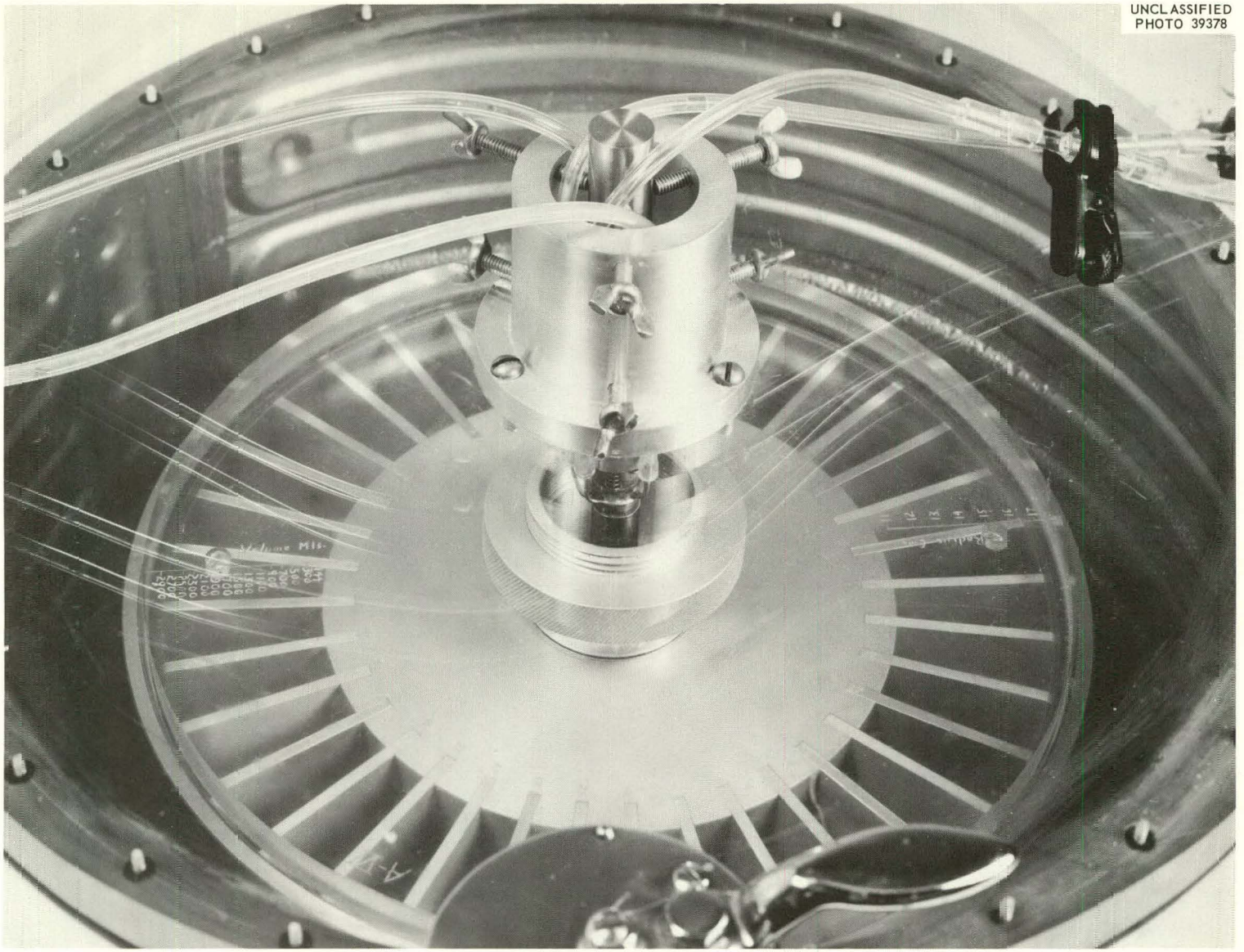

Fig. V-B-2. Rotor A-VI and Seal Assembly Mounted in PR-2 Centrifuge. The rotor is visible during operation through the plastic top of the centrifuge.

Three methods have been investigated for obtaining flow into and out of the centrifuge at operating speed. The first skimmers used[3] did not prove to be successful at the relatively low peripheral speed at the edge of the skimmer discs. As a second approach, a self-aligning ball-and-socket rotating seal was tested. This seal was ineffective because of distortion of the ball during attachment to the drive and to cold-flowing of the reinforced Teflon of the static seal when under pressure. A third, flat modified face seal has proven effective.

One top-end cap for rotor A-VI has been fabricated from Lucite to permit viewing of the rotor contents completely across the rotor diameter. At the center of the rotor, a large nut limits deflection of the cap and reduces the stress level. With a stroboscopic light the rotor contents can be observed in detail.

Power limitations of the PR-2 drive motor have restricted the top test speed in practice to 5160 rpm. Critical speeds of the spindle system which occur at 700 to 900 rpm have been passed with no difficulty.

At the end of this report period, studies using biological materials had just begun. It is contemplated that rotor A-VI will be extremely useful for the isolation of nuclei, amphibian egg yolk platelets, paramylum granules, and for the separation of cells differing in size or density. The possibility of separating sperm on the basis of whether they contain X or Y chromosomes is also being considered.

C. ROTOR A-VII

N. G. Anderson C. A. Price R. E. Canning

1. Design

To test the reorienting gradient concept outlined in Chapter III-B, a small methacrylate rotor, shown diagrammatically in Fig. V-C-1, was built and mounted in a brass holder attached to a heavy flywheel rotor as shown in Fig. V-C-2. The large mass allowed smooth, controlled acceleration and deceleration in the International PR-2 Centrifuge. This rotor, designated rotor A-VII, has a capacity of 127 ml. The gradient, when reoriented vertically during rotation, is 1.27 cm thick.

2. Performance

To test the rotor, 27 ml of a pH 7.5 sodium phosphate-NaCl buffer, $\mu = 0.1$ (ref 4) was pipetted to the bottom of the rotor at rest. An 80-ml linear density gradient was formed using a two-cylinder gradient apparatus, and was pumped to the bottom of the rotor using a Technicon proportioning pump with a flow rate of 1.89 ml/min. The gradient extended from 17% to 60% (w/w) sucrose. A 20-ml underlay of 60% sucrose was pumped in after the gradient. After 15 min the gradient was pumped out of the rotor from the bottom using the same pump and flow rate, and was collected in 5-ml volumes. The same experiment was performed with the rotor slowly accelerated to 3000 rpm, and decelerated to rest over a 15-min interval. The gradients

---

[3] N. G. Anderson, *Anal. Chem.* 33, 970–71 (1961).

[4] G. L. Miller and R. H. Golder, *Arch. Biochem.* 29, 421 (1950).

Fig. V-C-1. Drawing of Rotor A-VII. The hollow interior is divided into four sector-shaped compartments by vertical septa. The shallow conical bottom extends below the septa. Filling and emptying is through a narrow tube inserted through the top opening to the bottom of the rotor. At 3000 rpm the gradient extends from the edge of the rotor only as far in as the edge of the center upper hole. The gradient does not, therefore, completely fill the rotor at rest. A rubber stopper is inserted to minimize effects of air friction during operation.

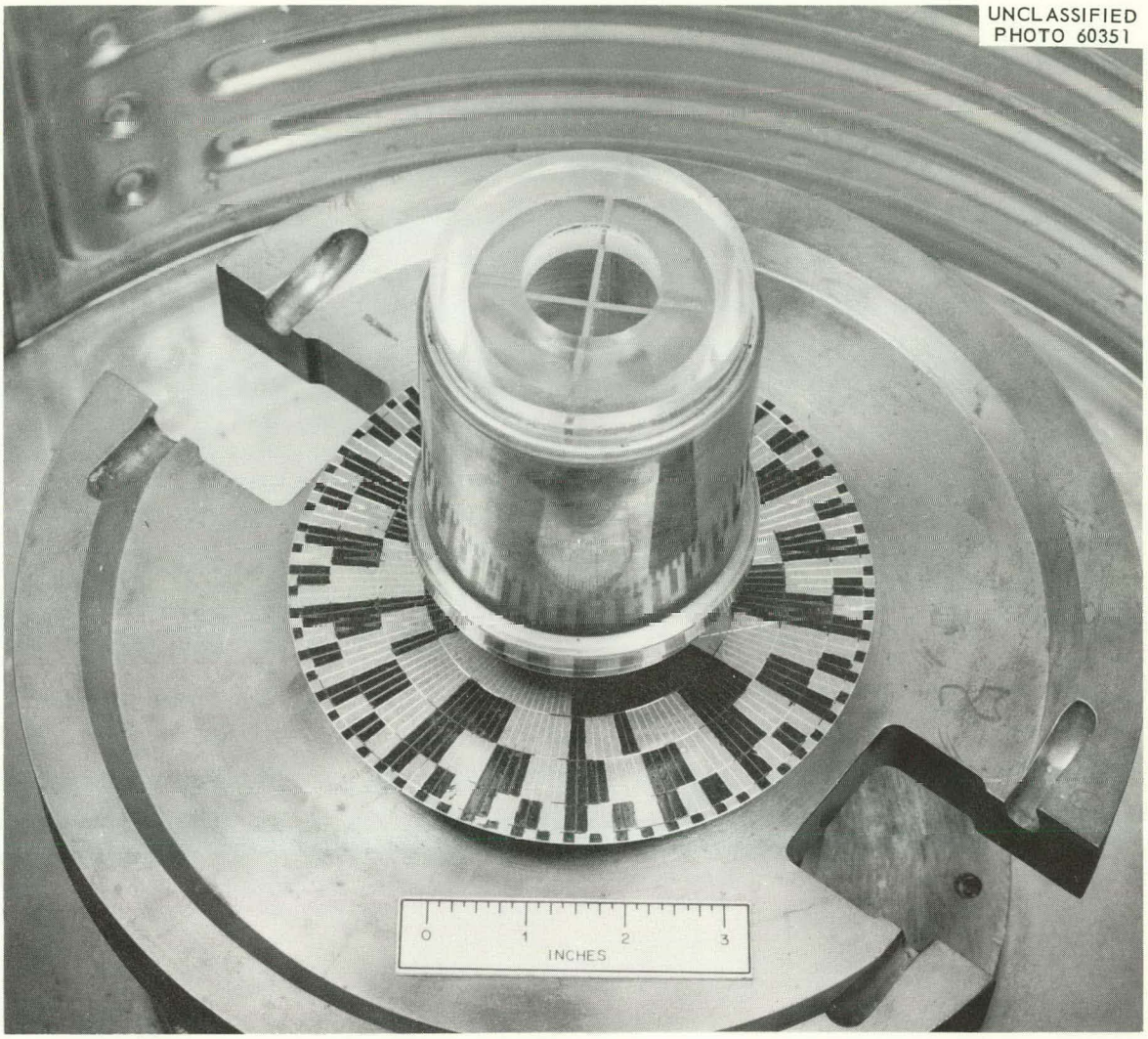

Fig. V-C-2. Complete A-VII Rotor Assembly.

were analyzed for sucrose content refractometrically, and the results are recorded in Fig. V-C-3. It is evident that very little disturbance in the gradient occurred during the transition from rest to 3000 rpm and back to rest.

To determine whether a sample zone could be maintained in position during the rest-to-rotation transition, 1 ml of an 8% solution of bovine serum albumin was introduced to the bottom of the rotor between the overlay and the sucrose gradient. After acceleration to 3000 rpm and deceleration to rest over a 15-min period, the rotor contents were pumped out through an ultraviolet absorption analyzer, which was set at 280 mμ with a 0.2 cm light-path flow cell.[3] The results, replotted in terms of rotor radius with the rotor volume also included, are shown in Fig. V-C-4. The sample introduced had a calculated width of approximately 0.1 mm. After acceleration to 3000 rpm and deceleration to rest, the width of the sample peak at

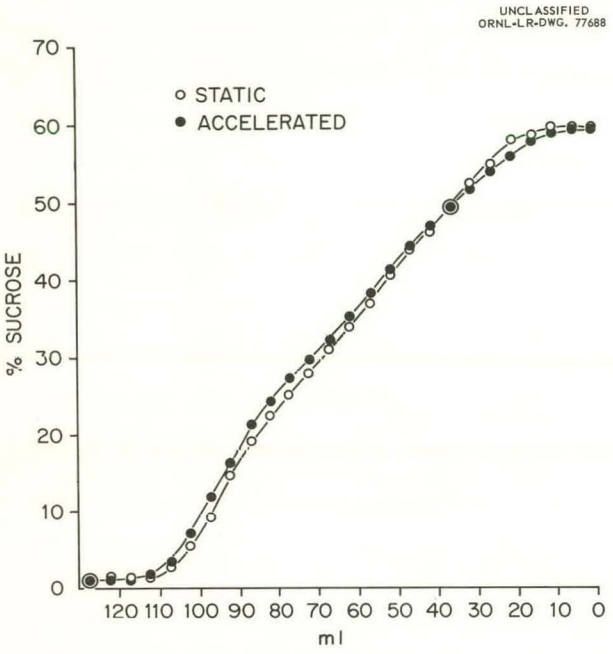

Fig. V-C-3. Analysis of Density Gradients Recovered from Rotor Filled and Emptied at Rest, and Rotor Accelerated to 3000 rpm Between Filling and Emptying.

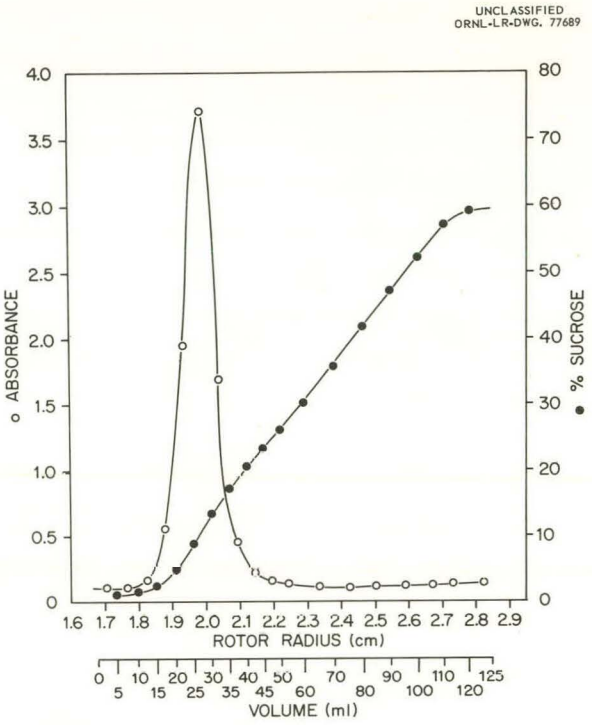

Fig. V-C-4. Stability of Sample Layer During Acceleration to 3000 rpm and Deceleration to Rest. The sample layer was 1.0 ml of 8% BSA layered over a sucrose gradient.

half-height as observed by the monitoring system was 1.0 mm. This amount of broadening, which is probably due to both diffusion and laminar mixing in the fluid lines, is not prohibitively large for the purposes described.

To see whether a zone of material banded sharply further down the gradient could be recovered with good resolution, 40 mg of ragweed pollen in 2 ml of 8% sucrose was used as the sample layer. The experimental conditions were identical with those described for the BSA experiment. After deceleration from 3000 rpm to rest, the absorbance at 280 mμ and the sucrose concentration were determined as shown in Fig. V-C-5. A clear yellow pigment released from the pollen grains accounted for nearly all of the absorbance in the region of the starting zone. Extraction of the pigment from the pollen grains as they sedimented through the gradient probably accounts for the skewed tail observed in the starting zone curve. A small number of pollen grains were found through the starting zone. These may have been cells that had begun to swell in the sucrose solution. The majority of the cells banded in a narrow zone at the 43% (w/w) sucrose level. The width of the peak at half-height corresponds to a zone thickness of 0.87 mm in the rotor during rotation. In these experiments the pollen was not treated with alcohol, a procedure that is generally done when the grains are used as standards for particle counters.

Since the diameter of a high-speed rotor is determined and limited by the strength of available materials, large rotor capacity can only be obtained by using elongated cylindrical configurations. A zone occupying a narrow band in the density gradient during rotation will, when the rotor is returned to rest, be physically thicker as its cross sectional area is decreased. This is true even though the zone occupies the same volume of fluid during rotation and at rest. Band-widening by diffusion and by laminar mixing along the wall during unloading, therefore, is minimized.

In these experiments, the density gradients have been preformed. It is evident that reograd rotors may be used with preformed gradients for separations based either on sedimentation rate or on density alone by isopycnic banding, or that the gradients for the latter type of separation may be formed in the rotor by the centrifugal field.

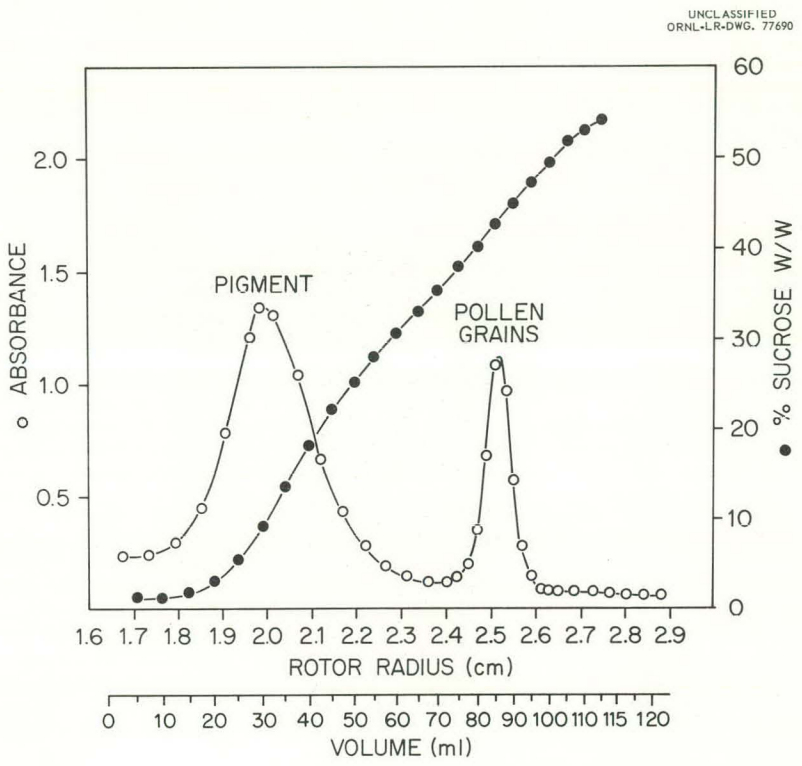

Fig. V-C-5. Banding of Ragweed Pollen Grains in a Sucrose Gradient.

VI. Intermediate-Speed Zonal Rotors

A. ROTOR B-I

N. G. Anderson

Rotor B-1 (Fig. VI-A-I) was constructed under the original Union Carbide-Spinco contract and proved to be very unstable during tests. Study of this rotor is continuing under this program because the radius and capacity are those of choice for biological studies. If the reasons for instability can be fully understood, many difficulties in future designs will be avoided.

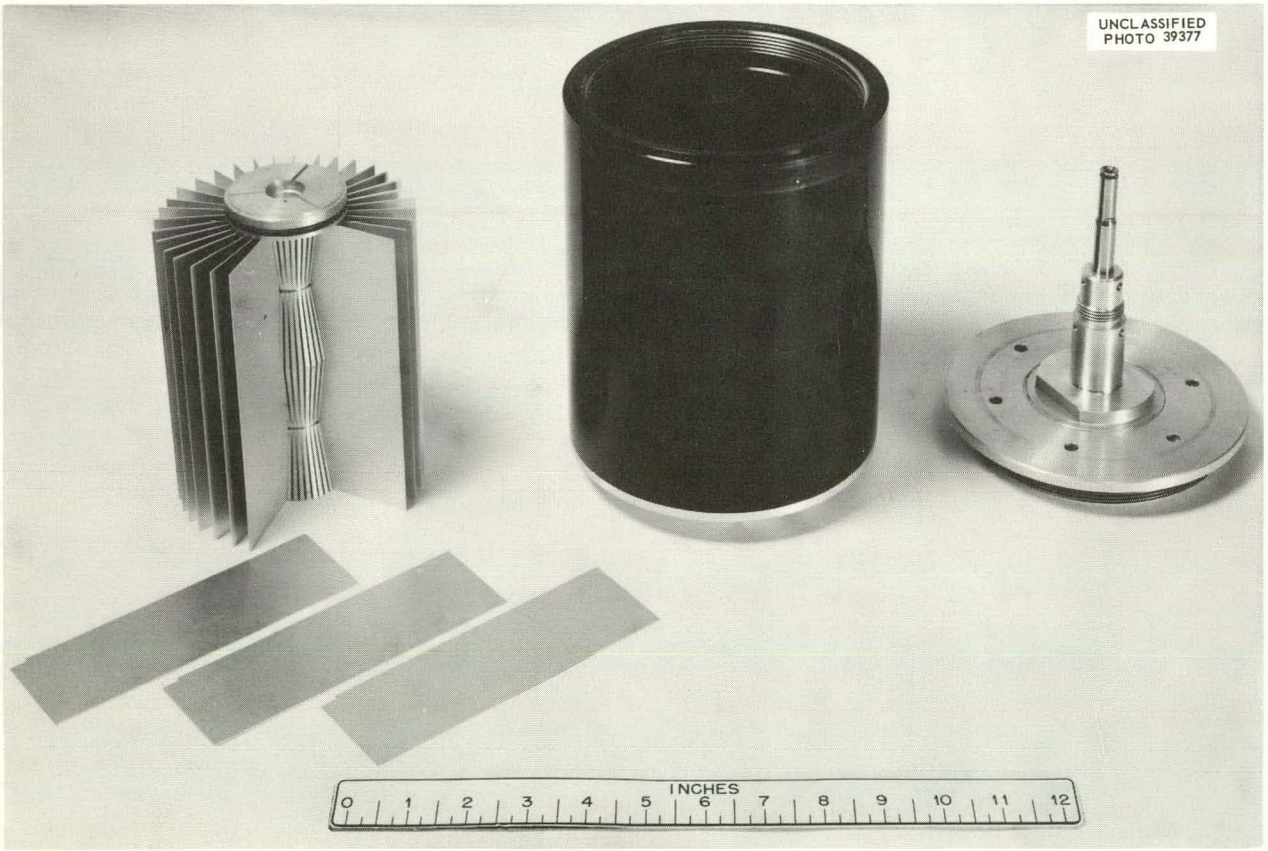

Fig. VI-A-1. Rotor B-1. Core and septa are shown on the left, rotor chamber in center, and the upper end cap and upper shaft on the right.

B. ROTOR B-II

N. G. Anderson

1. Description of the Rotor

The greater part of the experimental work done with biological materials during this report period has been done with the intermediate-speed B-II zonal rotor. Details of the construction and operation of this rotor are given since these have not all been published. Representative separations are presented here.

The rotor is shown in an isometric projection in Fig. VI-B-1. The rotor chamber is 25.72 cm long, with an inside diameter of 10.16 cm and a wall thickness of 1.27 cm. The rotor is driven from below by a Spinco Model L preparative ultracentrifuge drive. This arrangement necessitates making the fluid line connections at the top. An upper bearing is also used to center the rotor and to provide a vacuum seal.

The total internal volume of 1625 ml is divided into 36 sector-shaped compartments by thin aluminum septa that fit into slots in the rotor core. The stainless steel upper shaft is hollow and contains a small, additional center tube. Fluid may be pumped into and out of the rotor through either the small center tube or in the annular space between the center tube and the hollow upper shaft.

The center line in the upper shaft connects to the rotor wall through six horizontal channels in the upper rotor end caps. The outer line in the upper shaft connects to the central rotor core. The upper shaft ends in a flat face seal made of Teflon filled with a metallic oxide. It presses against a flat, static seal of aluminum coated with tungsten carbide. Both the upper seal and the upper bearings are cooled by circulating cold water.

It is essential in high-resolution work to eliminate as far as possible tangential flow in the rotor due to Coriolis forces. Fluid flowing to the rotor edge must be suitably channeled to accelerate it to the tangential velocity obtaining at the edge of the fluid chamber. Similarly, as the gradient is displaced in toward the core during unloading, it is greatly decelerated. In the absence of vertical septa, the energy involved will be dissipated as heat in the process of swirling the rotor fluid. A steep gradient may withstand the resulting laminar flow without complete mixing, but considerable resolution will be lost. Compartmentalization of the rotor is, therefore, considered important and contributes greatly to rotor stability.

The upper static seal must be held against the rotating seal to prevent leakage. Rather than keep the seal at all times under the maximum pressure required during the loading and unloading procedure, a double-chambered pressurizing cylinder is used which exerts a force on the seal proportional to the pressure in the fluid lines. The line from the gradient engine enters the lower of the two cylinder chambers before flowing through the seals and into the rotor. To minimize the length and hold-up volume of the line leading to the rotor core, through which the sample is introduced and the separated zones recovered, the center line does not flow to the pressurizing cylinder. Instead, the nitrogen gas line used to force the sample into the rotor is attached to the upper chamber of the seal pressurizing cylinder.

The core (Fig. VI-B-2) is doubly constricted to guide each zone in the density gradient out of the rotor with a minimum of laminar mixing owing to vertical flow along the core.

The vertical septa are inserted in vertical slots in the core and are supported by the rotor chamber during rotation. The assembled core is positioned in the rotor as shown in Fig. VI-B-3. The assembled rotor is shown in Fig. VI-B-4.

Fig. VI-B-1. Cutaway Drawing of Zonal Ultracentrifuge Rotor. Note divisions of internal volume into sector-shaped compartments by vertical septa, central collecting core, and coaxial lines leading to upper seal.

1. Tubular rotor wall
2. Lower rotor cap
3. Upper rotor cap
4. Rotor core
5. Septa
6. Fluid line crossover
7. Upper rotor shaft
8. Center upper fluid line
9. Upper bearing
10. Coolant lines
11. Oil line
12. Rotor chamber top
13. Upper bearing housing
14. Rotating seal cup
15. Rotating seal
16. Upper static seal
17. Fluid line leading to rotor center
18. Fluid line leading to rotor edge
19. Seal pressurizing cylinder
20. Fluid line to rotor center running through pressurizing cylinder
21. Fluid line to rotor edge running through pressurizing cylinder
22. Fluid line opening at rotor edge
23. Fluid line opening in central core

From N. G. Anderson, *J. Phys. Chem.* 66, 1984 (1962).

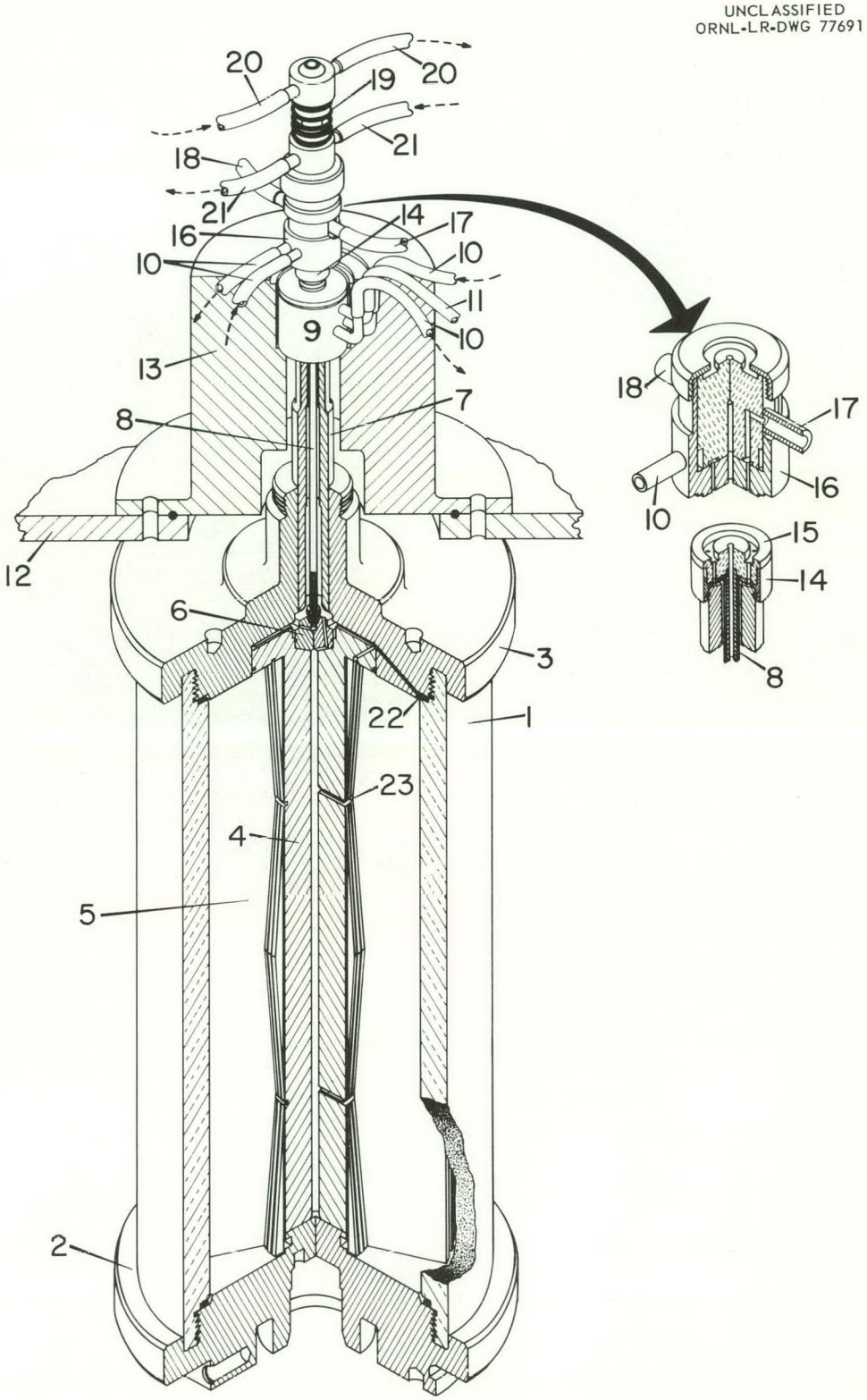
UNCLASSIFIED
ORNL-LR-DWG 77691
20
19
20
21
18
21
14
17
16
10
10
11
9
10
13
7
8
12
6
3
22
1
23
4
5
2
18
17
16
10
15
14
8

Fig. VI-B-1

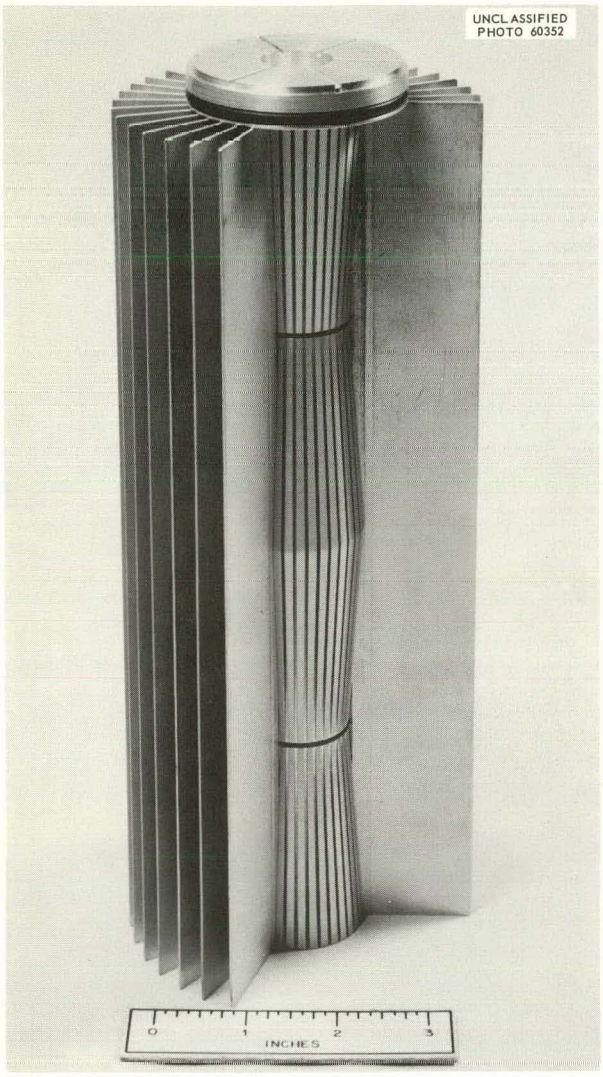

Fig. VI-B-2. Partially Assembled Core of Rotor B-II.

Fig. VI-B-3. Core Inserted in Rotor Casing of Rotor B-II.

In operation, the centrifuge is surrounded by a group of instruments (Fig. VI-B-5), including the gradient engine (Fig. VI-B-6), and analytical devices (Chapter XV) for measuring in the gradient as it is recovered – ultraviolet absorption, total protein, radioactivity, and enzymic activity.

2. Operation of the Centrifuge System

The empty, prechilled rotor is accelerated to 3000 rpm *in vacuo* and is then filled with the density gradient. This is done by pumping a 1200-ml gradient to the rotor wall, light end of the gradient first using a four-piston gradient engine. The gradient most generally used for tissue fractionation ranges from 17 to 55% sucrose (w/w). For virus and ribosome fractionation a 12 to 30% sucrose gradient is employed. After the gradient is in the rotor, a "cushion" of concentrated sucrose (55 or 66%) is pumped to the rotor edge

Fig. VI-B-4. Assembled Rotor B-II with Upper Bearing and Static Seal in Place.

until the light end of the gradient begins to flow out of the core exit line, indicating that the rotor is completely full. During filling, the connection to drain between the seal pressurizing cylinder and the gradient pump is kept closed. The sample (generally 12.5 ml) is placed in chamber 1 of the sample gradient system and an equal volume of 8% sucrose is placed in chamber 2. The connections between chamber 1 and 2 are then opened, and the linear sample gradient allowed to flow into the sample and overlay container. The sample gradient is then moved into the rotor after the connections to the sample gradient system and the monitoring systems have been closed. Introduction of the sample into the spinning rotor causes part of the cushion to be displaced out of the rotor through the edge line. This displaced fluid is allowed to flow out.

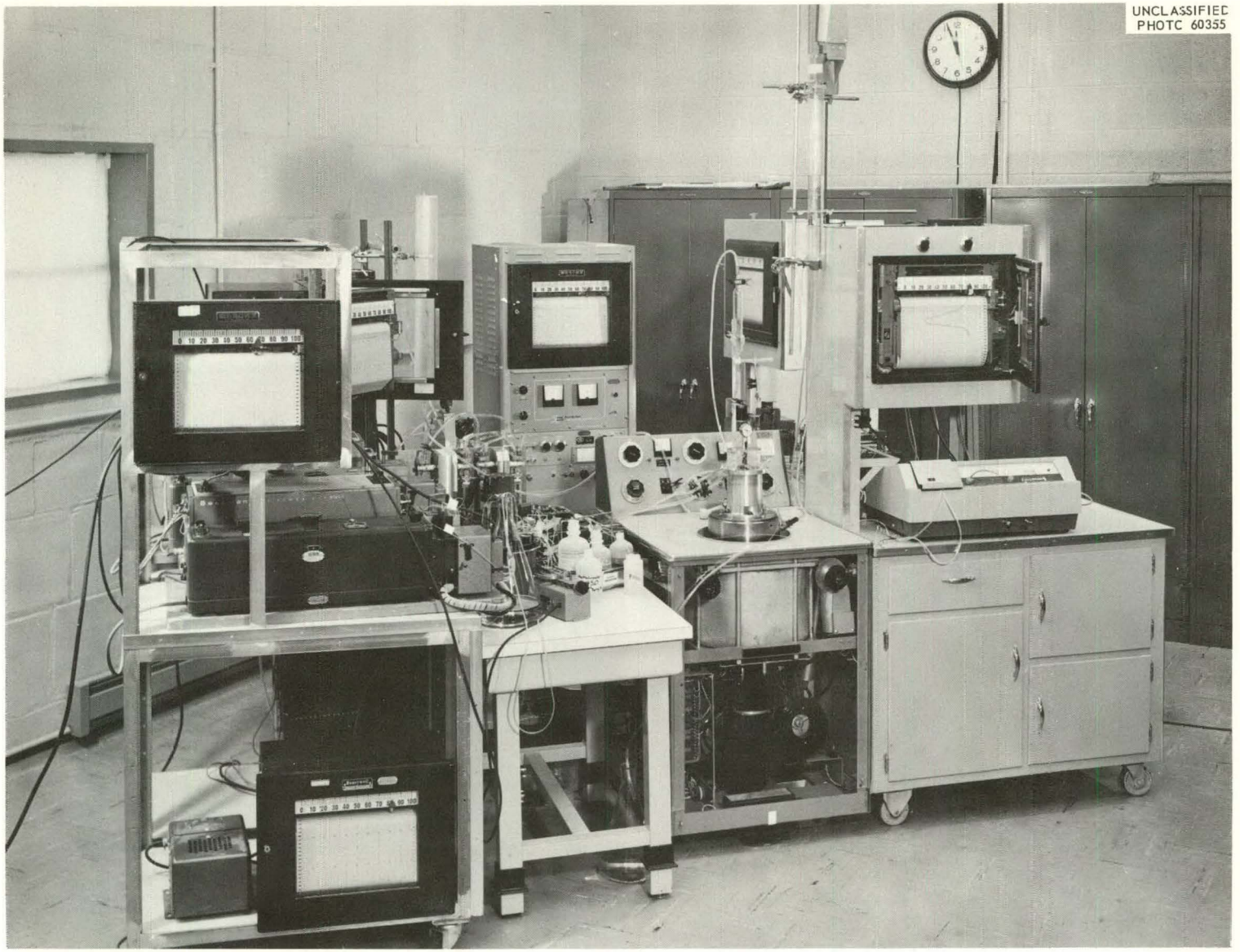

Fig. VI-B-5. Completed B-II Zonal System with Auxiliary Automated Analytical Units. Centrifuge is in center right, ultraviolet monitor on right, uricase system in front left, acid phosphatase system in rear right, and radioactivity monitoring unit in rear center.

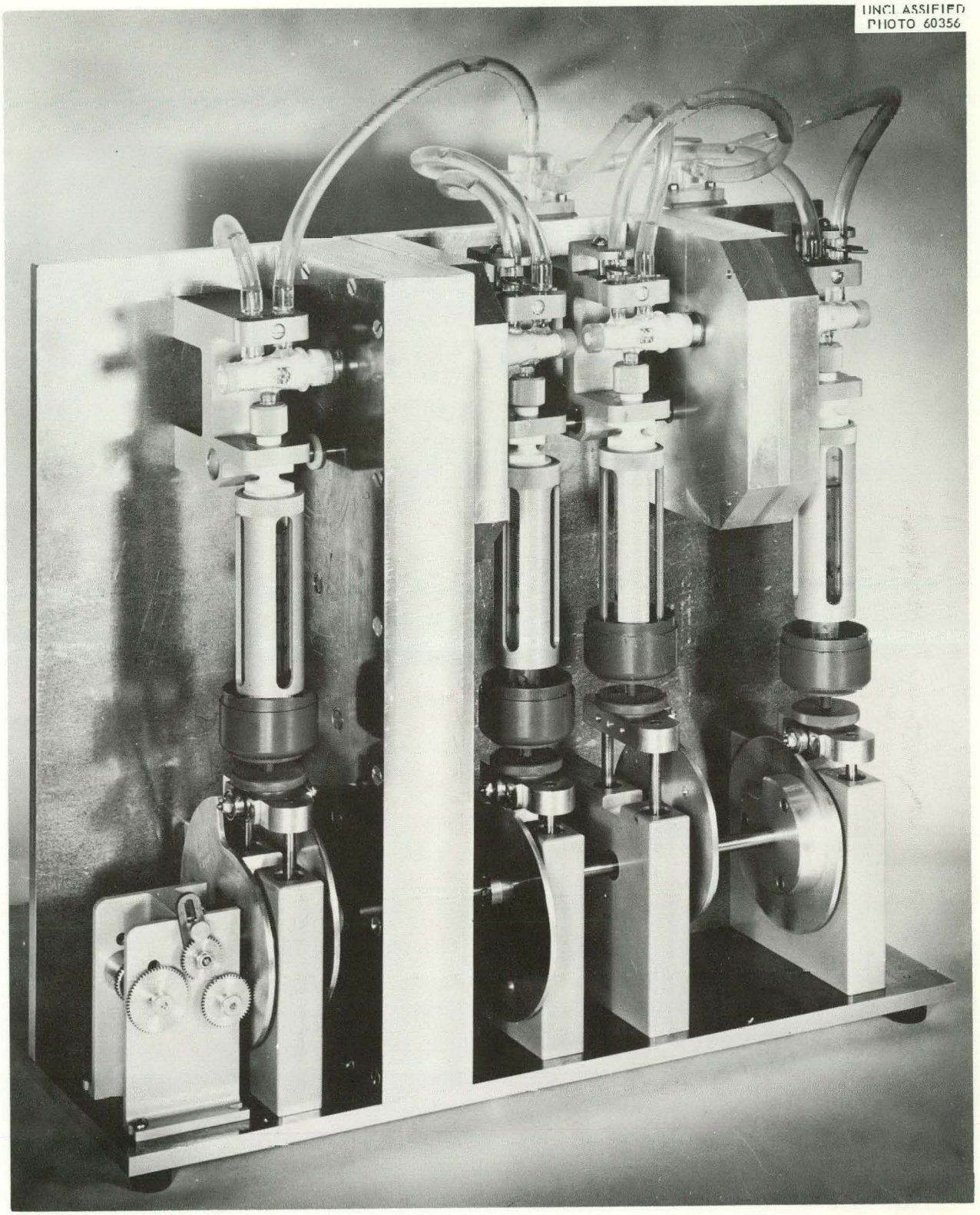

Fig. VI-B-6. Four-Piston Gradient Engine for Zonal Centrifuge.

When the sample container has been emptied, the nitrogen pressure is released and the container is filled with the light overlay fluid (100-300 ml). This is also moved into the rotor under pressure.

Any air now trapped in the rotor should be removed. When the sample and overlay container is empty it is filled with distilled water to a mark, and about 30 ml forced into the rotor with nitrogen pressure. As this is being done, the gradient engine is started pumping 55 to 66% sucrose, which passes down the drain line along with part of the cushion being displaced out of the rotor. At this moment the nitrogen pressure is released and the drain line closed, forcing the distilled water back into the sample container. This flow is continued until the distilled water level has returned to the mark. The gradient engine is then stopped and the lines to the rotor edge closed. The line from the sample chamber is kept open during operation so that fluid may flow into the rotor during acceleration to compensate for rotor expansion.

The centrifuge is then accelerated to operating speed (up to 30,000 rpm). After the desired separation has been completed, the centrifuge is decelerated to 5000 rpm, and the gradient displaced out through the center core by pumping 55 or 66% sucrose to the rotor edge. The line to the sample and overlay container is closed and the recovered gradient allowed to flow through the ultraviolet monitor and the proportioning pump to the several automated analytical systems. In most instances, forty 40-ml fractions are collected.

3. Fluid-Line Seals

The fluid-line seals presently used in the B-II rotor system are satisfactory for most operations. However, for work with pathogenic viruses it is imperative to eliminate any leakage into the atmosphere. A variety of seals and seal configurations are being explored with the aim of developing a suitable biologically tight seal system.

A seal test system with an electrically driven spindle operating at speeds up to 80,000 rpm has been constructed which is capable of sustaining the axial loads normally required for liquid seals.

Flat-face seals using an impregnated fluorocarbon runner and a hardened 440 stainless steel runner have been constructed and tested. The entire seal is encased to provide a buffer cavity for a disinfectant to inactivate any virus particles that may leak out between the seal faces. The performance requirements for the seal are (1) minimum leakage of sample or gradient fluid out between the seal faces during operation, (2) complete elimination of leakage of the live virus out of the seal enclosure, (3) no in-leakage of the disinfectant solution into the rotor or fluid line, and (4) a reasonable operating lifetime.

Experiments to date suggest these requirements can be met.

4. Performance

a. Sample Zone Thickness. – To see whether a concentrated sample layer maintains its position in the centrifuge, we layered a sample gradient (made from 10 ml of 8% bovine serum albumin in distilled water and 10 ml of 17% sucrose) over a 1200-ml gradient varying linearly with rotor radius from 17 to 55% sucrose (w/w). After the sample was introduced, the rotor was accelerated to 25,000 rpm for 5 min, decelerated to 5000 rpm, and unloaded. The ultraviolet absorbance of the effluent stream was recorded and the results were recalculated in terms of the rotor radius. The sample zone at a radius of 25.3 mm would be

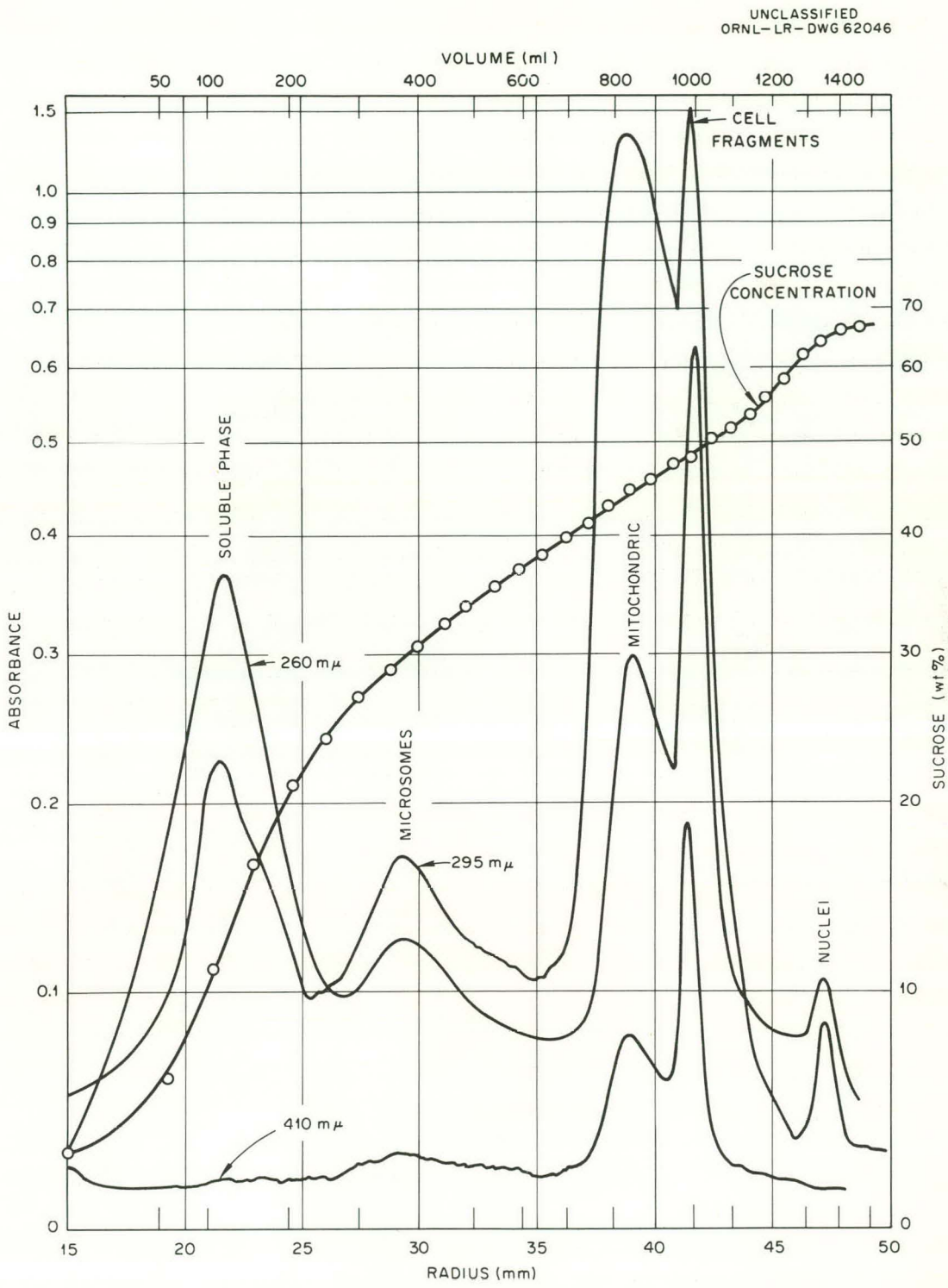

Fig. VI-B-7. Fractionation of Rat Liver Brei Obtained at 19,500 rev/min in 3 Hours. Recordings at 2600 and 4100 A were made after dilution (in a continuously flowing system) with an alkaline buffer (pH 10). The recording at 2950 A was made directly (without dilution) on the gradient flowing out of the centrifuge and through a quartz flow cell. (Anderson and Burger, *Science* **136**, 646, 1962; Reprinted from *Science* by permission.)

0.65 mm thick if no mixing or diffusion occurred. The peak recovered had a width of 1.6 mm at half-height, indicating that only a small amount of band-spreading had occurred, due in part to the fact that the core used assumed vertical zones.

b. Tissue Profiles. – The separation obtained with a brei (25%, w/v) of perfused rat liver in 8.5% sucrose is shown in Fig. VI-B-7. The nuclei which are free of cytoplasmic contamination are in the zone marked "nuclei," whereas nuclei associated with cytoplasmic "tabs" or in whole cells appear just to the right of the level marked "cell fragments." After more prolonged centrifugation (4 hr at 20,000 rev/min), the nuclei are more sharply banded away from the "cell fragments" or membrane fraction. The results of enzymatic studies on these fractions will be reported elsewhere. While much theoretical and experimental work remains to be done before optimal fractionation conditions are achieved, these results suggest that quantitative separations of gram quantities of tissue can now be achieved.

c. Ribosome Separations. – Rapidly growing *Escherichia coli* cells were chilled, concentrated by centrifugation, and broken in a constant pressure French press. The ribosomes were concentrated by centrifugation and resuspended in 0.01 *M* $MgCl_2$-Tris Cl (pH 7.5) buffer, and layered over a 10-30% sucrose gradient in Rotor B-II. The rotor was run at 24,600 rpm for 6 hr and then unloaded. The results are shown in Fig. VI-B-8. The results agree extremely well with the pattern obtained in the analytical ultracentrifuge. This work opens up many new possibilities in the biophysical study of ribosomes.

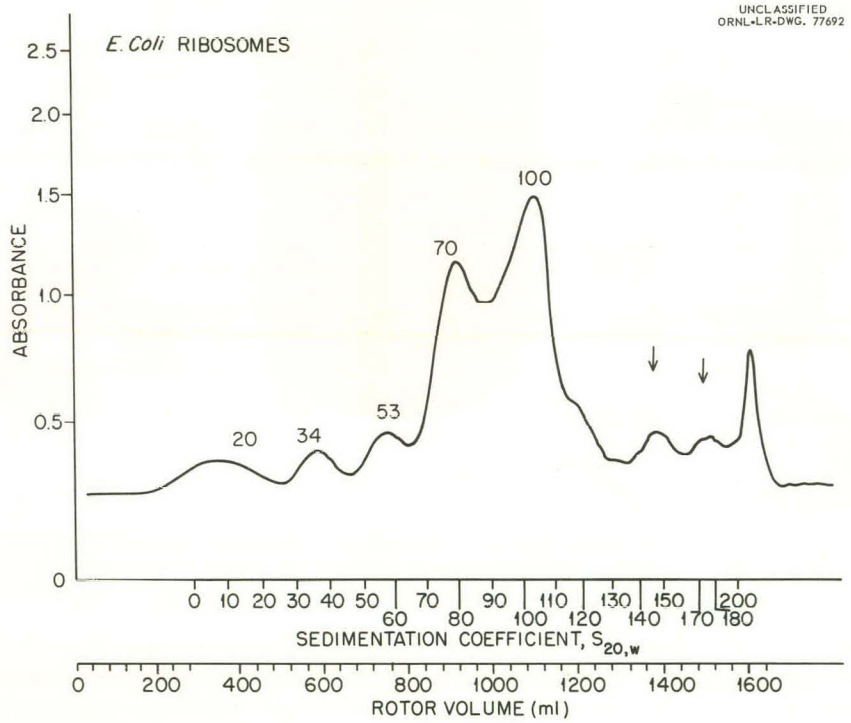

Fig. VI-B-8. Separation of *E. coli* Ribosomes in B-II Zonal Rotor.

C. ROTOR B-III

N. G. Anderson R. E. Canning C. T. Rankin

1. Description of Rotor

Rotor B-III (Fig. VI-C-1) uses the lower end cap and rotor tube from rotor B-I. New septa, core and upper end cap have been adapted to test the reorienting gradient principle with a larger rotor. The total internal volume is 1450 ml. A removable coaxial filling plug inserted into the upper end cap permits fluid to flow directly to the bottom of the rotor through the center core. Fluid flowing out the top is directed outward by the upper flared-out portion of the core, and inwardly by the conical lower portion of the upper end cap; it flows out through the upper portion of the core and out the removable coaxial filling plug (not shown).

2. Preliminary Performance Studies

A sucrose gradient was introduced into the rotor at rest and recovered by displacement out through the top. Comparison of the gradient as introduced, as recovered when run through the rotor, and as recovered after acceleration of the rotor to 15,000 rpm and deceleration to rest revealed only very small changes in the gradient.

Fig. VI-C-1. Parts of Zonal Rotor B-III. Core assembly is shown on left, rotor body in center, and upper end cap at right. Gradient is static loaded through the center line leading from the upper end cap to the bottom of the core. When the gradient flows out the upper end cap annular constriction, the sample layer is forced back into the upper portion of rotor on top of gradient. Gradient is recovered by pumping dense fluid to bottom of chamber at rest, forcing gradient out top.

To determine the effect of passage through the rotor and of reorientation on the thickness of the sample zone, a 1200-ml sucrose gradient (17-55% w/w) was introduced into the rotor at rest, and a sample gradient (10 ml of 4% BSA in 8.5% sucrose grading into 10 ml of 17% sucrose) backed in on top of it. The sample layer was moved down into the rotor by overlaying with 200 ml of Miller-Golder buffer ($\mu = 0.1$, pH 7.5). The absorbance recording obtained after static unloading with the rotor held stationary, and after acceleration to 1500 rpm and deceleration approximately 1 hour later, is shown in Fig. VI-C-2. The amount of zone widening is more than that observed with the B-II rotor, but is acceptable for many purposes. On the basis of these results, B series reograd rotors appear worthy of continued study, especially since their construction and operation is so simple.

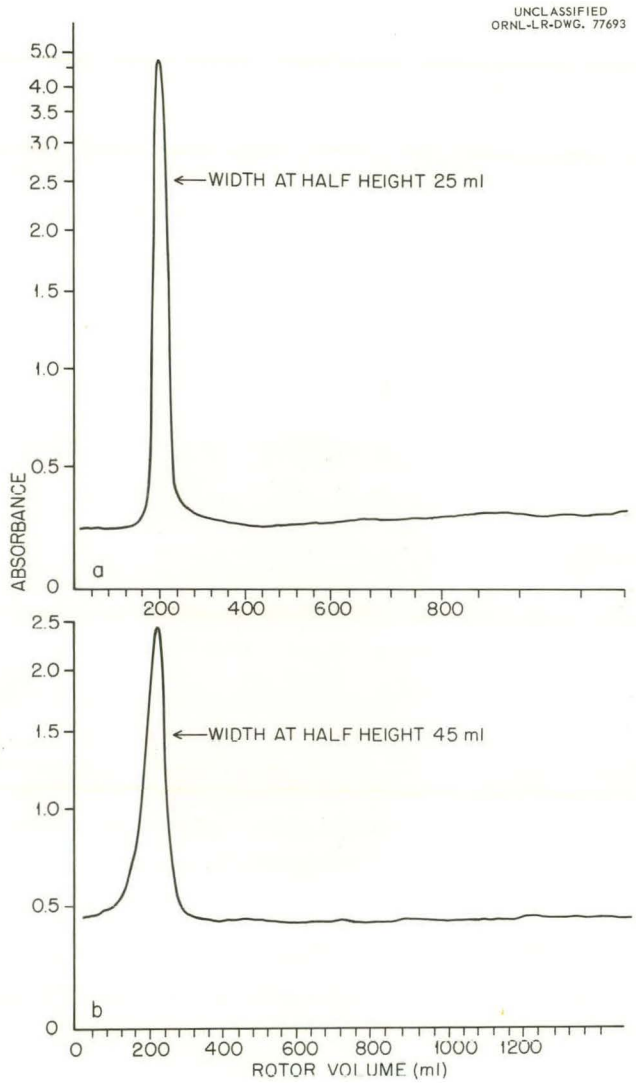

Fig. VI-C-2. Widening of Sample Zone in Reograd Rotor B-III During Gradient Reorientation. In (*a*) the 20-ml sample zone was introduced and recovered from the gradient at rest. In (*b*) a similar zone was introduced and recovered at rest, but while in the rotor it was reoriented to a vertical position during acceleration to 1500 rpm, and then brought back to a horizontal position during deceleration to rest.

VII. High-Speed Zonal Rotors

A. ROTOR C-1

N. G. Anderson

Rotor C-I was originally designed to test the reorienting gradient concept at speeds up to 60,000 rpm using a commercially available analytical ultracentrifuge drive. Work on this rotor was discontinued as soon as it became evident that much higher speeds would be available with new ultracentrifuge drive mechanisms designed and constructed at Oak Ridge. Since the C-I rotor may prove to be of general use in laboratories equipped with analytical ultracentrifuges, work will be resumed on this rotor later.

B. ROTOR C-II

H. P. Barringer

1. General Considerations

Speeds in excess of 60,000 rpm and force fields of more than 250,000 $\times g$ have not been generally available for biological studies. The purpose of the C-II rotor system has been to provide an extremely simple centrifuge system, requiring no critical adjustments, which may be routinely operated at extremely high speeds by untrained personnel. Since the rotor is intended primarily for work with cesium chloride solutions, a fluid density of 1.7 has been used in the design calculations. Using solutions of this density, the SW 39 rotor is limited to a total capacity of approximately 12 ml at 33,000 rpm, while the Spinco analytical AN rotor is operated at 44,770 rpm with approximately 0.7 ml of solution. It did not appear feasible to explore much higher speeds if the rotor volume would be cut down at the rate suggested by the capacities of currently available equipment. Fortunately, the reograd concept makes the use of tubular, sector-compartmented rotors feasible. Since it was considered important for future planning to know as soon as possible whether or not this concept, configuration, and drive system would be suitable for biological studies, the C-II rotor was designed, constructed, and tested to 90,000 rpm in somewhat less than 3 weeks.

2. Rotor Design

Rotor C-II has a design speed of 141,000 rpm (310,000 $\times g$ at R_{max}) when loaded with 100 ml of fluid having a density of 1.7. With lighter fluids, proportionately higher speeds may be obtained.

The rotor is a hollow, reorienting gradient type of zonal centrifuge, which is loaded and unloaded at rest. The density gradient may be formed with a suitable gradient engine and introduced together with sample zone at rest for rate-zonal molecular sedimentation studies, or the gradient may be formed by the centrifugal field as is often done in isopycnic zonal centrifugation.

The configuration of the rotor is shown in Figs. VII-B-1 and VII-B-2. The chamber is divided into four compartments by a single piece core so that angular momentum can be imparted to the fluid mass during acceleration and deceleration without stirring or mixing. The drive assembly and associated housing are shown in Fig. VII-B-3.

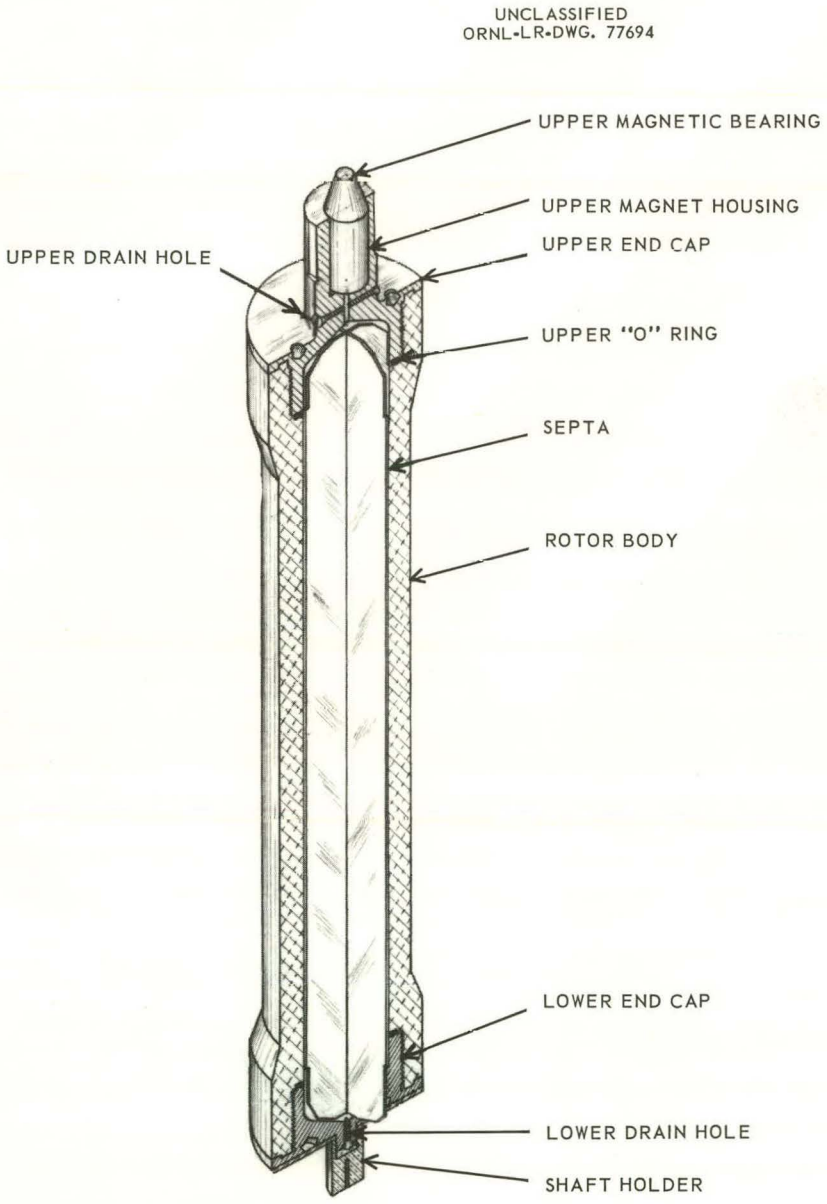

Fig. VII-B-1. Assembly Drawing of Rotor C-II.

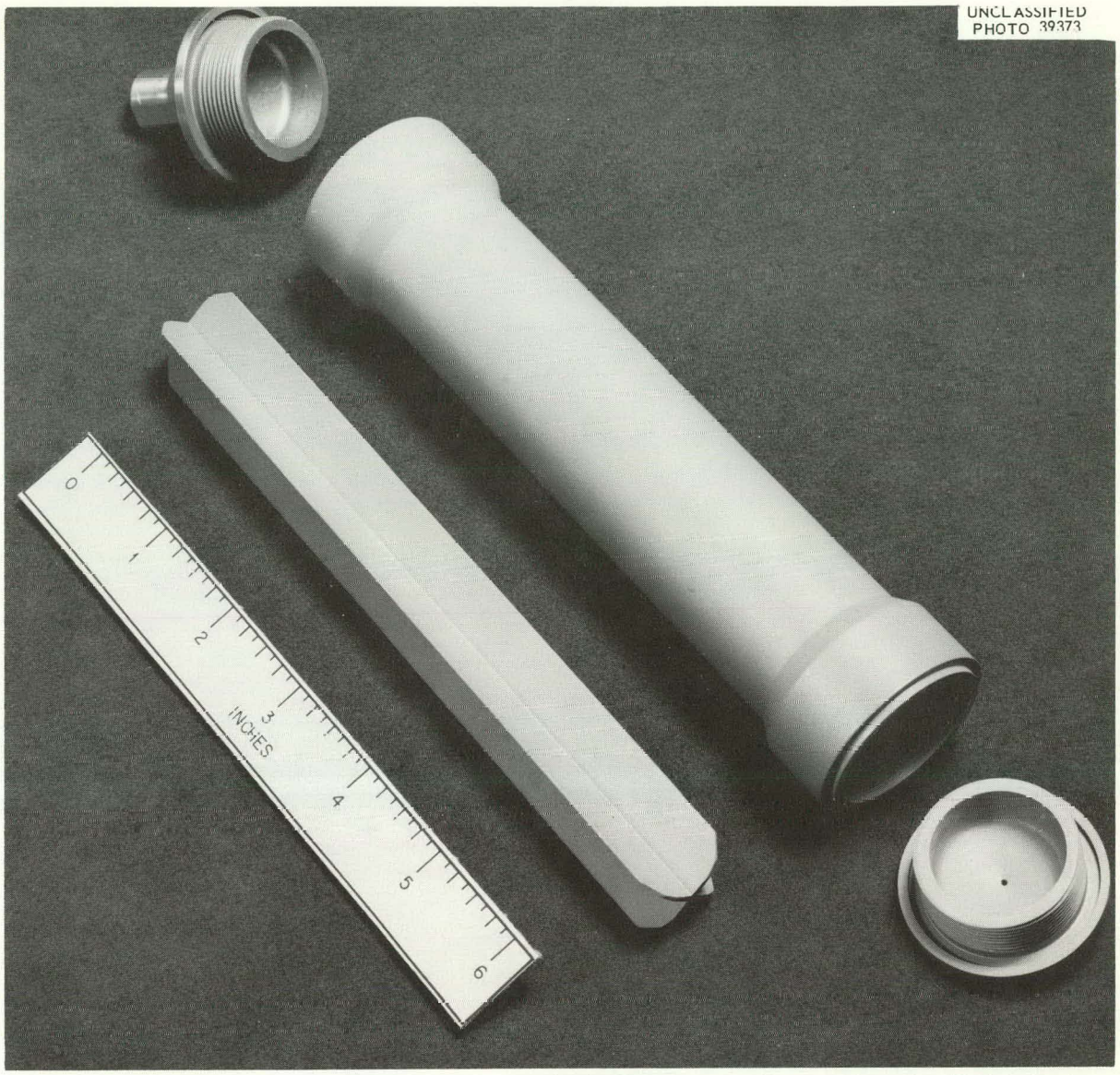

Fig. VII-B-2. Disassembled Rotor C-II.

The rotor support bearing is a simple pivot at the bottom and a magnetic bearing at the top to support the rotor as it spins about a vertical axis. Elastomeric damping of both bearings is provided to give the rotor sufficient stability to pass certain critical vibrational frequencies. The rotor is driven by a hysteresis motor that used a conventional radial air-gap stator as an axial air-gap motor. The armature is attached to the lower end of the rotor and covers part of the stator laminations. The rotor can be locked into the frequency of the rotating magnetic field. Thus, by increasing the driving frequency, the centrifuge can be accelerated with almost zero slip and with virtually no heat input to the rotor. Multiphase power is supplied to the motor by conventional motor-alternator power supplies or by a variable-frequency electronic power supply designed for this purpose.

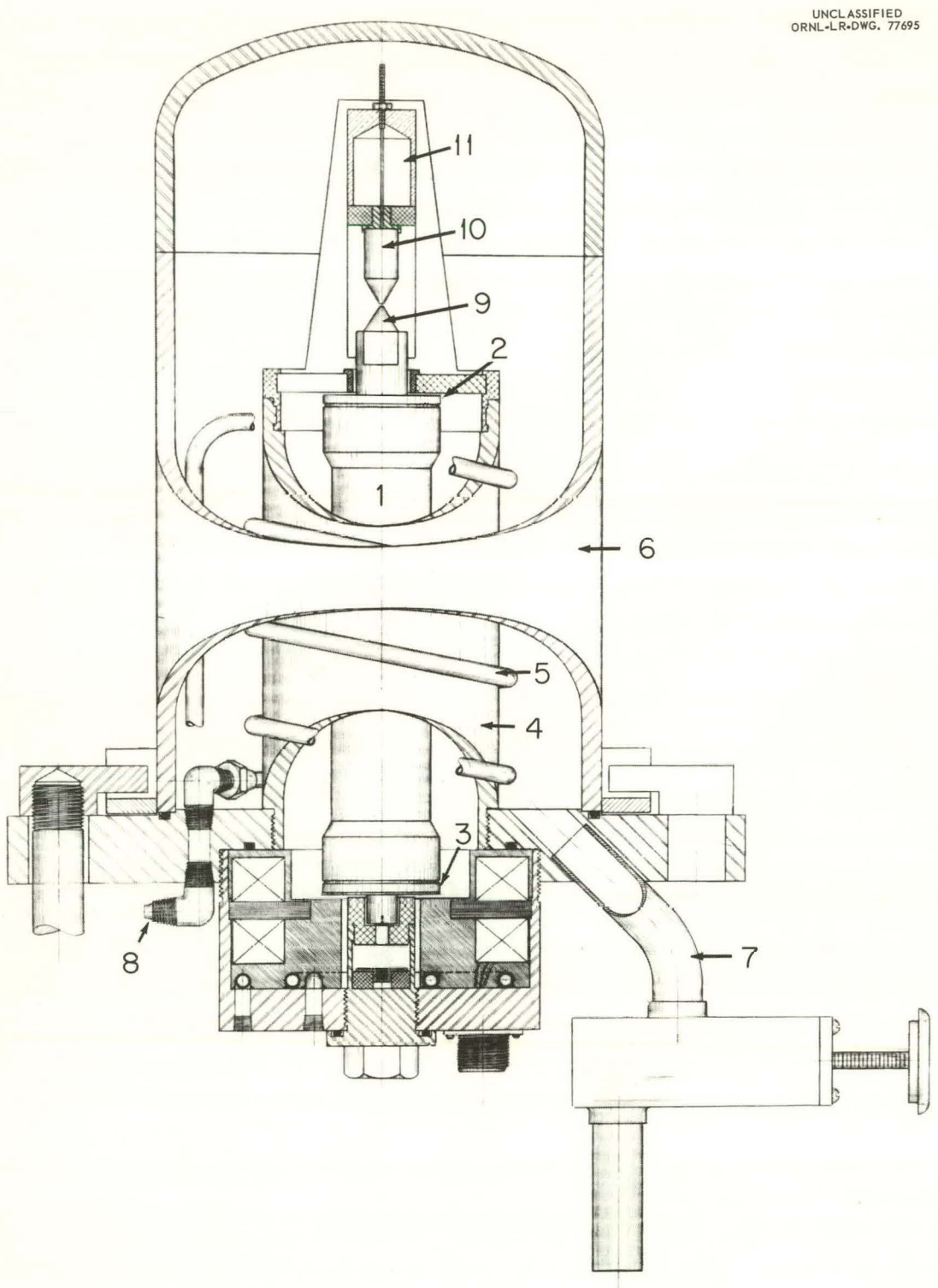

Fig. VII-B-3. Drive Assembly, Vacuum Chamber, Armor Shield, and Bearing Systems for Rotor C-II. (1) Rotor body; (2) upper end cap; (3) lower end cap; (4) cooling jacket; (5) cooling coil; (6) vacuum jacket; (7) vacuum line; (8) coolant inlet; (9) upper magnetic bearing, rotating member; (10) upper magnetic bearing, stationary member; (11) upper bearing suspension.

The rotor is operated *in vacuo* with suitable cooling coils to remove any heat generated by the high peripheral speeds employed. Both the cooling coils and the rotor surface have high emissivity values to provide excellent radiant heat transfer. Rotor speed is determined by placing a proximity probe adjacent to two machined depressions on the rotor. The two pulses per revolution thus generated are fed either to a rate meter or a pulse counter. With the latter, rotor speed can be accurately determined to ±1 of 4700 pulses per second (±0.021%) when the rotor is operated at 141,000 rpm.

The rotor is designed for optimum use of rotor materials and operates safely below the first flexural critical frequency of the rotor body. It provides the maximum volume and maximal centrifugal force for the rotor materials used and the capacity required. The end caps are sealed by conventional "O" rings and fill plugs are provided in both end caps.

3. Operation

The C-II rotor proved to be an extremely stable and rugged centrifuge. At 141,000 rpm the rotor run-out has been less than 0.001 in. peak to peak. The rigid body vibration modes at low speeds have been limited to less than 0.010 in. (peak to peak) excursions. Owing to an error in the assembly of the lower damping system on one occasion, the rotor was suddenly decelerated from 141,000 rpm to rest. Only small scratches on the rotor body were observed.

Over 300 hours of run time at various speeds between 98,400 rpm and 141,000 rpm have been accumulated. The rotor is estimated to have a life in excess of 8000 hours at 141,000 rpm (68×10^9 revolutions).

4. Performance

The C-II rotor has been tested using cesium chloride gradients formed by the centrifugal field to band DNA and virus particles at speeds up to 141,000 rpm. Since the large rotor volume (100 ml) allows milliliter or larger fractions to be recovered, sufficient material is available for accurate refractometric determination of cesium chloride concentration. A new refractometer has been ordered for this purpose. Banding of T3 phage particles in 9 hours at 100,000 rpm is illustrated in Fig. VII-B-4. The band as recovered was 0.85 mm thick at half-height, as calculated back to the band position in the rotor.

In similar experiments, at speeds up to 141,000 rpm, two bands have been observed with milligram quantities of calf and rat thymus DNA. These experiments will be reported in more detail in the next report.

This work makes it possible to determine easily whether or not a labeled drug or other substance becomes attached to DNA in the cell.

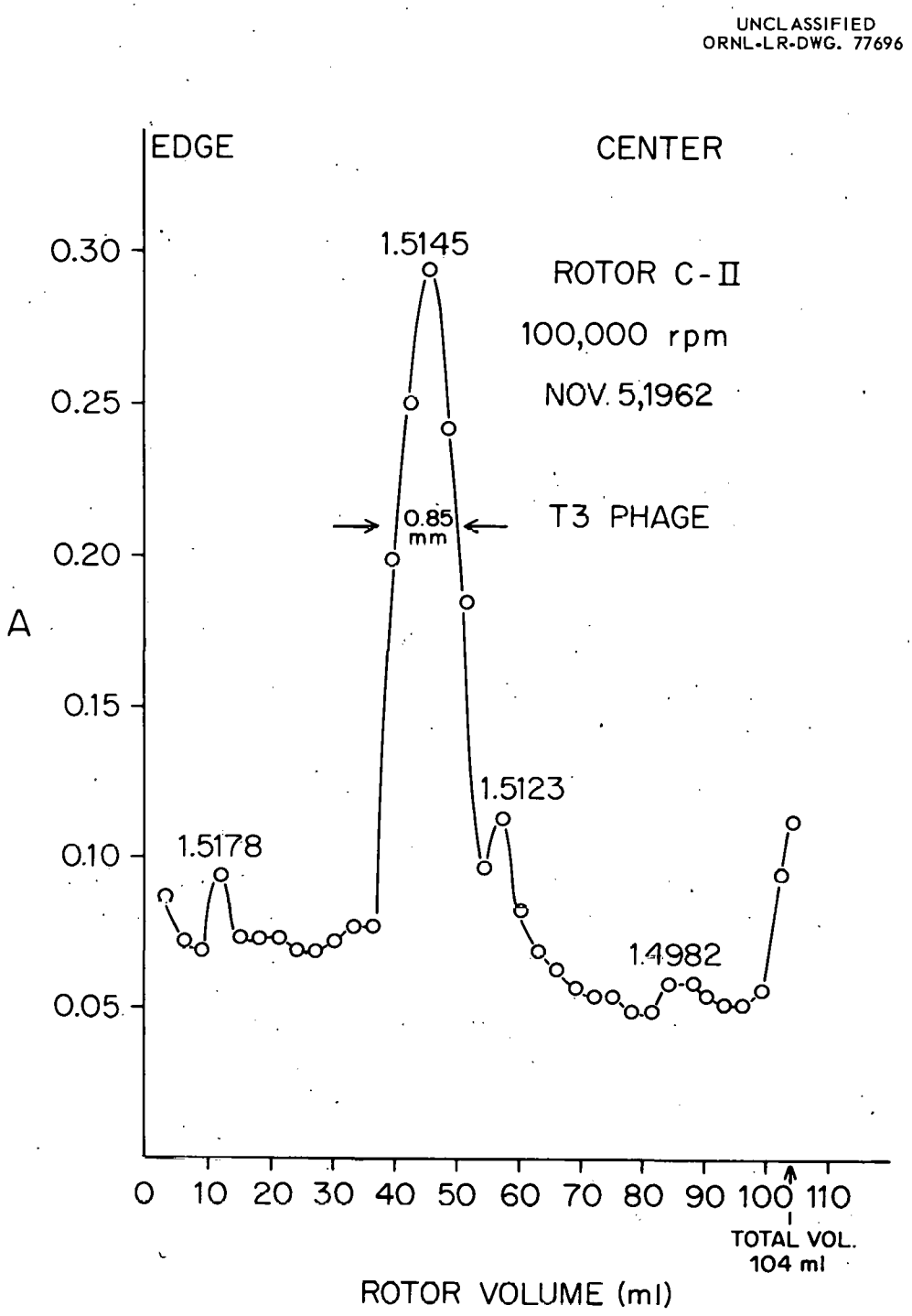

Fig. VII-B-4. Banding of T-3 Phage in CsCl in Zonal Rotor C-II.

VIII. Ultrahigh-Speed Rotor Systems for Equilibrium Centrifugation

A. DESIGN OF D SERIES ROTOR SYSTEMS AND DRIVES

H. P. Barringer D. A. Waters

Because of the very low diffusivity of DNA and other large macromolecules, molecular equilibrium centrifugation or "banding" in cesium chloride or other salt solutions is successful with previously available centrifuges. With lower molecular weight substances, the band width with a homogeneous substance may become excessively large, making it difficult to resolve two components differing slightly in density. With a given system (such as DNA, cesium chloride, and water) resolution is not increased with increasing centrifugal force, since as the steepness of the gradient is increased, bands of DNA differing in density move closer together and also narrow. To increase resolution markedly, the centrifugal field must be greatly increased without a proportional increase in gradient steepness. By using deuterium oxide and mixtures of salts or organic substances of lower molecular weight than cesium chloride, the steepness of the gradient in a given centrifugal field can be decreased and still include regions having the desired density. Because the centrifugal field may then become the limiting factor in achieving high resolution in a reasonable time, it is of interest to explore the limits set by existing materials and technologies on the construction of ultrahigh-speed rotors.

The ultrahigh-speed D series rotors are currently in the conceptual design stage. These rotors will be characterized by very high speeds, very high centrifugal fields, and by the uniqueness of the design concept. Rather unusual materials are being considered for fabrication, and the drive systems are unconventional.

The first rotor, D-I, will have a design speed of 400,000 rpm and will produce 1.2 million $\times g$ for extended periods of time. The rotor chamber will be constructed of ultrahigh-strength steel with a yield strength of 260,000 psi. At these speeds the volume of fluid must be restricted to 10 ml. For the initial tests, the D-I rotor will be operated in a similar manner to the C-II rotor with the fluid being sealed in the rotor chamber during operation. A schematic drawing of D-I is shown in Fig. VIII-A-1.

Conceptually, the D-II rotor will utilize several components of the D-I rotor, but rather than steel end caps, the end enclosures will be transparent windows permitting observations and optical measurements to be made. The rotor will be suspended magnetically in the initial test drive system. While many objects having a small length-to-diameter (L/D) ratio have been successfully suspended and rotated in magnetic

fields up to 6×10^7 rpm, objects having a large L/D ratio, *i.e.*, $I_{spin}/I_{transverse} \ll 1$, are much more difficult to operate successfully. Rotor D-II is shown diagrammatically in Fig. VIII-A-1.

A third rotor design, D-III, utilizing a different L/D ratio, with fairly large-diameter quartz, ultrahigh-strength glass, or sapphire windows is being considered. This centrifuge will be the very high speed counterpart of the E series rotors considered in the next chapter. Rotor D-III will be useful for basic studies on the formation and capacity of density gradients. Because of the small L/D ratio of D-III, the rotor can be supported by either a magnetic field alone, or by a magnet-pivot system.

Rotor D-IV will be discussed in a subsequent report. For maximal centrifugal field studies, Rotor D-V is being considered. It has transparent end windows, magnetic support, a 0.75-ml capacity, maximal centrifugal force of 2.5 million $\times g$ at 840,000 rpm (275 m/sec inner peripheral velocity) and an inside diameter of 1 mm. This rotor would be useful for studies on the effects of high hydrostatic pressure on the density of macromolecules.

It should be emphasized that the D series rotors are still in the early design stages. However, they conform to principles demonstrated in larger systems. Many difficult theoretical and engineering problems remain to be solved before D series rotors are available for use in biological studies. By centering attention on a specific series of rotor configurations, the supporting activities required for their completion are more clearly defined.

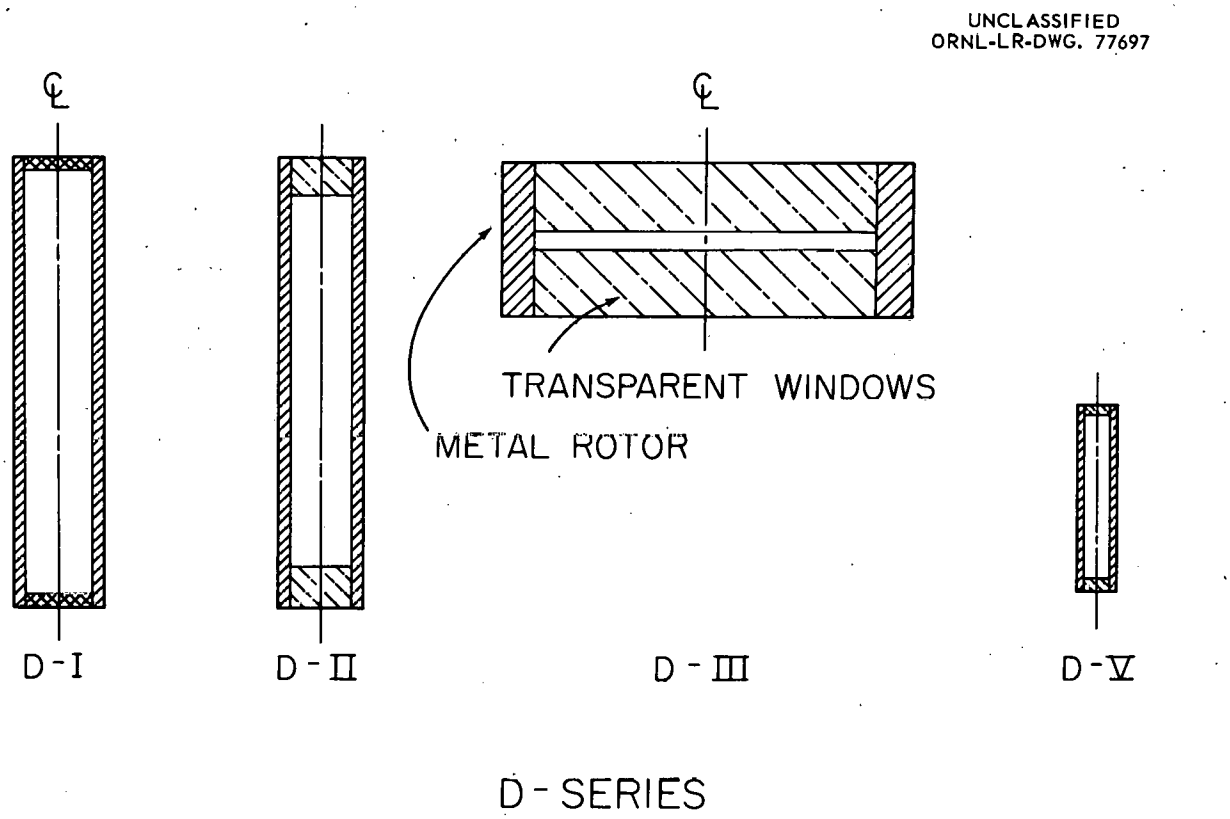

Fig. VIII-A-1. D Series Rotors – Conceptual Design.

IX. Analytical Zonal Centrifuges

A. DESIGN OF E SERIES ROTOR SYSTEMS

N. G. Anderson

It is desirable for several reasons to make direct measurements of the rate of sedimentation of particles in density gradients. For large particles this can now be done in rotor A-V and A-VI (Chapter VA, B). For smaller particles, however, much higher fields will be required. Rotor systems of this type for intermediate-speed operation (ca 30,000 rpm) are designated as Series E rotors.

An alternate approach to the problem of measuring sedimentation rates at several points in a gradient is to make multiple runs with a B-II rotor and plot the sedimentation rate as a function of gradient density, viscosity, and osmotic pressure from this data. However, it is considered preferable to observe the behavior of particles in the gradient directly.

In instances where particles tend to behave osmotically, the effective particle density is a function both of the position in the gradient and the length of time the particle has spent in the gradient. While attempts have been made to treat the sedimentation of mitochondria theoretically and to predict the behavior of the particles in a density gradient, experimental observation shows that all mitochondria do not behave identically and the apparent bulk properties cannot be applied to the individual particles. At a given level in the gradient, dense unswollen mitochondria together with swollen mitochondria are found. It is important to determine directly the behavior of such particles in a density gradient.

An additional reason for constructing Series E systems is to study experimentally the capacity of gradients to support particle zones. While the theoretical capacity of a gradient for particles of a given density in a given band width may be easily calculated, in practice the capacity of the gradient is much less than expected. By direct observation it is hoped to observe the causes of the low capacity.

X. Ultrafast-Freezing Centrifuge

N. G. Anderson J. G. Green P. Mazur

A. THEORY

Many cell types survive freezing and thawing if they are initially cooled at a relatively slow rate. At more rapid cooling rates, survival drops markedly. However, in theory, if cells could be frozen fast enough to vitrify the water they contain, high survival should result. These conditions have been difficult to meet experimentally. The purpose of this work has been to examine centrifugal methods for approaching the theoretical limits for the cooling rates of cells. The work is of interest in relation to the preservation of cells, viruses, and other biological materials.

Numerous experiments have been performed on the effects of freezing and warming rates on whole cells including the studies of Mazur[1,2] performed in this laboratory. The freezing of droplets of cell suspensions in liquid nitrogen introduced by Meryman and Kafig[3] and further utilizied by Rinfret and Doebbler[4] appears as a suitable starting point for the development of techniques for producing very rapid cooling rates. The experimentation described here employs the method of rapid freezing of droplets in liquid nitrogen with the droplets separated from an insulating gas barrier using a centrifugal field.

Initially, rotor design and experimental procedures were conditioned by the objectives of attaining maximal freezing rates of droplets and minimal extraneous stress on contained cells to permit the evaluation of results in terms of freezing and thawing rates only.

Rigorous mathematical treatment of the factors involved in centrifugal freezing has been delayed until further experimental work has been done; however, the following sequence of events is thought to occur. On contact with the vertical meniscus of the liquid nitrogen, which has a surface velocity of 670.2 cm sec^{-1} at 5000 rpm in the F-I-f and F-II-f rotors, a droplet is deformed and breaks into many smaller droplets which at first have a tendency to spin. Passage of the droplet through the liquid nitrogen occurs in two intergrading phases, an initial transient pre-equilibrium phase involving acceleration of the particle to the rotational velocity of the liquid nitrogen and a subsequent equilibrium phase involving movement of the droplet

[1] Peter Mazur, *Ann. N.Y. Acad. Sci.* 85, 610 (1960).

[2] Peter Mazur, *Biophys. J.* 1, 247 (1961).

[3] H. T. Meryman and E. Kafig, *Proc. Soc. Exptl. Biol. Med.* 90, 587 (1955).

[4] A. P. Rinfret and G. F. Doebbler, *Biodynamica* 8, 181 (1960).

to the wall of the plastic insert. In the latter phase, the particle would move centrifugally according to the equation:

$$T_s = \frac{18\eta}{d^2(\sigma - \rho)} \cdot \frac{\ln R_{max} - \ln R_{min}}{\omega^2}, \quad (1)$$

where

T_s = time in seconds for particle transit,
η = viscosity of the medium in poises,
d = diameter of the particle,
σ = density of the solvated particle,
ρ = density of the medium,
R_{max} = radius to the outer periphery of the liquid nitrogen,
R_{min} = radius of the surface of the liquid nitrogen,
ω = angular velocity of the rotor in radians sec^{-1}.

Assuming typical values of 0.001 poise, 0.1 cm, 1.0^2 gm cc^{-1} and 0.808 gm cc^{-1} for n, d, σ and ρ, respectively, and measured values of 2.8 cm, 1.6 cm and 2.74×10^5 radians sec^{-1} for R_{max}, R_{min} and ω^2 at 5000 rpm respectively, a particle in the F-I-f and F-II-f rotors will complete its transit to the rotor wall in 1.73×10^{-5} sec with an average theoretical velocity through the medium of 6.9×10^4 cm sec^{-1}. These calculations represent the upper theoretical limits for particle velocity, and are probably not reached in practice.

At such speeds, the droplet continues to fragment into smaller droplets so long as it remains fluid. Therefore, the particle size may be an indicator of the freezing rate. Owing to the initial inertia and the velocity the particle attains, it is unlikely that an insulating gas envelop forms but, rather, that the particle leaves a trail of superheated liquid nitrogen in its wake which vaporizes only after the particle has passed. In addition, the lack of adhesion and relative sphericity of the frozen droplets indicate that the particle must be sufficiently solidified to prevent distortion upon contact with the wall of the rotor. Heat transfer from the droplets must be extremely rapid under these conditions.

B. SERIES F ROTORS

Figure X-B-1 depicts the initial rotor, designated F-I-f, utilized in this series of experiments. The rotor consists of an outer brass shell containing an inner methacrylate plastic cup. The frozen droplets were removed from this rotor by pouring.

To improve transfer procedures a transfer cap was attached to rotor F-I-f (Fig. X-B-2). This is designated F-II-f. To effect transfer of the frozen droplets, the prechilled transfer cap is first attached to the rotor using a film of silicone stopcock grease as a seal and lubricant. After most of the liquid nitrogen has evaporated, the rotor is inverted and the droplets are expelled from the plastic cap by the nitrogen gas generated within the rotor.

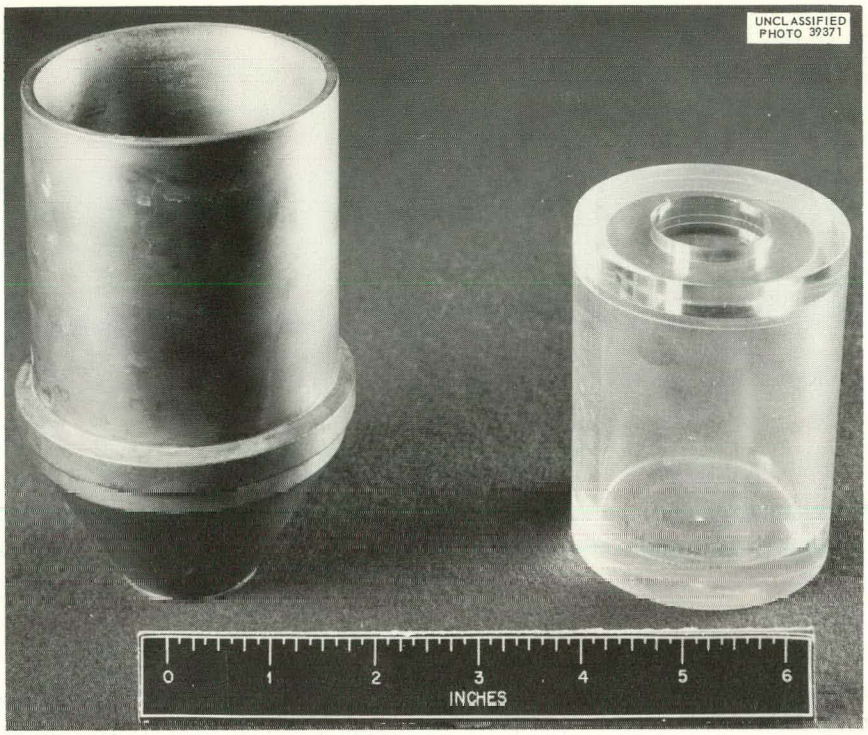

Fig. X-B-1. Rotor F-I-f.

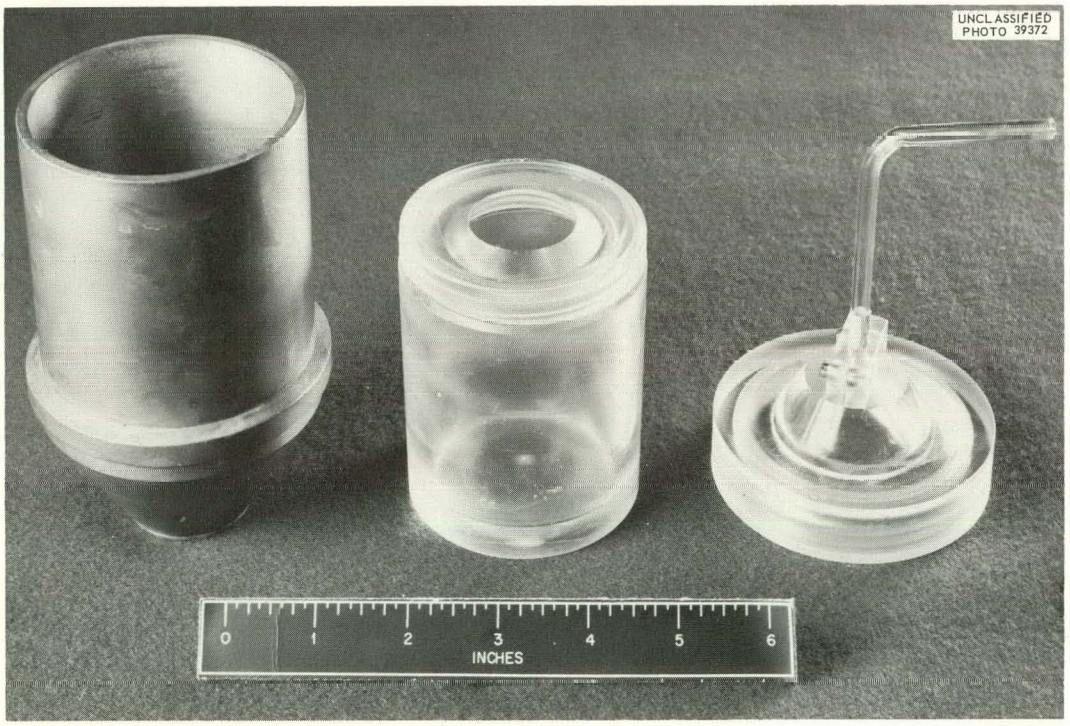

Fig. X-B-2. Rotor F-I-f, with Transfer Cap Shown. When assembled, it is rotor F-II-f.

To explore centrifugal warming techniques, rotor F-III-t of Fig. X-B-3 was formed by hollowing an International Equipment Company No. 855 duraluminum angle head rotor.

Rotors F-I-f and F-II-f are driven by an International Refrigerated Centrifuge Model PR-2. In use they were precooled with liquid nitrogen immediately before the cell suspensions were introduced into the nitrogen-filled rotor. At operational speeds, the liquid nitrogen assumed a vertical orientation; thus the volume was limited by the rim of the plastic top. Observation of the performance of the rotor and injection of the experimental material into the rotor were facilitated by a transparent cover of polymethacrylate plastic fitted to the centrifuge as shown in Fig. X-B-4.

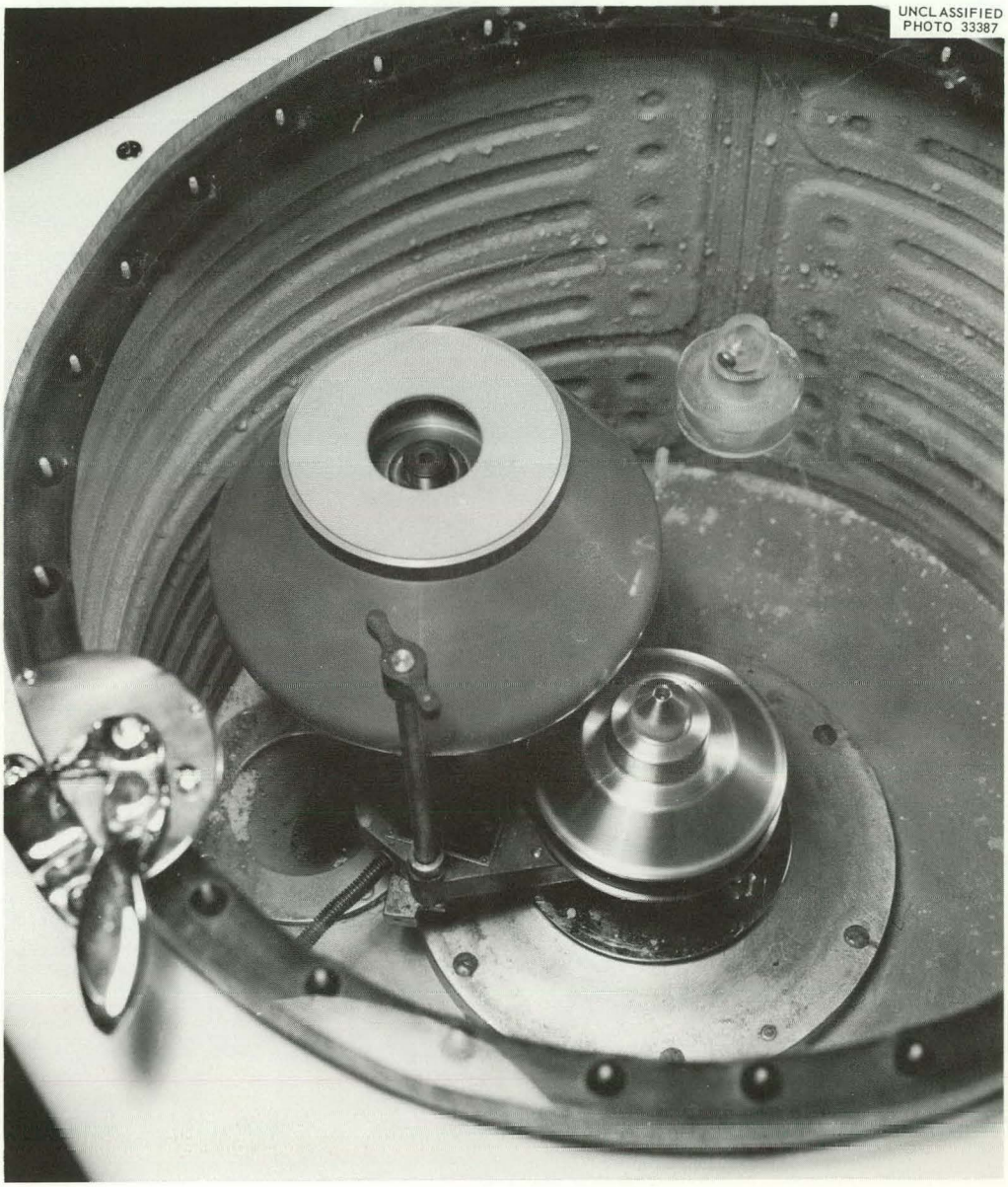

Fig. X-B-3. Rotor F-III-t, Used for Rapid Thawing of Yeast Cells.

Fig. X-B-4. Technique for Ultrarapid Freezing of Cells by Injection into Liquid Nitrogen into Rotor F-I-f.

The material to be frozen was injected into the rotor in short, repeated pulses through a 5.1 cm No. 23 gauge cannula from a hypodermic syringe placed to direct a stream into the liquid nitrogen. Preliminary experiments have been conducted with (1) water, to assess droplet formation, (2) versenated whole rat blood, to evaluate droplet formation of a cell suspension and (3) suspensions of washed yeast cells (*Saccharomyces cerevisiae*), to determine effects of treatment on cell viability. The first was tested at various rotor speeds while (2) and (3) were tested at 5000 rpm.

Droplet formation was evaluated photographically by transferring the frozen droplets in liquid nitrogen from the F-I-f rotor to a petri dish. The frozen droplets were observed through a dissecting microscope and photographed when only traces of liquid nitrogen remained in the dish.

C. FREEZING AND THAWING OF YEAST CELLS

Three types of experiments, differing in warming procedures, have been performed with yeast suspensions (Table 1).

1. With slow warming, the frozen droplets were allowed to remain in the rotor until melted and were then transferred to a beaker containing 1 liter of 0.96 *M* potassium phosphate plating diluent.

2. With rapid warming, the frozen droplets were transferred from the F-I-f rotor to a dish fabricated from aluminum foil and placed in the bottom of a 1500 ml beaker. When nearly all of the liquid nitrogen had evaporated, 1 liter of plating diluent (35°C) was poured over the contents of the foil dish.

3. The frozen droplets were transferred from rotor F-II-f, as described previously, to the F-III-t rotor spinning at 1800 rpm but containing 1 liter of 35°C plating diluent. To minimize metal contamination, the thawed cells were transferred immediately to a beaker for plating.

Table 1. Results of Freezing and Thawing Experiments with Yeast Suspensions

Experiment	Rotor	Percent Survival[a]
Slow warming	F-If	0.0
Rapid warming	F-If	10.5
Fast freezing and rapid thawing	F-IIf F-IIIt	76.1

[a] Corrected for viability of controls.

Viability of the frozen-thawed yeast cells was assessed by suitable counting and plating procedures. Control samples were treated similarly except for freezing. The cell culturing and plating techniques have been described by Mazur;[2] however, in this case, aliquots for plating of the frozen-thawed cells were taken directly from the beakers of cells in plating diluent and from a 1000-fold dilution of the thawed suspension. Although special precautions other than the use of sterile thawing and plating media were not observed, contamination of the culture by extraneous organisms was rare. The counting and plating procedure utilized with yeast suspensions is diagrammed in Fig. X-C-1.

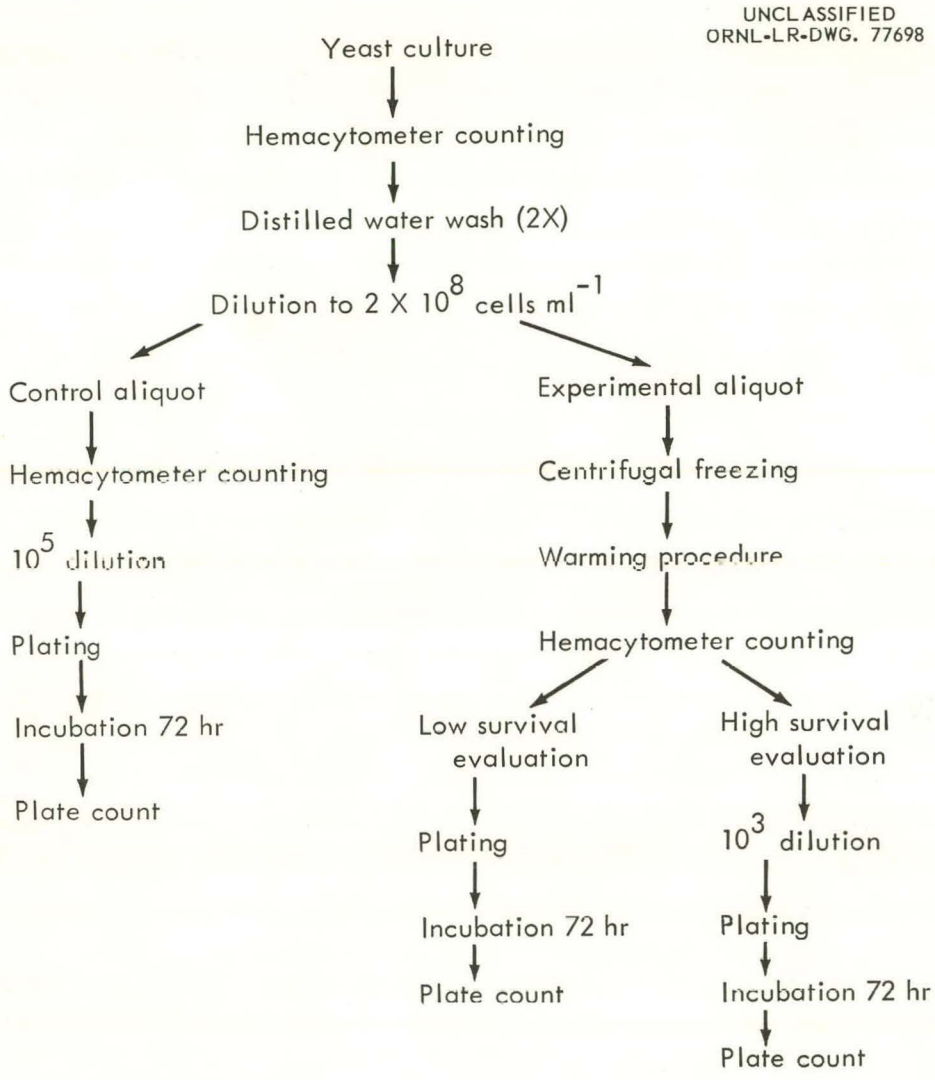

Fig. X-C-1. Diagrammatic Representation of Experimental Procedure with Yeast Suspensions.

Photographs of droplets obtained when water was injected into liquid nitrogen in rotor F-l-f at rest and at speeds of 1000 to 5000 rpm are shown in Fig. X-C-2. When the rotor was stationary, particles varying from 0.1 to 10 mm or more in diameter were obtained. The smaller droplets were spherical but the larger droplets were irregularly shaped. When the rotor was spun faster, successively smaller and generally spherical particles were obtained. It is likely that contact of the injected stream with the rapidly moving surface of the liquid nitrogen dispersed the droplets before freezing occurred and that the droplets remained fluid at least until surface tension forces produced a typical spherical shape.

Figure X-C-3 shows that when whole rat blood was injected into the F-l-f rotor at 5000 rpm, spherically shaped droplets similar to those obtained with water were obtained; however, the larger droplets show evidence of cracking. The cause of this fracturing has not been ascertained, although the observer-directed orientation of the fractures suggests that they may result from warming occurring during the time for observation.

UNCLASSIFIED
PHOTO 60357

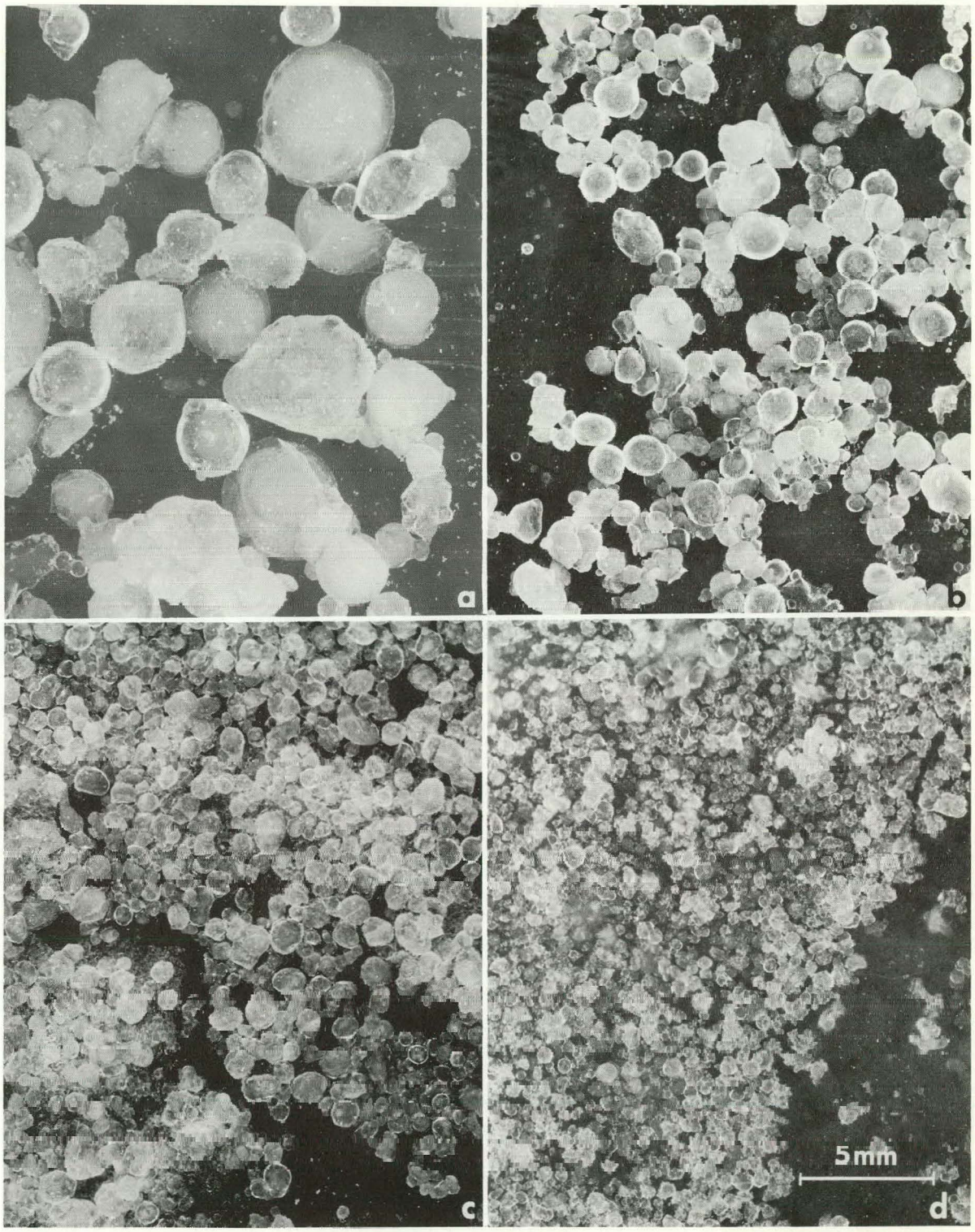

Fig. X-C-2. Water Injected into Liquid Nitrogen at Rest (*a*), and into Liquid Nitrogen Spinning in Rotor F-I-f at 1000 rpm (*b*), 3000 rpm (*c*), and 5000 rpm (*d*).

The viability of the treated yeast suspensions indicates the practicability of centrifugal freezing and thawing procedures. Refinement of techniques will follow additional theoretical and experimental work, and other applications of the method may then be explored.

UNCLASSIFIED
PHOTO 60358

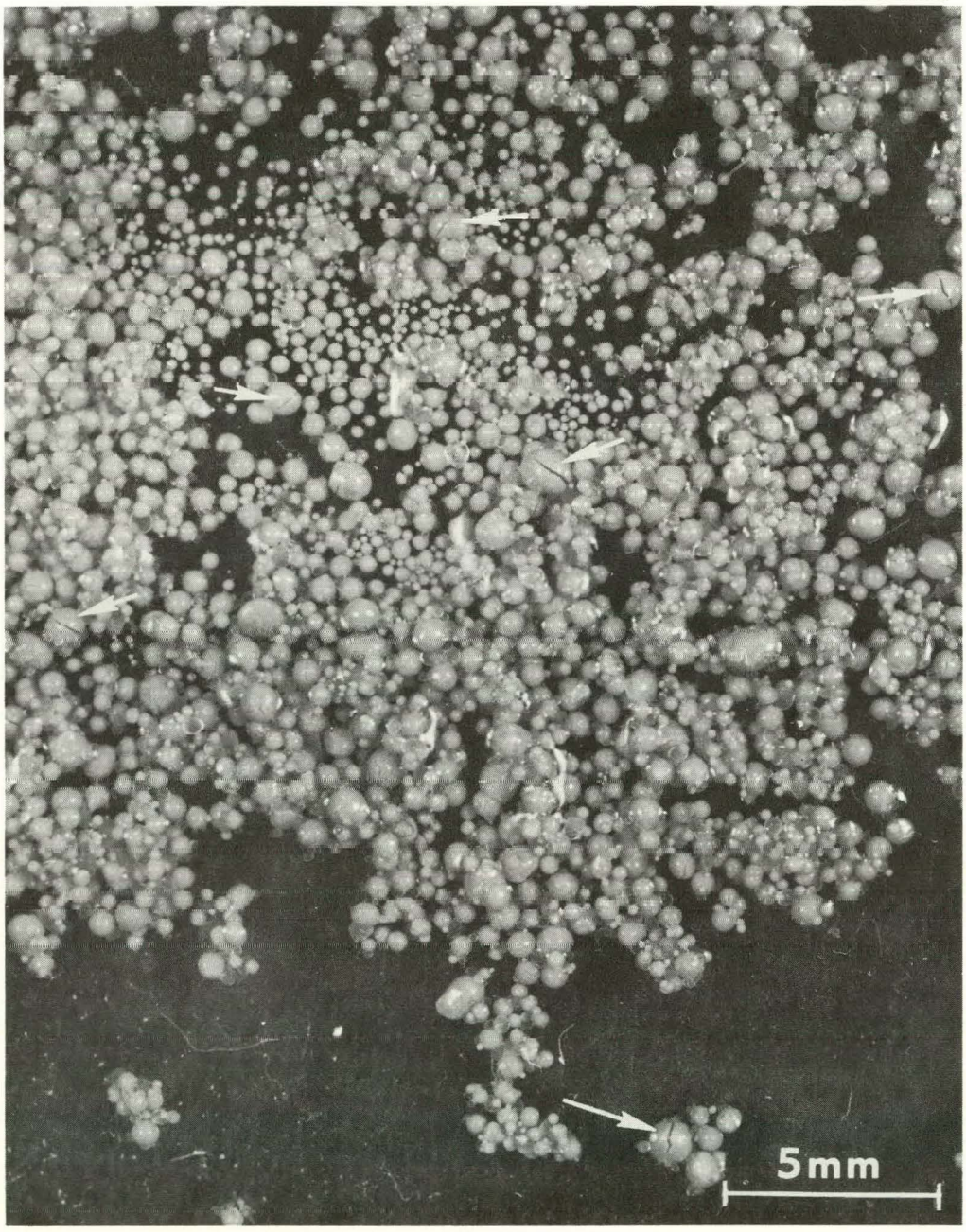

Fig. X-C-3. Whole Versenated Rat Blood Injected into Liquid Nitrogen in the F-l-f Rotor at 5000 rpm. Note cracks in larger particles.

XI. Biochemical Studies on Cell Fractions

A. GRADIENT SYSTEM FOR METABOLICALLY ACTIVE NUCLEI

W. D. Fisher G. B. Cline

Since many of the synthetic activities of isolated thymus nuclei are dependent upon the tonicity of the isolation medium[1] nuclei isolated in conventional sucrose gradients are not suitable for metabolic studies. For example, nuclei isolated in an isotonic sucrose-$CaCl_2$ solution are able to incorporate labeled amino acids into protein and certain RNA precursors into RNA,[2] but lose these properties when exposed to hypertonic sucrose.[3] Isotonic sucrose is not unique in its capacity to preserve nuclear synthetic function since active nuclei may be obtained in 0.25 *M* solutions of other disaccharides (maltose and lactose) and also monosaccharides (fructose and glucose).[3] This suggests that metabolically active nuclei might be isolated in a gradient composed of sucrose grading into more concentrated dextran arranged to be essentially isotonic throughout.

The effect of exposure to various concentrations of dextran on the incorporation of C^{14}-leucine by isolated calf thymus nuclei is shown in Fig. XI-A-1. The nuclei were prepared in 0.25 *M* sucrose–0.006 *M* $CaCl_2$ (ref 3), immersed in dextran solutions varying from 10 to 36% (w/w) for 1 hour, concentrated by centrifugation, and washed twice with the original sucrose-$CaCl_2$ isolation medium. Maximal incorporation (80% of that occurring in the original nuclear preparation) was obtained in nuclei exposed to 30% dextran, which has approximately the same freezing point depression as the isolation medium.

The amino acid incorporation activity of nuclei isolated in a sucrose-dextran gradient is presented in Table 2. A 20% (w/w) calf thymus brei was prepared in 0.33 *M* sucrose–0.006 *M* $CaCl_2$ and the nuclei isolated in parallel using 0.25 *M* sucrose–0.006 *M* $CaCl_2$ and conventional centrifugal procedures, and with a sucrose-dextran gradient (grading from 0.25 *M* sucrose–0.006 *M* $CaCl_2$ into 30% dextran–0.006 *M* $CaCl_2$, pH 7.0) using zonal rotor A-V. The gradient stream recovered after centrifuging for 20 min at 500 rpm was monitored by following absorptivity at 260 mμ (0.2-cm path cell) or by visual observation of the nuclear zone in the transparent centrifuge head. Purity of the nuclei was checked by phase contrast microscopy. The nuclei were collected from the dextran by centrifugation, washed twice with the 0.25 *M* sucrose–0.006 *M* $CaCl_2$ medium, and incubated with labeled amino acids. Recoveries varied from 50–98% of that obtained with batch nuclear isolation methods.

---

[1] V. G. Allfrey, p 279 in *The Cell* (ed. by J. Brachet and A. E. Mirsky), Academic Press, New York, 1959.

[2] V. G. Allfrey, p 170 in *The Cell Nucleus* (ed. by J. S. Mitchell), Butterworths, London, 1960.

[3] V. G. Allfrey, A. E. Mirsky, and S. Osawa, *J. Gen. Physiol.* 40, 451 (1957).

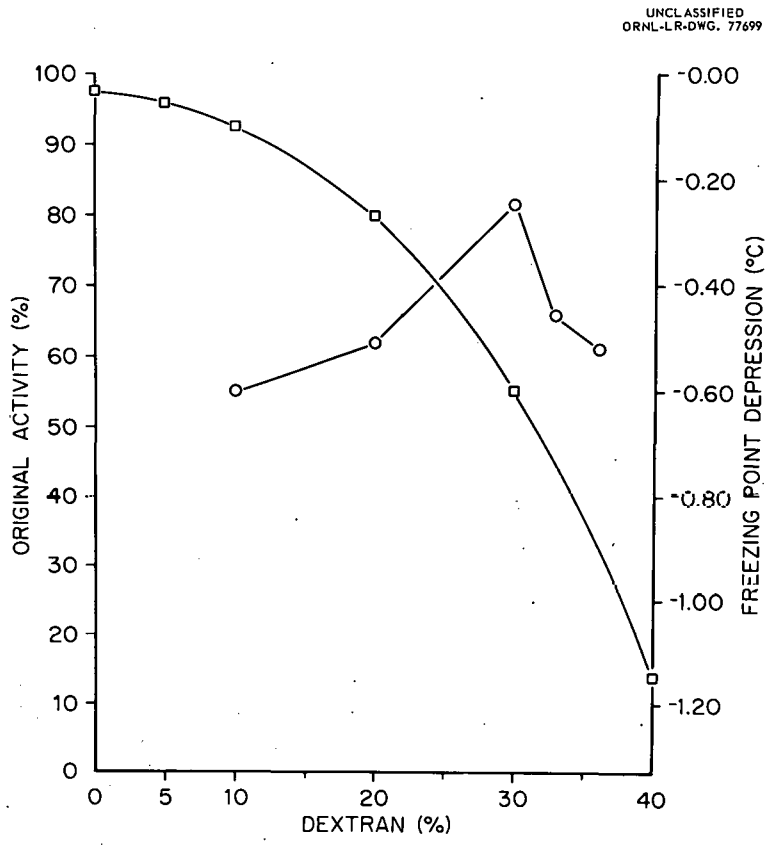

Fig. XI-A-1. Incorporation of C^{14}-Leucine Into Proteins of Isolated Calf Thymus Nuclei Exposed to Various Concentrations of Dextran in 0.006 *M* $CaCl_2$ O——O, and the Freezing Point Depression of Dextran Solutions □——□. The incubation medium consisted of 0.1875 *M* sucrose, 0.02 *M* glucose, 0.0285 *M* NaCl, 0.025 mg L[1-C^{14}] leucine (1.7 μc), and 250 mg wet weight nuclei buffered with 0.025 *M* tris-HCl at pH 7.1 in a final volume of 2.0 ml. Preparation of the protein and assay of radioactivity were done as described by Allfrey (p 170 in J. S. Mitchell, *The Cell Nucleus*, Butterworths, 1960). Incubation time was 90 min at 37°. The activity of the control nuclei was 88 counts/min/mg protein. Freezing points were determined in a freezing point apparatus using a Beckman thermometer. [From W. D. Fisher and G. B. Kline, *Biochim. Biophys. Acta* (in press)].

Table 2. A Comparison of Amino Acid Incorporation in Nuclei Isolated in 0.25 *M* Sucrose-0.006 *M* $CaCl_2$ and in a Dextran-Sucrose Gradient

Incubation and assay as described in the legend to Fig. 1, employing 0.025 mg of labeled amino acid

Amino Acid	Nuclei from Gradient (counts/min/mg protein)	Nuclei Prepared in Sucrose (counts/min/mg protein)
L[1-C^{14}] leucine (1.7 μC)	42	43
DL[1-C^{14}] glycine (1.7 μC)	37	54
L[C^{14}] lysine (1 μC)	100	230
L[C^{14}] lysine (0.5 μC)	75	83

The results demonstrate that sucrose-dextran density gradients yield nuclei which approach the metabolic activity of those prepared in isotonic sucrose, and that zonal centrifugation, with its increased resolution, is useful for preparing nuclei for metabolic studies. The density range of the gradient (1.02–1.10) is large enough to permit the construction of gradients of reasonable capacity. Because of the nonideal freezing depression of dextran solutions, the central portion of the gradients prepared by mixing sucrose and dextran solutions will be slightly hypotonic. Experimentally, the center of the gradient had a freezing point depression of −0.50° as compared to −0.60° for the original dextran and sucrose solutions. This small difference did not appear to affect appreciably the metabolic activity of the nuclei.

Two-component, essentially isotonic gradients in zonal rotors hold promise for the isolation of subcellular components with minimal damage and provide one solution to the problems encountered with pure sucrose gradients discussed by de Duve, Berthet, and Beaufay.[4]

B. ACID PHOSPHATASE IN CELL FRACTIONS

H. Schuel N. G. Anderson

1. Introduction

The classical procedures for the separation of subcellular components have been severely hampered by the poor resolution that can be achieved with differential centrifugation, and the consequent excessive handling required to obtain purified fractions.[5,6]

The application of high-speed density gradient centrifugation in swinging-bucket rotors greatly improved the obtainable resolution,[5,7] but this approach was restricted by the small volume and difficulties in loading the tubes with the gradient and recovery of the gradient with its separated zones after centrifugation. These difficulties have been largely overcome by the development of the B-II rotor described above. This device is capable of swinging a 1.6-liter gradient at speeds up to 30,000 rpm with a force in excess of 51,000 × g at the rotor edge, and has achieved high-resolution separation of subcellular components (soluble phase, ribosomes, microsomes, mitochondria, membranous fragments, and nuclei) from gram quantities of tissue during a single centrifugation.

On the basis of the enzymatic analysis of brei fractionated by differential and density gradient centrifugation, de Duve (1959) has postulated the existence of a new family of subcellular particles in rat liver, called lysosomes. The lysosomes are believed to be intermediate in size between microsomes and mitochondria and to contain a variety of acid hydrolases. These enzymes appear to be inactive on external substrates and would thus be prevented from digesting the major biochemical components of the cell. The breakdown of these particles and the release of the constituent hydrolases may be associated with injury as well as with physiological and pathological autolysis.

---

[4] Ch. de Duve, J. Berthet, and H. Beaufay, *Progr. Biophys. Biophys. Chem.* 9, 325 (1959).

[5] N. G. Anderson, pp 299–352 in *Physical Techniques in Biological Research* (ed. by Gerald Oster and Arthur W. Pollister), Academic Press, New York, 1956.

[6] Ch. de Duve and J. Berthet, *Intern. Rev. Cytol.* 3, 225 (1954).

[7] Ch. de Duve, pp 128–59 in *Subcellular Particles* (ed. by T. Hyashi), Ronald Press, New York, 1959.

It thus appeared desirable to test the performance of rotor B-II by attempting to isolate lysosomes from rat liver. "Acid phosphatase," the key enzyme in the development of the lysosome concept, was employed as the biochemical marker.

2. Method

Adult male Sprague-Dawley rats were used in this study. The animals were decapitated, and the livers were perfused with cold Locke's solution prior to homogenization in a Potter and Elvenhjem grinder in cold 8.5% sucrose. The brei was fractionated in zonal ultracentrifuge rotor B-II according to the procedure described elsewhere (Chap. VI, B2). A 1200-ml sucrose gradient, varying linearly with radius from 17 to 55% (w/w) with a cushion of 66% sucrose at the rotor edge, was employed.

Acid phosphatase activities were measured automatically with the Technicon Autoanalyzer[8] by means of a modified King-Armstrong procedure.[9,10] The substrate was disodium phenyl phosphatate (Technicon Instruments Corp.), and enzyme activity was estimated by measuring the amount of free phenol produced. Sodium malonate (Eastman Organic Chemicals) was used as the buffer. To release particle-bound enzymes a 0.2% solution of the nonionic detergent Turgitol NPX (ref 11) (Union Carbide Chemical Co.) was included in the substrate. Assays were made *in stream* on the gradient recovered from rotor B-II and also on each of the forty 40-ml fractions collected.

The protein content of the isolated fractions was estimated in the autoanalyzer according to the Folin-phenol method[12] on the material left after extraction of acid soluble nucleotides with 70% ethanol and 1% perchloric acid, lipids with Bloor's solution, RNA with cold 0.5 *N* perchloric acid, and DNA with hot (70°) 0.5 *N* perchloric acid.

Microscopic observations were made on the isolated fractions with a phase-contrast microscope using a dark-medium objective.

3. Experimental

Preliminary experiments suggested the presence of several enzymes with acid phenyl phosphatase activity in rat liver brei in the presence of malonate buffers. In untreated brei, pH-activity maxima were observed at pH 3.2 and 5.5. The addition of the Turgitol resulted in the preferential release of considerable

---

[8] L. L. Skeggs, *Am. J. Clin. Pathol.* **28**, 311 (1957).

[9] M. E. A. Powell and M. J. H. Smith, *J. Clin. Pathol.* **7**, 245 (1954).

[10] P. R. N. Kind and E. J. King, *J. Clin. Pathol.* **7**, 322 (1954).

[11] Similar in composition to Triton X100 used by de Duve (1959). These products are described as mixtures of alkyl phenyl esters of polyethylene glycol and have the following general formula:

$$C_8H_{17}-\langle\bigcirc\rangle-(OCH_2\cdot CH_2)_{\overline{9\text{-}10}}\,OH$$

[12] O. H. Lowry, N. J. Rosebrough, A. L. Farr, and R. J. Randall, *J. Biol. Chem.* **193**, 265 (1951).

additional activity between these optima. These observations confirm the results reported by other workers.[13] Since it was not practical to run similar complete pH activity spectra on each of the some 40 fractions obtained from a typical run with zonal ultracentrifuge rotor B-11, it was decided, instead, to monitor phenyl phosphatase activity at pH 3.2, 4.0, 5.0, and 5.5 in order to obtain some idea of the overall distribution pattern.

Assays of acid phenyl phosphatase activities were made in liver breis subjected to a wide range of centrifugal fields, 10,000–30,000 rpm for 60–180 min. Under these conditions, separations of subcellular components are achieved on the basis of sedimentation to the isopycnic position for the larger particles and on the basis of sedimentation rate for the smaller particles. The results of an experiment in which rat liver brei was subjected to 22,000 rpm for 120 min can be seen in Fig. XI-B-1. The phenyl phosphatase activities monitored at pH 4.0, 5.0 and 5.5 exhibited a similar distribution pattern, with considerable activities present in the soluble phase (sample layer of gradient) and particulate-mitochondrial and membranous fractions. The pH 3.2 activity, however, exhibited a rather different distribution pattern, with just a trace observed in the soluble phase, while most of the activity was associated with the cytoplasmic granules. Integration of the areas under these curves suggests that the phenyl phosphatase activities at each of the monitored hydrogen ion concentrations have a unique distribution between "soluble" and "particulate" phases in fractionated rat liver brei.

A rather different distribution pattern emerges when the data from this run are expressed in terms of specific activity, as seen in Fig. XI-B-2. The region in the gradient between the microsomes and the mitochondria appears to have the highest concentration of all the acid phenyl phosphatase activities measured, while the regions occupied by the soluble phase and larger cytoplasmic particles appear to be relatively poor. Examination of this part of the gradient by phase microscopy reveals large numbers of small apparently dense granules which may be the so-called lysosomes. The significance of the specific activity data in the gradient beyond the membranous-fragments fraction is questionable at present because the measurements of protein and phenyl phosphatase are just at the lower limits of resolution of the respective assay systems.

In low-speed runs (10,000 rpm for 60 min) a much larger portion of the activities is found in the region between the ribosomes and mitochondria. The ultraviolet absorbance in this area is about the same in both high- and low-speed runs. These observations suggest that at least part of the acid phenyl phosphatase activities are associated with small dense granules which sediment slower than either mitochondria or membranous components.

All the activities in the gradient beyond the soluble phase (sample layer) were bound to particles. This is based on the following evidence: Liver brei first subjected to 10,000 to 20,000 rpm for 60 min in zonal ultracentrifuge rotor B-II showed a distribution pattern of acid phenyl phosphatase activities similar to that seen in Fig. XI-B-1. Aliquots from this run were diluted slightly with 8.5% sucrose (to make it possible to sediment particles that had reached their isopycnic position in the gradient), and then centrifuged

[13] G. A. J. Goodlad and G. T. Mills, *Biochem. J.* 66, 346 (1957).

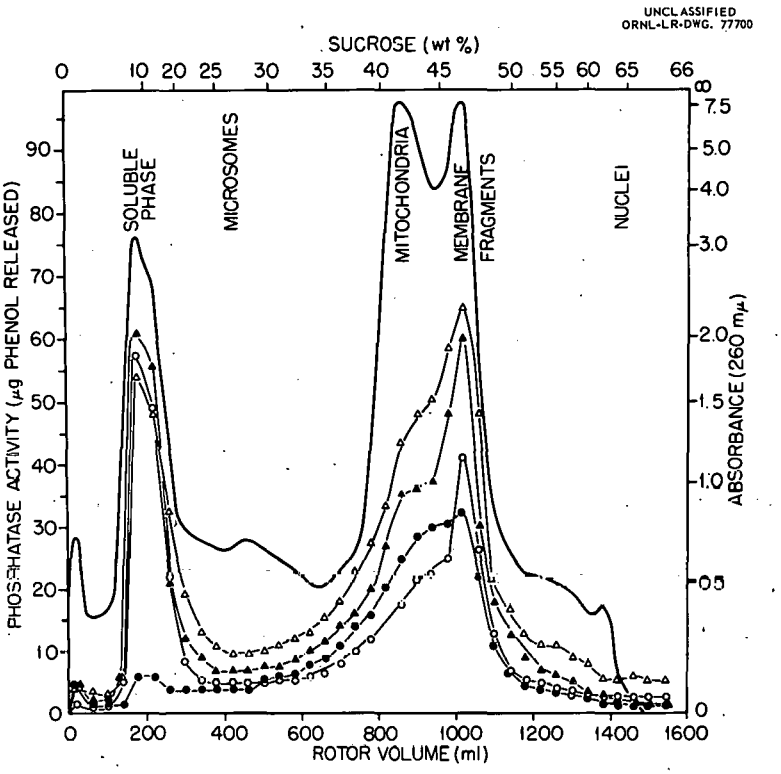

Fig. XI-B-1. Distribution of Acid Phenyl Phosphatase Activities at pH 3.2, 4.0, 5.0, and 5.5 in Rat Liver Brei Subjected to 22,000 rpm for 120 min in Zonal Ultracentrifuge Rotor B-II. Assays made with sodium malonate buffers in the presence of Turgitol NPX.

for 90 min at 40,000 rpm (105,536 × *g* avg) in the Spinco Model L Preparative Ultracentrifuge. The supernatants taken from aliquots of these fractions beyond the soluble phase peak in the gradient were found to be almost completely devoid of acid phenyl phosphatase activities.

Essentially all of the acid phenyl phosphatase activities present in the original brei measured under these conditions was recovered after fractionation in zonal ultracentrifuge rotor B-II.

4. Discussion

The experiments just described illustrate the kind of work in tissue fractionation that can be accomplished with zonal ultracentrifuge rotors. Furthermore, it is evident that the components of cells can now be visualized in a new way – as a continuous spectrum of particles. Devices of this type have the further advantage of being preparative as well as analytical; subcellular components are readily separated in mass and are available for subsequent chemical and morphological analysis, and the distribution of classes of particles in the gradient might also be diagnostic for various types of physiological manipulations. Fractionation systems built around various types of zonal centrifuges have a number of applications in biological research when used with suitable systems for further chemical and physical analysis.

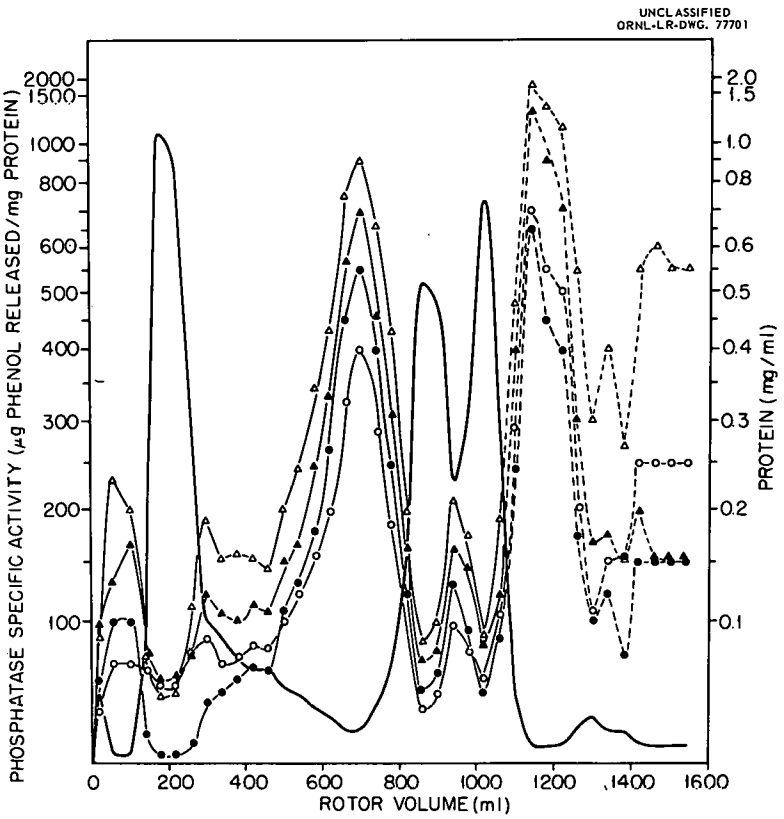

Fig. XI-B-2. Specific Activities of Acid Phenyl Phosphatase at pH 3.2, 4.0, 5.0, and 5.5 in Rat Liver Brei Subjected to 22,000 rpm for 120 min in Zonal Ultracentrifuge Rotor B-II. Protein assays made on material remaining after extraction of acid-soluble nucleotides, lipids, RNA, and DNA. —— protein phosphatase: ● pH 3.2; △ pH 4.0; ▲ pH 5.0; O pH 5.5.

With respect to the lysosomes believed to be in rat liver, it is clear that rotor B-II with a sucrose gradient failed to separate them into a single fraction. In addition, it appears that the distribution of acid phosphatases in liver brei is much more complicated than the work of de Duve[7] and his colleagues originally suggested. Preliminary experiments, which will be discussed in detail in a subsequent report, demonstrate that all the cytochrome "c" oxidase and hence all the mitochondria are banded in a sharp peak around 43% sucrose. This part of the gradient also contains large numbers of acid phenyl phosphatase containing granules, the identity of which is uncertain at present. This heterogeneity of cytoplasmic particles is confirmed by preliminary observations with the electron microscope (also to be discussed in a subsequent report). Class A rotors now under development will permit a more satisfactory separation of the larger cytoplasmic particles on the basis of differences in sedimentation rate.

Future work will be directed along two lines: (1) experiments designed to test the performance of class A and B rotors in the fractionation of whole cells and subcellular components, and (2) experimental studies on subcellular physiology using zonal centrifuges as a tool.

XII. An Integrated System for Virus Isolation

N. G. Anderson

Vaccines for human use are now generally prepared from whole-tissue-culture supernatants without purification or concentration of the virus. Foreign protein antigens from the tissue culture cells, therefore, may be included. The number of different vaccine preparations that could be tolerated by the population is limited in part by the danger of a gradual build-up of sensitivity to these proteins. Unwanted or adventitious viruses have also in the past been included in vaccines. Unfortunately, at present only those adventitious viruses that have been and can be identified are excluded in vaccine preparation. In some instances, effective vaccines cannot be prepared because the concentration of virus in the original culture fluid is too low to produce immunity in man. For these reasons, as well as for attempts to isolate viruses from human and animal tumors, it is considered urgent to complete the developmental work on the integrated system described here in the shortest possible time.

The immediate aim is a system capable of concentrating virus particles from large volumes of culture fluid, and of isolating from the concentrate only the particles having the physical properties of the desired virus. The amount of foreign protein antigen and the as yet unidentified adventitious viruses differing in physical properties from the desired virus would thus be reduced in quantity by many orders of magnitude. Multiple vaccines containing only purified, inactivated virus particles could be prepared.

In initial studies[1] formaldehyde-treated types I, II, and III poliovirus were purified from tissue-culture supernatant concentrates. Most of the mass in the starting zone in the centrifuge proved to be material which did not sediment appreciably under the conditions used. A single virus peak was observed in each instance which, when reconcentrated and observed in the analytical ultracentrifuge, gave only one peak having the expected sedimentation coefficient. With crude extracts containing brome mosaic virus a single virus peak was also observed, while a very skewed peak was seen with crude tobacco mosaic virus (TMV)-containing extracts.

For more extensive investigations T3 *coli* phage from cells grown on a synthetic medium was used. As a test material, 20 liters of a phage-infected *E. coli* culture were pumped through the rotor running at 20,000 rpm. The flow rate was approximately 100 ml/min. The sedimented material was scraped off the rotor wall and resuspended in buffer at pH 7.0. A small amount of this lysate concentrate was placed in 20 ml of

[1] N. G. Anderson, *J. Phys. Chem.* 66, 1984 (1962); and *Science*, in preparation.

buffer and used as the sample layer in the run shown in Fig. XII-1. The sample contained some soluble material, phage particles, and lysed cells. An event-marking pen along the lower edge of the chart registers each 40 ml fraction as it is collected. The sedimentation coefficients were calculated using the method described in Chapter XIII. The sedimentation coefficient for the virus peak agrees very well with the value of 476 S reported by Swaby.[2] When examined using phase-contrast microscopy the peak on the far right was found to contain lysed cell fragments. This run indicates the resolution that may be obtained with the present zonal ultracentrifuge prototype. Similar experiments were done with T2 phage where the separation was followed by infectivity assays.

Rotor B-II is not ideally suited to continuous flow work since flow through the rotor in the absence of a density gradient is not distributed evenly over the inner surface of the rotor. The following exploratory experiment was done, however, to see if a combination of continuous flow and equilibrium-zonal centrifugation was feasible.

Fifteen liters of a low titer T3 phage lysate was pumped through the rotor at approximately 2 liters/hr with the rotor spinning at 20,000 rpm at 5°C. The rotor was then decelerated to 5000 rpm and 100 ml each of 1:3, 1:1, and 3:1 dilutions of a stock cesium chloride solution (130 g in 70 ml H_2O) were pumped in to the rotor edge in that order. This was followed by 250 ml of the stock cesium chloride. These solutions form very thin layers at the rotor edge and rapidly diffuse to form a continuous density gradient.

[2] L. G. Swaby, Ph.D. thesis, University of Pittsburgh, 1962.

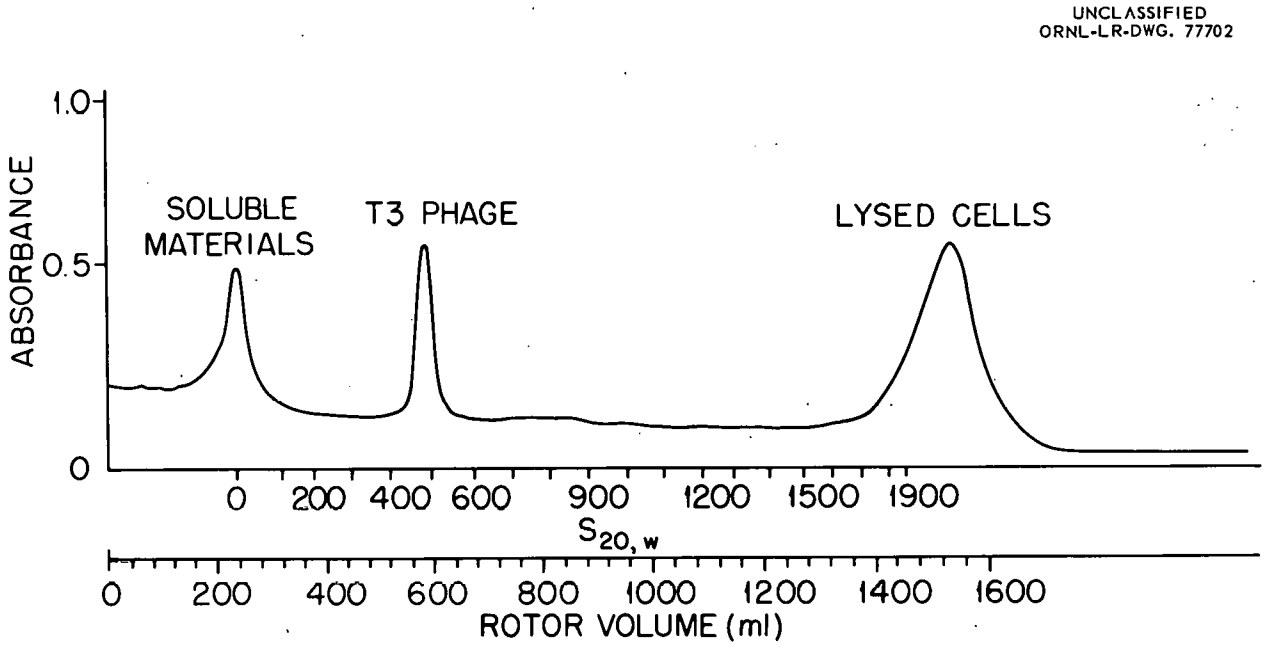

Fig. XII-1. Concentrated T3 Phage Lysate Centrifuged 1 Hour at 20,000 rpm at 5° in B-II Zonal Ultracentrifuge Rotor Using a 10–30% 1200-ml Sucrose Gradient.

The run continued for 2 hours at 20,000 rpm, then the speed was slowed to 5000 rpm for 3 hours at which time the gradient was recovered by pumping stock cesium chloride to the rotor edge. The ultraviolet absorbance of the effluent rotor stream was recorded and is shown in Fig. XII-2. Samples from the three peaks were examined using phase contrast microscopy. The first peak contained lysed bacterial cells and debris, the second only whole cells. The third was optically empty, with the center of the peak at a density of 1.5, which is the density of T3 phage.[2] The ragged recording of the first peak is due to the presence of large clumps of material in the effluent stream.

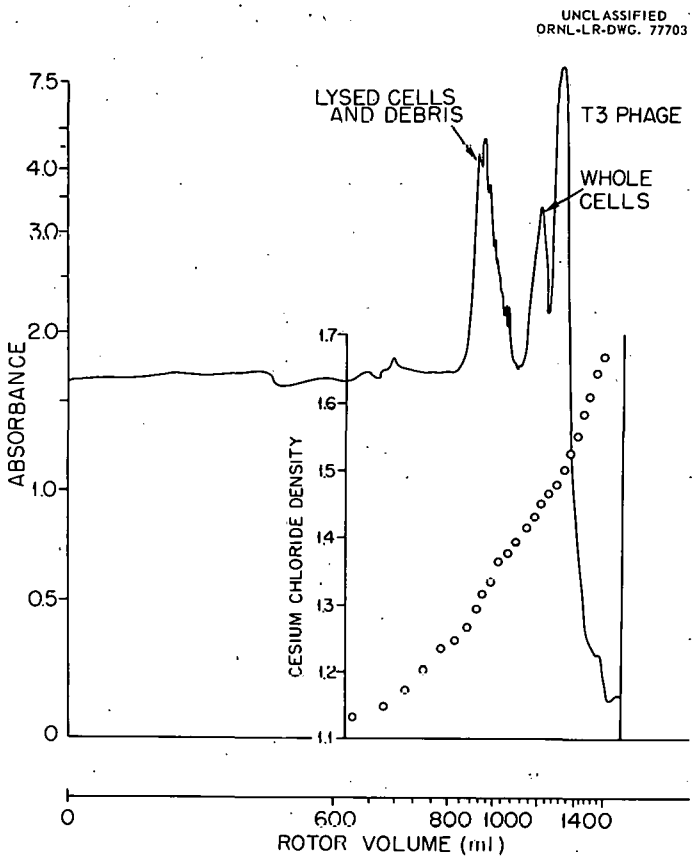

Fig. XII-2. Banding of T3 Phage Lysate in CsCl in Rotor B-II After Concentration by Continuous Flow Centrifugation.

The material in the third peak was diluted to decrease the density of the solvent and the virus was recovered by centrifuging at 150,000 × *g* for 1 hour. The pellet was suspended in 0.1 ionic strength Miller-Golder[3] buffer at pH 7.5 and rerun in the zonal centrifuge with the same gradient used for the separation shown in Fig. XII-1, but with a centrifuge run time of 2 hours at 20,000 rpm. The results shown in Fig. XII-3 demonstrate that excellent purification of virus particles may be obtained using the combined continuous-

[3]G. L. Miller and R. H. Golder, *Arch. Biochem.* 29, 421 (1950).

flow density-gradient method. Rotors are now being designed which will allow a cesium chloride gradient to be stabilized at the rotor wall while the dilute virus suspension is flowing through the rotor. The virus particles would then sediment into the density gradient directly rather than to the rotor wall and subsequently back into the cesium chloride gradient as was done here.

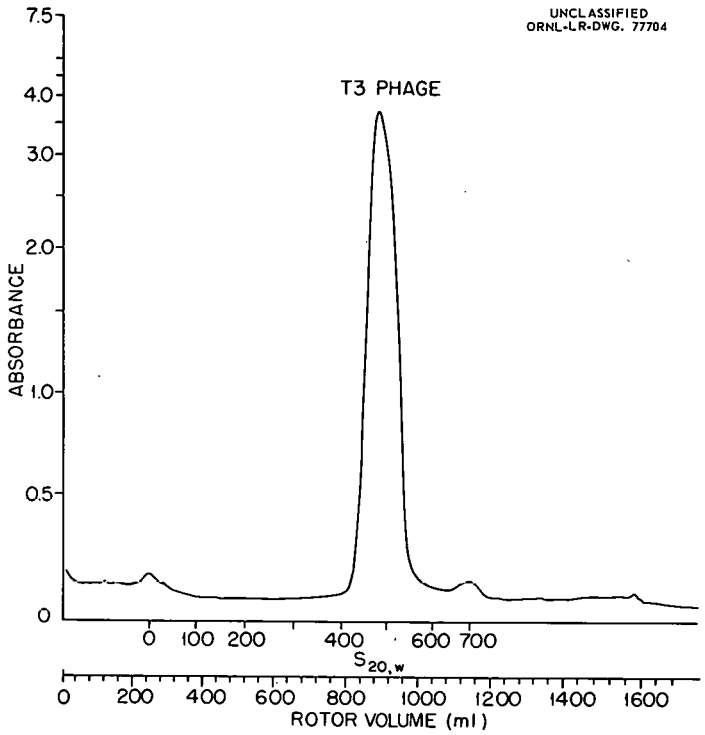

Fig. XII-3. Rate Zonal Sedimentation of T3 Phage from Phage Peak Shown in Fig. XII-2. Centrifugation done in 10–30% sucrose gradient for 2 hours at 20,000 rpm at 5° in rotor B-II.

These experiments demonstrate the feasibility of zonal rotors for the large-scale purification of virus particles by rate-zonal and isopycnic-zonal centrifugation, and, in addition, show that the latter may be combined with continuous-flow centrifugation for the concentration of virus from large volumes of solution.

Adventitious viruses have recently been discovered in vaccines previously considered safe for human use.[4,5] Since only those contaminating viruses for which specific tests are available can be detected, it is considered important to develop methods of large-scale virus purification which would decrease markedly concentration of particles and viruses differing in sedimentation rate or density from the virus desired.

In instances where the viral nucleic acid may be removed by chemical treatment[6] or where a fraction of the naturally formed particles are devoid of nucleic acid, the possibility of isolating such hollow-headed or "top-component" particles for the preparation of noninfective vaccines may now be considered.

---

[4] R. N. Hull, J. R. Minner, and C. C. Mascoli, *Am. J. Hyg.* 68, 31 (1958).

[5] B. H. Sweet and M. R. Hilleman, *Proc. Soc. Exptl. Biol. Med.* 105, 420 (1960).

[6] J. M. Kaper, *J. Mol. Biol.* 2, 425 (1960).

XIII. Data Reduction

A. COMPUTER PROGRAM FOR THE ZONAL ULTRACENTRIFUGE

N. G. Anderson R. E. Lybarger

1. General Outline

In the zonal ultracentrifuge, particles sediment through a gradient of increasing density and viscosity. It is important to be able to determine sedimentation coefficients routinely and to relate these values and the absorption recordings to other on-stream analyses made during a centrifuge run. Unfortunately, the computations involved are extensive and very time-consuming. Arrangements have, therefore, been made to program the sedimentation coefficient determinations, area integrations, and corrections for nonlinearity of analytical methods for a computer. This program was not completed during this report period; however, the elements of some of the methods used are recorded here.

Equations required:

- Viscosity of sucrose solutions as a function of both concentration and temperature.
- Density of sucrose solutions as a function of both concentration and temperature.
- Volume of rotor as a function of radius starting with the edge of the rotor core.

Input data:

- Volume increments.
- Running time at beginning of first and end of each volume collected.
- % sucrose in each volume.
- $\int \omega^2 t$
- Particle densities.
- Optical densities and analyzer readings.
- Analyzer lag corrections.

Output:

- Sedimentation coefficients plotted along radius for each particle density.

2. Method

Sedimentation coefficients are determined using a modification of the trapezoidal approximation of Martin and Ames (*J. Biol. Chem.* **236**, 1372, 1961). In a medium, m, at temperature, T, the sedimentation constant is given by:

$$s_{T,m} = \frac{dx/dt}{\omega^2 x} \tag{1}$$

where dx/dt is the velocity of movement of the boundary, ω^2 is the angular velocity of the rotor in radians per second, and x is the distance from the rotor center to the inflection point of the boundary or center of the zone. It is customary to extrapolate to a standard state, in this instance water at 20° using the equation:

$$s_{20,w} = s_{T,m} \frac{\eta_{T,m}(\rho_p - \rho_{20,w})}{\eta_{20,w}(\rho_p - \rho_{T,m})} \tag{2}$$

where $\eta_{T,m}$ is the viscosity of the medium at the temperature of centrifugation, $\eta_{20,w}$ is the viscosity of water at 20°, ρ_p is the density of the particle in aqueous solution (this is equal to the reciprocal of the partial specific volume, $\bar{V}$), $\rho_{T,m}$ is the density of the medium at the rotor temperature, and $\rho_{20,w}$ is the density of water at 20°C. The term ρ_p is for practical purposes considered a constant, since the partial specific volume of most proteins varies little with temperature.

Equation (2) applies to sedimentation in a uniform solvent and also in a density gradient. In the gradient, however, the viscosity ($\eta_{T,m}$) and the density ($\rho_{T,m}$) are functions of the sucrose concentration through the gradient. If equations (1) and (2) are combined, then

$$\omega^2 s_{20,w}\, dt = \frac{(\rho_p - \rho_{20,w})\eta_{T,m}}{(\rho_p - \rho_{T,m})\eta_{20,w}} \cdot \frac{1}{x}\, dx \tag{3}$$

Integrating the left side of equation (3):

$$\int_0^t s_{20,w}\omega^2\, dt = s_{20,w}\omega^2 t \tag{4}$$

The right-hand side of equation (3) can be approximated as follows:

$$\frac{(\rho_p - \rho_{20,w})}{\eta_{20,w}} \int_0^{x_{i+1}} F(x)\, dx = \frac{(\rho_p - \rho_{20,w})}{\eta_{20,w}} \sum_0^{x_{i+1}} F(x_i)(x_{i+1} - x_i) \tag{5}$$

Using standard tables or the equations listed at the outset, the density and viscosity of the sucrose solutions corresponding to different levels of the gradient are determined. Then

$$F(x) = \frac{\eta_{T,m}(x_i)}{[\rho_p - \rho_{T,m}(x_i + x_{i+1}/2)]\, x_i} \tag{6}$$

is calculated for each distance, x_i. The right side of the equation may then be integrated for each value of ρ_p.

In the original method of Martin and Ames a second term is included in equation (5) to take care of the fact that sedimentation constants were determined for particles at fixed points along the gradient (along the radius x), and that the sucrose concentrations are given for the same fixed points. It was, therefore, necessary to average $F(x)$ between two consecutive points, and use the average to determine the sedimentation rate of a particle between the two points.

In the zonal ultracentrifuge the sedimentation constants are calculated for radii equal to the radii (in the rotor during rotation) of the last drop of fluid collected in each fraction tube. The sucrose concentrations, however, are determined for the whole (usually 40 ml) fraction. In this manner, the average of the sucrose concentration through the zone represented by one tube is obtained. The second term in equation (5) is, therefore, omitted.

In all future runs, the volume of the overlay will be chosen so that the end of one 40-ml collection corresponds to the center of the sample zone:

$$\frac{V_o + L_v + \frac{1}{2}A_v}{40} = N \tag{7}$$

where V_o is the overlay volume, L_v is the line volume, A_v the sample volume, and N is a whole number.

3. B-II Rotor Volume

The equation relating V to X (volume to radius) in the B-II rotor is:

$$X = \sqrt{\frac{V - V_c + \pi X_c^2 h + A_v}{\pi h}} \tag{8}$$

where X is the radius of a zone recovered in volume V from the rotor, V_c is the volume of fluid within the maximum core diameter area and in the lines, X_c is the maximum radius of the core, A_v is the volume occupied by the septa, and h is the internal rotor height. The volume of the septa outboard of the core is given by the equation.

$$A_v = N_a h T_a (X - X_c)$$

where N_a is the number of septa, h is the height of the septa, and T_a is the thickness of each septum.

XIV. Remote Facility Design

N. G. Anderson E. C. Evans E. F. Babelay R. E. Brockwell

During the Joint NIH-AEC Zonal Centrifuge Program, centrifuge systems will be developed that will allow the isolation of very large amounts of virus materials. As these come into general use, it becomes imperative to consider the hazards that may be involved. It is evident that these will depend on the types of viruses being purified. However, if adventitious pathogenic viruses are present in otherwise innocuous virus preparations, the pathogens may also be sufficiently concentrated to become an unexpected hazard. Further, the effects of massive amounts of otherwise harmless viruses on human subjects are difficult to evaluate. For these reasons, we consider it our responsibility to examine the possibility of developing virus isolation facilities which would minimize the hazards mentioned.

For highly pathogenic material, triple containment is being considered, with double and single containment for less-hazardous materials. The first containment system will be the centrifuge rotor itself, with associated lines and seals. The second is the rotor chamber and chambers containing the fluid line seals, fluid lines, and samples, which are thus sealed off from the room in which the centrifuge is operated. The third barrier would be the room in which the centrifuge is operated. This room should be constructed so that it can be sealed and sterilized.

Sterilization methods, remote handling techniques, biologically tight seal systems and associated problems are, therefore, being investigated.

XV. Zonal Centrifuge Monitoring Systems

T. J. Lewis J. T. Dalton N. G. Anderson

A. MONITORING OF ULTRAVIOLET ABSORBANCE OF THE GRADIENT AS RECOVERED FROM THE ROTOR

For maximum resolution it is desirable to analyze the density gradient exit stream as it flows out of the rotor. This is done most conveniently by following the ultraviolet absorbance at 260 or 280 mμ continuously. Three systems have been examined and the most generally applicable appears to be a Beckman-DU monochromator with a Gilford Photocell and Hydrogen Lamp Power Supply. A flow cell having an optical path of 0.2 cm and a holdup volume of 56λ (ref 1) is conveniently used. It has been found desirable to keep the photocell as close to the flow cell as possible since a small amount of refractive bending of the light beam due to the density gradient occurs which produces spurious peaks when long light-path double beam spectrophotometers are employed.

B. CENTRIFUGE CONTROL AND MONITORING SYSTEM

All indicating and electrical control systems, with the exception of the mechanical tachometer now on the modified Spinco L Centrifuge used to drive the B-II rotor, are being removed and mounted on a separate rack to allow the centrifuge to be operated remotely. The same control and monitoring rack will serve for other centrifuge systems now being developed. A schematic diagram of the instrumentation is shown in Fig. XV-1.

In addition to a digital display of rotor speed, instrumentation is being developed for obtaining a similar display of the time integral of the acceleration of the centrifuge bowl as is required for the computations discussed in Chapter XIII. Indicators for continuous rotor speed (rpm) and ω^2, the angular velocity squared, are being developed. The integral of ω^2 with respect to time will be indicated as decimal digits in units of radians squared/sec. The integrator will have a capacity large enough for an operating time of at least 12 hours. It is expected that the overall accuracy of the system will be 3% or better. The method of obtaining the desired information includes taking a pulse signal from a distance detector probe mounted to a collar at the top of the rotor. This collar will be made with two diametrically opposed flats, which will impart two pulses/rev to the probe. These voltage pulses will be amplified and fed into a frequency meter whose

[1] N. G. Anderson, *Anal. Chem.* 33, 970 (1961).

UNCLASSIFIED
ORNL-LR-DWG. 77705

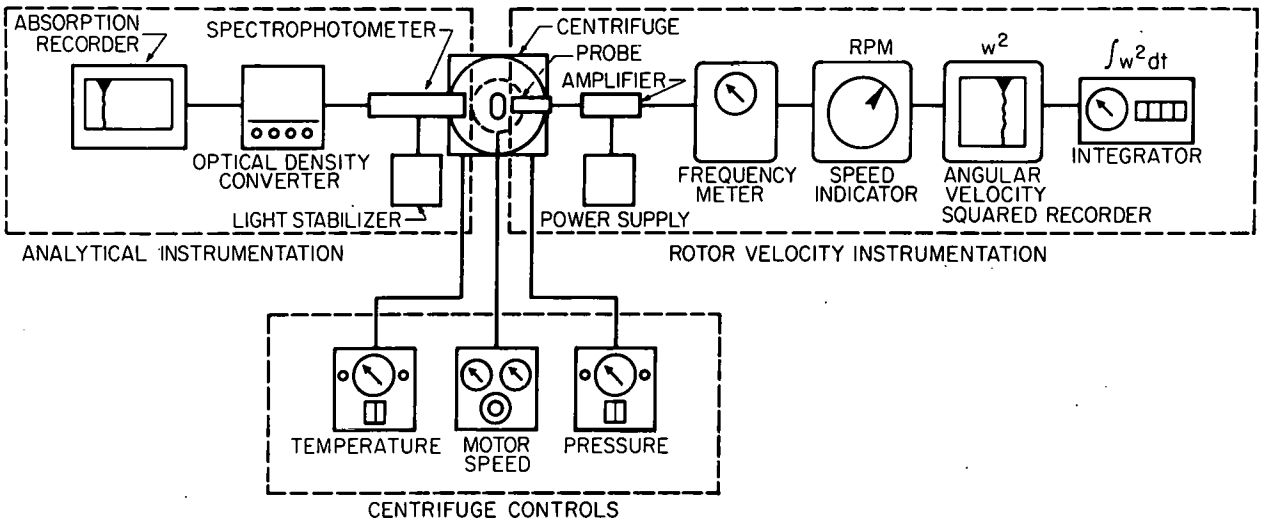

Fig. XV-1. Proposed Zonal Centrifuge Instrumentation.

dc output will be proportional to the frequency of the pulses. This direct voltage will be measured and indicated by a self-balancing potentiometer calibrated to read the instantaneous value of angular velocity.

To obtain ω^2, the direct voltage representing ω will pass to a squaring circuit, thence to another self-balancing potentiometer which, in this instance, is part of an instrument calibrated to record the square of the angular velocity. An integrating circuit with a digital readout uses the output from the recorder to perform the integration

$$\int_{t=t_0}^{t_1} \omega^2 \, dt \, .$$

C. BIOANALYTICAL INSTRUMENTATION

The intracellular distribution of enzymatic activity may be readily determined by on-stream analysis in the recovered gradient stream. In this report period, the major part of the effort has been directed toward the study of acid phosphatases in rat liver using the Technicon Autoanalyzer (Chapter XI-B). Automated systems for total protein, uricase, and cytochrome oxidase determinations in sucrose gradients are under development and will be described in detail later. A new system for determining picogram quantities of carbon in solid organic materials is also being investigated.

XVI. Preparation of Cells for Study in Zonal Centrifuge Systems

T. W. James R. H. Stevens

For studies on changes occurring in cells during cell division it is desirable to have large masses of cells in the same stage of the cell cycle. Ultimately, it is desirable to use synchronously dividing mammalian cells. A prototype cell synchronizer has been built and used to evaluate methods for producing synchronization and for monitoring continuously cell concentration.

On the basis of this research a conceptual design (Fig. XVI-1) is being developed for a high-capacity, protozoan cell culture system capable of automatically and precisely synchronizing up to 30 liters of culture media. The system will provide either light or temperature synchronization of the solution on a preprogrammed basis, allowing automatic withdrawal of culture solution and admission of fresh culture media at any point in the synchrony cycle. The culture vessel is also expected to provide constant temperature operation for up to 60 liters of culture. Particular attention is being given to the system's capability for rapidly and uniformly raising and lowering the solution temperature without creating thermal zones whose temperatures are lethal to the culture cells. The general operational criteria for the system include:

1. Equipment to control the culture to within ±0.1°C at either of two temperature levels, and the capability of raising and lowering the culture temperature as rapidly as possible from one level (for example, 14°C) to the other (for example, 28°C) on a prescheduled basis.

2. Designs for "fail-safe" operation to limit the upper temperature of the recirculating heating liquid to 35°C in the event of stirring failure in the culture vessel. Normally, the temperature of the culture vessel will approach the operating temperature exponentially without exceeding the operating value.

3. Provision for in-place steam sterilization of required equipment, or means for easily disconnecting and locating these items in an autoclave. Also, provisions for sterilizing by ultrafiltration the nutrient make-up solution and air purge to the culture vessel.

4. Provision for monitoring the oxygen and carbon dioxide tensions, pH, and temperature of the culture solution.

5. Provision for viewing the culture medium through glass during growth, and for admitting light to the culture for light-dark synchrony purposes.

6. Means for inoculating the system with cells, and for automatically and/or manually adding and withdrawing solution at any time.

7. Means for determining the concentration of cells continuously, for recording cell number as a function of time, and for controlling the synchronizing temperature changes by time and length of the division burst.

The system will consist of (1) a mobile, autoclavable housing containing the culture vessel and its auxiliary equipment for the automatic addition and removal of solutions, (2) a small instrument console for the timing and valve controlling equipment and (3) two precisely temperature-controlled, 50-gallon water baths to change or to maintain the temperature of the culture at the proper values. The culture vessel will be a conical-bottomed, double-walled metal tank, 21 in. in diameter by 17 in. deep. It will be fitted with a removable cover through which all stirring and probing functions can be performed. Two glass ports in the vessel wall will permit visual observation and light-cycling of the culture. The double-wall design permits circulation of heating or cooling water through the annulus, thus obtaining a greater surface area-to-volume ratio for heat transfer than possible with immersed coils, and provides a smooth, easily cleaned inner surface.

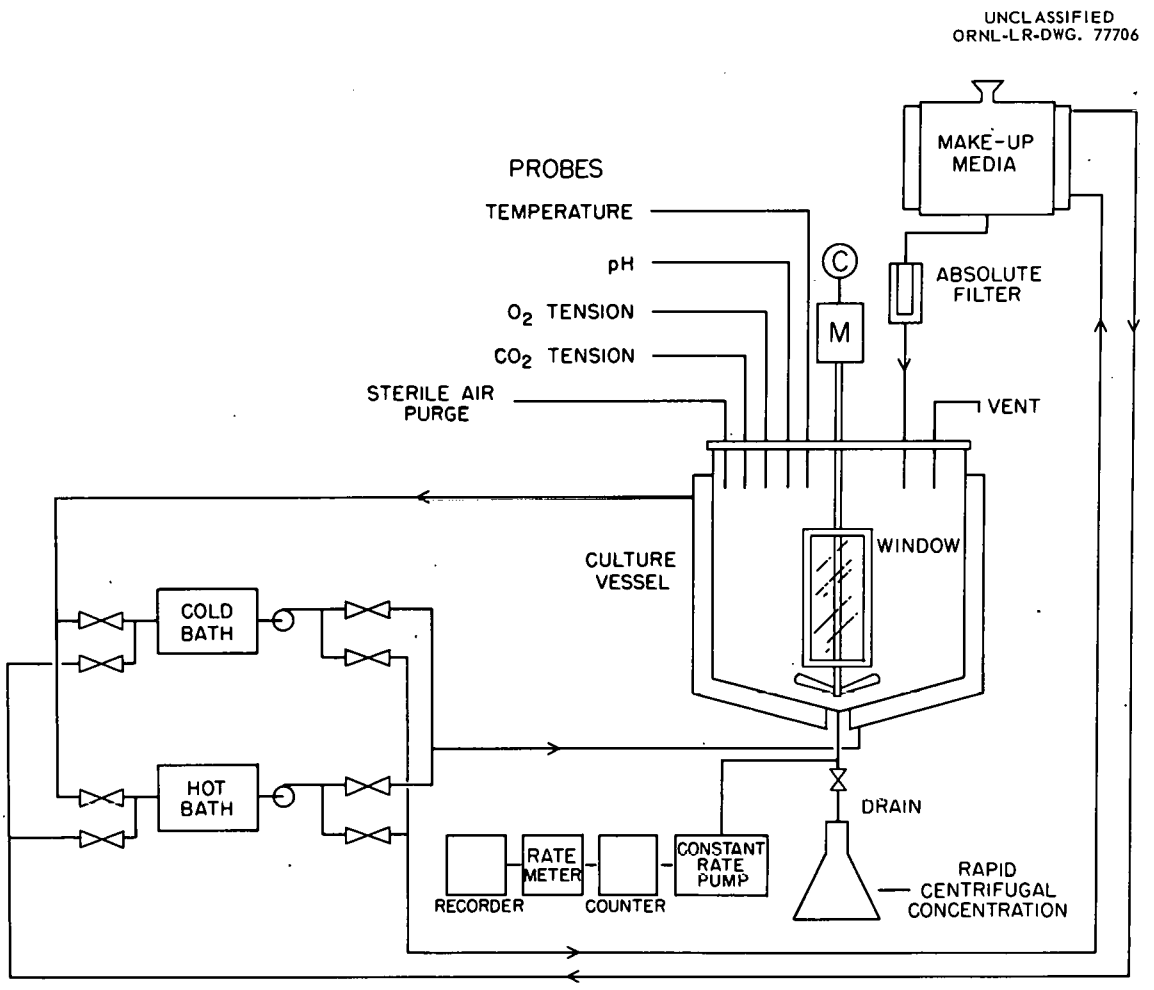

Fig XVI-1. Conceptual Design of Cell Synchronizing System.

THIS PAGE

WAS INTENTIONALLY

LEFT BLANK

Organization of the Joint NIH–AEC Zonal Centrifuge Development Program

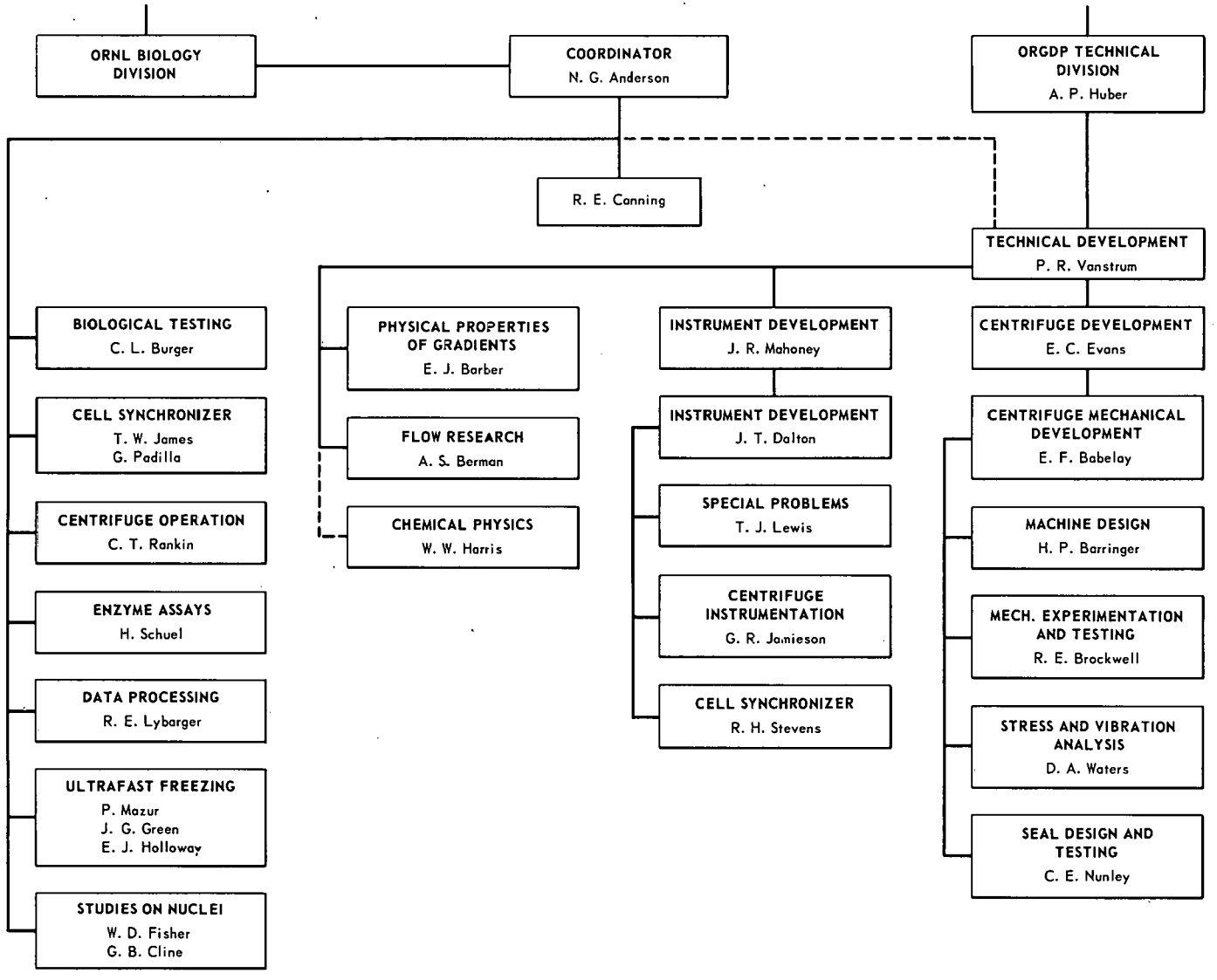

Consultants: C. A. Price, Rutgers University
B. T. Cole, University of South Carolina

THIS PAGE

WAS INTENTIONALLY

LEFT BLANK

ORNL-3415
Special

INTERNAL DISTRIBUTION

1. S. I. Auerbach
2. R. Baldock
3. R. E. Biggers
4. A. L. Boch
5. D. S. Billington
6. E. P. Blizard
7. C. J. Borkowski
8. G. E. Boyd
9. D. D. Cowen
10. C. J. Collins
11. F. L. Culler
12. P. B. Dunaway
13. J. L. Fowler
14. J. H. Frye, Jr.
15. R. F. Hibbs
16. A. S. Householder
17. J. S. Johnson
18. R. W. Johnson
19. W. H. Jordan
20. K. A. Kraus
21. M. T. Kelley
22. J. A. Lane

23–24. C. E. Larson

25. T. A. Lincoln
26. S. C. Lind
27. R. S. Livingston
28. K. Z. Morgan
29. J. P. Murray (K-25)
30. D. J. Nelson
31. M. L. Nelson
32. J. S. Olson
33. M. E. Ramsey
34. R. M. Rush
35. M. J. Skinner
36. J. A. Swartout
37. E. H. Taylor
38. A. M. Weinberg
39. H. I. Adler
40. J. F. Albright
41. R. C. Allen

42–46. N. G. Anderson

47. W. A. Arnold
48. W. E. Barnett
49. R. H. Baum
50. A. C. Bell
51. M. A Bender
52. W. F. Bertsch
53. F. J. Bollum
54. H. E. Brockman

55–56. C. L. Burger

57. I. L. Cameron
58. P. Cammarano
59. S. F. Carson
60. A. Castellani
61. B. M. Cattanach
62. E. H. Y. Chu
63. G. Cleffmann
64. W. E. Cohn
65. C. C Congdon
66. G. E. Cosgrove
67. G. Cudkowicz
68. E. B. Darden
69. F. J. de Serres
70. D. G. Doherty
71. M. I. Dolin
72. J. L. Fairley
73. F. J. Finamore
74. W. R. Fisher
75. P. J. Fritz

76–78. D. A. Fuccillo, Jr.

79. M. E. Gaulden
80. J. W. Goodman
81. D. G. Gosslee
82. J. E. Graebe
83. J. G. Green
84. E. H. Grell
85. R. F. Grell
86. W. D. Gude
87. G. Giudice
88. A. H. Haber
89. A. Hollaender
90. I. H. B. Hoppe
91. K. B. Jacobson
92. J. Jagger
93. T. W. James
94. A. Kaji
95. H. Kaji
96. S. Karasaki
97. M. A. Kastenbaum
98. F. T. Kenney
99. J. X. Khym
100. R. F. Kimball

101. J. S. Kirby-Smith
102. D. R. Krieg
103. Sr. R. Lanigan
104. D. L. Lindsley, Jr.
105. T. J. Long
106. T. Makinodan
107. R. J. Mans
108. P. Mazur
109. C. G. Mead
110. O. L. Miller, Jr.
111. S. Nishimura
112. G. D. Novelli
113. E. F. Oakberg
114. T. T. Odell, Jr.
115. G. M. Padilla
116. H. D. Peck, Jr.
117. E. H. Perkins
118. A. P. Pfuderer
119. E. F. Phares
120. R. A. Popp
121. D. M. Prescott
122. M. L. Randolph
123. R. R. Rinehart
124. P. Roberts
125. Stanfield Rogers
126. L. Rosen
127. L. B. Russell
128. W. L. Russell
129. T. Sado
130. N. G. Sansing
131. H. Schuel
132. J. K. Setlow
133. R. B. Setlow
134. F. Seto
135. L. H. Smith
136. G. E. Stapleton
137. C. M. Steinberg
138. G. E. Stone
139. M. P. Stulberg
140. D. C. Swartzendruber
141. P. A. Swenson
142. C. Takata
143. R. L. Tyndall
144. A. C. Upton
145. R. M. Valencia
146. E. Volkin
147. R. C. von Borstel
148. Vu Thi Suu
149. H. E. Walburg, Jr.
150. R. A. Wallace
151. B. B. Webber
152. W. J. Welshons
153. V. P. White
154. L. Wickham
155. A. K. Williams
156. J. P. Williams
157. S. Wolff
158. C. J. Wust
159. T. Yamada
160. M. Yoneda
161. E. F. Babelay
162. E. J. Barber
163. H. P. Barringer
164. A. S. Berman
165. H. A. Bernhardt
166. H. D. Culpepper
167. J. T. Dalton
168–177. E. C. Evans
178. J. Farquharson
179. R. L. Farrar, Jr.
180. W. W. Harris
181. A. P. Huber
182. G. R. Jamieson
183. E. C. Johnson
184. T. J. Lewis
185. J. R. Mahoney
186. C. E. Nunley
187. P. R. Vanstrum
188. D. A. Waters
189. S. J. Wheatley
190. W. J. Wilcox
191. E. Chargaff (consultant)
192. R. D. Hotchkiss (consultant)
193. Curt Stern (consultant)
194. M. M. Wintrobe (consultant)
195. P. C. Zamecnik (consultant)
196–197. Biology Library
198–199. Central Research Library
200. Reactor Division Library
201–202. ORNL – Y-12 Technical Library Document Reference Section
203–222. Laboratory Records Department
223. Laboratory Records, ORNL, R.C.
224. Laboratory Shift Supervisor

EXTERNAL DISTRIBUTION

225. R. W. McNamee, Union Carbide Corporation, New York
226. C. Baker, National Cancer Institute, Bethesda, Maryland
227. N. F. Barr, Atomic Energy Commission, Washington
228. N. Berlin, National Cancer Institute, Bethesda
229. H. D. Bruner, Atomic Energy Commission, Washington
230. W. R. Bryan, National Cancer Institute, Bethesda
231. J. C. Bugher, Puerto Rico Nuclear Center, Rio Piedras, P.R.
232. W. W. Burr, Jr., Atomic Energy Commission, Washington
233. R. S. Caldecott, Atomic Energy Commission, Washington
234. R. M. Chanock, National Institute of Allergy and Infectious Diseases, Bethesda
235. R. A. Charpie, Union Carbide Corporation, New York
236. W. D. Claus, Atomic Energy Commission, Washington
237. C. L. Dunham, Atomic Energy Commission, Washington
238. K. M. Endicott, National Cancer Institute, Washington
239. J. L. Fahey, National Cancer Institute, Bethesda
240. E. Frei, National Cancer Institute, Bethesda
241. H. Bentley Glass, Johns Hopkins University, Baltimore
242. H. N. Glassman, U.S. Army Chemical Corps, Fort Detrick, Maryland
243. S. T. Grey, Food and Drug Administration, Washington, D.C.
244. N. S. Hall, University of Tennessee
245. Fred J. Hodges, University of Michigan, Medical Center, Ann Arbor
246. J. G. Horsfall, Connecticut Agricultural Experimental Station, New Haven
247. R. D. Housewright, U.S. Army Chemical Corps, Fort Detrick, Maryland
248. R. J. Huebner, National Cancer Institute, Bethesda
249. K. W. Kohn, National Cancer Institute, Bethesda
250. P. Kotin, National Cancer Institute, Bethesda
251. R. E. Learmouth, National Cancer Institute, Bethesda
252. J. L. Liverman, Atomic Energy Commission, Washington
253. R. F. Loeb, College of Physicians and Surgeons, Columbia University, New York
254. R. G. Meader, National Cancer Institute, Bethesda
255. G. R. Mider, National Cancer Institute, Bethesda
256. Carl V. Moore, Washington University, St. Louis, Mo.
257. P. T. Mora, National Cancer Institute, Bethesda
258. M. A. Mufson, National Institute of Allergy and Infectious Diseases, Bethesda
259. R. Quimby, National Aeronautics and Space Administration
260. H. M. Roth, Research and Development Division, AEC, ORO
261. W. P. Rowe, National Institute of Allergy and Infectious Diseases, Bethesda
262. P. S. Sarma, National Institute of Allergy and Infectious Diseases, Bethesda
263. Shields Warren, New England Deaconess Hospital, Boston
264. C. S. Shoup, Atomic Energy Commission, Oak Ridge
265. H. A. Sober, National Cancer Institute, Bethesda
266. John Totter, Atomic Energy Commission, Washington
267. A. G. Wedum, U.S. Army Chemical Corps, Fort Detrick, Maryland
268. J. White, National Cancer Institute, Bethesda

269. H. G. Wood, Western Reserve University, Cleveland
270–271. C. G. Zubrod, National Cancer Institute, Bethesda
272. Atomic Energy Commission, Washington
273. General Electric Company, Richland
274. New York Operations Office
275. AEC Patent Branch, Washington
276. Division of Technical Information Extension, Oak Ridge
277. UCLA Medical Research Laboratory